Chemical Evidence for the Presence and Distribution of Macondo Oil in Deep-Sea Sediments following the Deepwater Horizon Oil Spill

Scott A. Stout, Ph.D.
NewFields Environmental Forensics Practice, LLC, Rockland MA
August 2015

Abstract
Sediments (2782) from high resolution cores (729) collected in 2010/2011 from the deep-sea following the *Deepwater Horizon* oil spill were chemically analyzed in order to (1) determine the presence of the spilled Macondo oil in the deep-seafloor, (2) assess the spilled oil's range of weathering after the spill, and (3) distinguish the spilled oil from deep-sea sediments containing oil from natural oil seeps and background (ambient) hydrocarbons. A forensic method reliant upon multiple lines of evidence (chemical fingerprinting, lateral and vertical hydrocarbon concentration trends, proximity to the well and known or apparent seeps, and the character of proximal samples – including nearby cores, novel "slurp gun" seafloor floc samples, and core supernatants) was used to meet these objectives and affirm the conceptual model that some liquid Macondo oil (not just dissolved hydrocarbons and gases) that had remained within the deep-sea was widely distributed by the deep-sea plume(s) and deposited in deep-sea sediments. General conclusions include:

- Macondo oil and synthetic-based drilling mud (SBM) were deposited within ~1 mile of the well, mostly within the top 3 cm but up to 10 cm deep (at least) in some locations.
- Beyond ~1 mile from the well a Macondo-derived oily floc was found in surface sediments (mostly top 1 cm) up to 19 miles southwest of the well, less in other directions.
- The Macondo oil present in sediments exhibited a range in weathering that, on average, increased with increasing distance from the well.
    - Minimally weathered oil typically co-occurred with SBM in sediments within ~1 mile of the well and is attributed to direct fallout of oil-SBM mixtures.
    - Severely weathered oil occurred at the seafloor surface (only) further from the well. These oils had suffered excessive dissolution and biodegradation during transport within the (well-established) deep-sea plume prior to being deposited on the seafloor (e.g., via marine oil snow or impingement).
- The distinct features of the severely weathered Macondo oil beyond a few miles from the well allowed it to be recognized at low concentrations and distinguished from pervasive background hydrocarbons and seep oils, the latter of which had retained susceptible hydrocarbons that had been removed from the Macondo oil due to the severe dissolution and biodegradation the (chemically and physically) dispersed Macondo oil experienced during its transport throughout the deep-sea.

Subsequently, sediments (805) from high resolution cores (201) collected in 2014 were collected, analyzed, and forensically evaluated for the same objectives. General conclusions include:

- Macondo oil (and SBM) was still present in sediments within ~1 mile of the well; however weathering due to biodegradation had progressed since 2010/2011.
- Macondo oil could still be recognized in surface sediments 1 to nearly 11 miles southwest of the well, less in other directions. Biodegradation had also affected this oil since 2010/2011.
- Overall, concentrations of Macondo-derived PAH are about 1 order of magnitude lower in 2014 than they were in 2010/2011.

Introduction

Crude oil released (April 20 to July 15, 2010) from the Macondo well at a water depth of ~1500 m following the explosion of the *Deepwater Horizon* drill rig experienced different environmental fates. Buoyancy forces caused most of the oil to be transported (roughly) vertically through the water column to the sea surface forming surface slicks, mousses, and sheens that were widely spread by wind and currents (Graettinger et al., 2015). However, it has been well established that some fraction of the crude oil released remained in the deep-sea.

Early sediment studies showed that some oil was directly deposited on the seafloor within ~2 miles (3 km) of the well, aided in part by the oil's co-occurrence with dense synthetic based drilling mud (OSAT-1, 2010). Another fraction of the oil that had remained within the deep-sea was advectively transported horizontally as physically or chemically-dispersed, neutrally buoyant droplets (< 40 μm) within an extensive deep-sea "plume" that formed between ~1000 to 1300 m water depth (e.g., Camilli et al. 2010; Hazen et al., 2010; Socolofsky et al., 2011; Atlas and Hazen, 2011; Ryerson et al., 2012; Payne and Driskell, 2015a). Deep water column studies tracked the plume in multiple directions (e.g., Spier et al. 2013), but mostly toward the southwest where oil droplets were still recognized ~96 miles (155 km) from the well while dissolved chemicals persisted much further; ~166 miles (267 km; Payne and Driskell, 2015a).

Multiple studies have shown that some of the oil that had reached the sea surface and some of the oil within the deep-sea plume was ultimately deposited on the seafloor. Some surface oil sank within aggregates of bacteria-mediated, mucus-rich marine snow that had proliferated in the near surface waters during the spill (Passow et al. 2012; Passow 2014; Fu et al. 2014). Direct evidence for this "marine oil snow" phenomenon was found through the study of sediment trap samples that showed a large flux of Macondo oily particles during the active spill, but not before or after the spill (Stout and German, 2015). Sinking marine snow particles formed at the surface that descended through areas where the deep-sea plume existed also likely "scavenged" deep-sea plume oil and carried it to the seafloor. In addition, bacteria-mediated marine snow also formed within the deep-sea plume itself as indigenous bacteria proliferated while consuming dissolved gas and oil (Hazen et al. 2010; Valentine et al., 2010) and formed "marine oil snow" at depth that sunk to the seafloor (Baelum et al., 2012).

The sinking of marine oil snow from the sea surface and deep-sea plume to the seafloor led to the widespread accumulation of oily "floc" on the seafloor, a phenomenon that has been referred to as "*marine oil snow sedimentation and flocculent accumulation*" or MOSSFA (Kinner et al. 2014), the so-called "dirty blizzard" (Schrope, 2013).

Evidence for the MOSSFA phenomenon and the widespread occurrence of seafloor floc containing Macondo oil was obtained from numerous studies of sediment chemistry

(Valentine et al., 2014, Hastings et al., 2015; Chanton et al., 2015; Brooks et al., 2015; Schwing et al., 2015), deep-sea corals (White et al., 2012; Hsing et al., 2013; Fisher et al., 2014a, 2014b; Brooks et al., 2015), sediment microbial communities (Kimes et al., 2013) and benthic infauna (Montagna et al., 2013). The collective results of these studies provide various means to assess the spatial extent, or "footprint", of the sunken Macondo oil (and floc) on the seafloor, although most of these studies were based upon observations made at only a few locations.

The natural resource damage assessment (NRDA), however, included the chemical analysis of 729 sediment cores collected in late 2010 and 2011 and an additional 201 sediment cores collected in 2014, four years after the spill. All of the 2010-2011 and 2014 cores were carefully collected in order to retain any surface floc (Payne and Driskell, 2015b) and subsequently split and analyzed at high resolution intervals (e.g., 0-1 cm, 1-3 cm, 3-5 cm, and 5-10 cm). In addition, 222 "pure" seafloor floc samples, collected using a specifically-designed ROV-mounted "slurp gun" (Payne and Driskell, 2015b) and 442 core supernatants, were also collected. All of the sediment intervals, slurp gun, and supernatant samples were analyzed to determine the concentrations and distributions of a large number of oil-derived chemicals in each. Collectively, these data provided a "chemical fingerprint" of any oil present.

In this study, the chemical fingerprints of any oil present in the sediments (and seafloor floc) and the spatial and depth trends in the chemical concentrations of oil-derived hydrocarbons in sediments were collectively used to establish the extent of "fingerprintable" Macondo oil deposited on the seafloor in 2010-2011, and then, what oil was still present in 2014. The oil's presence and character was important in assessing the exposure of seafloor and the deep-sea (benthic) resources.

Establishing the presence of the *Macondo oil* was important because deep-sea sediments in the study area undoubtedly contained some low(er) concentrations of pervasive ambient (background) hydrocarbons before the *Deepwater Horizon* oil spill (Cole et al., 2001; CSA, 2009; Wade et al., 2008; Rowe and Kennicutt, 2009) as well as high(er) concentration of localized hydrocarbons associated with natural oil seeps in the Mississippi Canyon region (e.g., BOEM, 2013; Sassen et al., 1993; 2006; Garcia et al., 2015; Crooke et al. 2015). This study also presents the degree to which Macondo oil was weathered when it was originally deposited (based on the 2010-2011 data), and then further weathered over the next few years (2014).

The results herein show that the highest concentration and thickest deposits of oil (and synthetic based drilling mud) occurred within 1 mile of the well. However, Macondo oil was also found up to 19 miles southwest of the well (less in other direction) and in a pattern consistent with the deep-sea plume's varying directions and depth. Surface (0-1 cm) concentrations of the oil tended to decrease with increasing distance from the well further supporting the conceptual model that most seafloor oil found away from the well was derived from oil entrained in the deep-sea plume. The chemical fingerprint of the oil transported within the deep-sea plume was changed due to severe weathering, but was recognizable and distinguishable from pervasive background hydrocarbons and localized impacts of oil from the area's natural oil seeps.

Samples

Sediments

Table 1 lists the 15 surveys/cruises and provides an inventory of the samples considered in this study. A complete list of all individual samples is provided in Attachment 1. Inspection of Table 1 reveals that a total of 2782 sediment samples were collected in

2010/2011 and an additional 805 sediment samples were collected in 2014. These samples were derived from 729 cores and 201 cores, respectively.

All of the sediment samples were collected in high-resolution cores in which between two and seven individual depth intervals were obtained for study. Cores considered to be high-resolution were those in which surface sediments were collected in 0 to 0.5, 0 to 1, 0 to 1.5, or 0 to 2 cm intervals. (Five of the 729 high resolution cores from 2010/2011 did not retain a surface interval but did have sufficiently high resolution deeper intervals, which were considered herein.) Cores (47) collected with low resolution surface intervals (0 to 3, 0 to 5, or 0 to 10 cm) were originally evaluated but were excluded in this study due to a general inability to recognize a surface impact (see next section).

Figure 1 shows the locations of all cores collected in 2010/2011 (Fig. 1A), including both high (729) and the low (47) resolution cores in 2010/2011. The location of all 201 cores from 2014, all of which were high resolution, are shown in Figure 1B.

Exclusion of Response and Early NRDA Sediment Cores: The deep-sea sediment cores collected as part of the response effort (OSAT-1, 2010) were evaluated but were also excluded from the synthesis of results presented herein. Response cores collected within about 2 miles of the wellhead indeed showed the presence of Macondo oil (and synthetic based mud), a conclusion also reached by OSAT-1 (2010). However, cores collected beyond this distance were equivocal with respect to the presence of Macondo oil. This result was attributed to (1) the difficulty of collecting any oily floc that may have been present and (2) the relatively low resolution of the cores, wherein the 0-3 cm intervals were homogenized and analyzed, potentially diluting any oily floc in the uppermost core (0-1 cm). Both of these shortcomings were explicable for at the time these cores were collected, the pervasive existence of the oily floc on the seafloor was not yet recognized.

Also excluded from this study are sediments from 47 low resolution cores collected early in the NRDA assessment during the cruises by the *Nancy Foster*, *Cape Hatteras,* and *Ron Brown* in 2010 (Fig. 1A). These cores were excluded as they were too low resolution (0-5 and 0-10 cm) to unequivocally recognize the impact of the Macondo oil to the surface sediment (0-1 or 0-2 cm) due to the diluting effect of analyzing 0-5 or 0-10 cm intervals. Five (atypical) low resolution cores from two *Hos Davis* cruises were also excluded from the same reason (Table 1). As the need for high resolution cores was realized, sediment cores from subsequent NRDA cruises were collected (1) with caution to preserve and collect any floc layer (see Payne and Driskell, 2015b) and (2) were analyzed at higher resolution, which allowed better recognition of any impact of Macondo oil to sediments (Table 1).

Core Supernatant Samples

On five of the NRDA cruises, the nepheloid layer (i.e., suspended particles in water found above the sediment core top) was poured off, collected, and analyzed as a water sample (Table 1). These samples are referred to herein as *supernatant* samples. There were 442 such samples collected, analyzed and considered herein (Table 1).

The absolute concentrations of hydrocarbons in the supernatants were not useful as these varied depending upon the amount of suspended particles present in the supernatant. However, the fingerprints of these samples were useful as they revealed the character of any particulates, i.e., "floc", floating above the sediment. The

fingerprints of the supernatant samples were considered as one line of evidence in classifying the specific nature of the surface (0-1 cm) sediments (see below).

Slurp Gun Filter Samples

On four of the NRDA cruises (Table 1) an attempt was made to collect surface floc directly from the seafloor surface using a vacuum operated "slurp gun" (Payne and Driskell, 2015b). This novel ROV-mounted device used suction to draw any surface floc and collect the floc on a filter(s) using an *in situ* filtration system. These samples were collected very proximal to areas where sediment cores were subsequently collected, i.e., in an effort to obtain completely undisturbed seafloor floc.

A total of 222 slurp gun filter samples were collected and analyzed as "solid" samples (Table 1). As was the case with the supernatant samples described above, the absolute concentrations of hydrocarbons in the slurp gun filter samples were dependent upon the amount of suspended oily floc particles collected on the filter(s). Therefore, the utility of the slurp gun filter samples was to assess the chemical fingerprints of, not the concentration of oil in, particles "slurped" off the seafloor. As with the supernatants, the chemical fingerprints of the slurp gun filters were considered as one line of evidence in classifying the specific nature of the surface (0-1 cm) sediments in the proximal cores (see below).

Methods

Analytical Methods

All of the samples were analyzed by Alpha Analytical (Alpha; Mansfield, Massachusetts) for detailed hydrocarbon composition in accordance with the Analytical Quality Assurance Plan (QAP; NOAA 2014) that included:

(1) *TPH and Selected Alkane Quantification and Fingerprinting*: a modified EPA Method 8015B was used to determine the total petroleum hydrocarbons (TPH) concentration (C_9-C_{44}) and concentrations of individual *n*-alkanes (C_9-C_{40}) and (C_{15}-C_{20}) acyclic isoprenoids (e.g., pristane and phytane), and simultaneously provide a high resolution gas chromatography-flame ionization detection (GC/FID) fingerprint of the samples. The concentrations of target compounds in sediments presented herein are reported in mg/kg_{dry} and are not surrogate corrected.

(2) *PAH, Alkylated PAH and Petroleum Biomarkers:* Semi-volatile compounds in each sample were analyzed using GC/MS via a modified EPA Method 8270. This analysis determined the concentrations of (1) 51 PAHs and alkylated PAHs including sulfur-containing aromatics and (2) 54 petroleum biomarkers (specifically, tricyclic and pentacyclic triterpanes, regular and rearranged steranes, and triaromatic steroids).

The sum of the 50 PAH, alkylated PAHs and sulfur-containing aromatics is referred to as $TPAH_{50}$ throughout this report. The concentrations of target compounds in sediments presented herein are reported in $\mu g/kg_{dry}$ and are not surrogate corrected.

An inventory of the analytes and their abbreviation used in figures throughout this report is given in Table 2.

All concentration data collected on these samples were reported through NOAA DIVER as surrogate corrected. As noted above, the concentrations discussed herein are non-surrogate corrected.

Degree of Weathering Quantification

The degree of weathering of the Macondo oil found was quantified based upon mass losses relative to the conservative internal marker within the oil, *viz.*, 17α(H),21β(H)-hopane (referred to hereafter as "hopane"), which has proven resistant to biodegradation (Prince et al. 1994). This approach was used to estimate the percent depletion of total PAHs ($TPAH_{50}$) and individual PAH analytes using the following formula:

$$\%\text{Depletion of A} = [((A_0/H_0) - (A_s/H_s))/(A_0/H_0)] \times 100 \qquad \textit{Eq. (1)}$$

Where A_s and H_s are the concentrations of $TPAH_{50}$, PAH analyte, and hopane in the sediment sample ($\mu g/kg_{dry}$), respectively, and A_0 and H_0 are the concentrations of $TPAH_{50}$, PAH analyte, and hopane in the average, fresh Macondo source oil ($\mu g/g_{oil}$; from Stout, 2015c). Although hopane can be degraded under some circumstances, if it (H_S) were in a given sample, any % depletions calculated would be underestimated.

As is common practice, and in order to eliminate the effects of varying surrogate recoveries on the %depletion calculations, non-surrogate corrected concentrations are used in all calculations.

Forensic Method

Determining the presence or absence of Macondo oil in deep-sea sediments is not simply a matter of conventional chemical fingerprinting, e.g., comparing the fingerprint of Macondo oil to the fingerprint of a sediment sample to see if they "match". Even when such comparisons are appropriate (e.g., oily matrices), the degree to which samples "match" must carefully consider the effects of weathering, mixing, and analytical precision (Stout, 2015a).

In the case of deep-sea sediments, chemical fingerprinting is complicated by the effects of mixing of any spilled oil deposited into sediments already containing ambient (background) hydrocarbons (e.g., Cole et al. 2001) and the effects of weathering, particularly biodegradation (e.g., Wenger and Isaksen, 2002; Dembicki, 2010). As will be shown below, weathering of the Macondo oil that remained within the deep-sea was rapid and intense and its chemical fingerprint was quickly and progressively changed. Thus, direct comparisons of the chemical fingerprint of the source (Macondo) oil to any oil residues in deep-sea sediments required an understanding of these effects. In the case of the *Deepwater Horizon* oil spill, the potential contributions of hydrocarbons associated with natural oil seeps (not just ambient background) warranted additional consideration. It is for these reasons that no "standard protocol" exists for oil spill fingerprinting in sediments, and certainly not for the particular (extreme) circumstances of the *Deepwater Horizon* oil spill.

Therefore, in this study a weight-of-evidence forensic method was developed and employed that included: (1) chemical fingerprinting, (2) chemical concentrations, considering a core's proximity to the Macondo well or to known or apparent natural oil

seeps, and vertically within a core's depth profile, and (3) consideration of results for proximal cores, supernatants, and slurp gun filters. Synthesis of all three of these components was used to collectively arrive at a *forensic* conclusion regarding the presence or absence of Macondo oil in all deep-sea sediment samples collected in 2010/2011 and 2014. The conclusions were given as one of five forensic classes, "A" through "E", as defined in Table 3. Importantly, all three components of this weight-of-evidence approach benefited from the knowledge gained after (nearly) the entire dataset was evaluated – when the conceptual model for oil's deposition throughout the deep-sea became clear (see below). Descriptions of these three components are given in the following sections.

Chemical Fingerprinting: Closer to the well, direct deposition of relatively high concentrations of minimally-weathered Macondo oil and synthetic based drilling mud (SBM) were easily recognized by their distinctive chemical fingerprints (see below). However further from the well, the chemical fingerprinting component necessarily considered the significant changes in Macondo oil due to weathering that became evident as the dataset grew and these changes were repeatedly observed and understood.

Details of these changes are given later in this report, but generally the chemical fingerprint of the Macondo oil found in seafloor sediments changed with increasing distance from the well. This indicated that the oil's advective transport within the deep-sea plume significantly affected its composition (fingerprint) – even affecting some compounds not typically thought to be particularly susceptible to weathering (e.g., selected biomarkers; see below).

The severity of weathering observed is attributed to the combined effects of dissolution and biodegradation, i.e., processes which were "super-activated" within the (chemically and naturally) dispersed oil droplets within the deep-sea plume. These severe weathering effects were also evident in water samples from the deep plume that contained dissolved and/or particulate oil (Payne and Driskell, 2015a,c). This super-activity was likely promoted by the small droplet size of the oil within the deep-sea plume, which having a large surface area to mass ratio, allowed for accelerated dissolution and biodegradation. Once these effects were recognized, they were then used to distinguish Macondo oil from low concentrations of background (ambient) hydrocarbons and, in some cases, seeped oil many miles from the well (see below).

The chemical fingerprinting component relied upon the overall character of the total petroleum hydrocarbons (TPH) extracted from the samples (as expressed by the GC/FID chromatograms). In addition, the hopane-normalized distributions of PAHs and related sulfur-containing aromatics and petroleum biomarkers were also used to assess whether differences were consistent with weathering or mixing, or if a different (non-Macondo seep) oil was present. Finally, diagnostic ratios (DRs) among selected PAH and petroleum biomarkers were compared (Table 4), although owing to the aforementioned difficulties surrounding weathering, mixing, and analytical precision in sediments, these comparisons were not made using any statistical criteria (e.g., 95% reproducibility limit, such as was appropriate for oily matrices; Stout, 2015b). The DRs were considered only qualitatively, e.g., sometimes showing depth trends within cores that became increasingly "Macondo-like" at the surface.

Chemical Concentration Trends: The concentration of hydrocarbons in sediments was considered in three ways in reaching a forensic conclusion, *viz.*, distance from the Macondo well, proximity to known or apparent seeps, and depth (vertical) profiles within each core.

The concentrations of Macondo oil deposited near the well were expectedly higher due to the direct fallout, often in conjunction with SBM (as had been recognized by OSAT-1, 2010). However, the main mechanism by which oil that had remained within the deep-sea was transported away from the well was within the deep-sea plume that formed between ~1000 and 1300m. Although multiple factors (e.g., bathymetry, plume oscillation, hydrodynamic processes, marine snow abundance) undoubtedly affected the frequency at which oil droplets were transported out of the plume to the seafloor, synthesis of the 2010/2011 sediment dataset eventually revealed that the concentrations of Macondo oil showed an overall decrease with increasing distance from the well (see below; Stout et al., 2015; Valentine et al. 2014). This overall decrease in concentration of Macondo oil in surface sediments was thereby a factor in assessing the forensic character of each core's surface sediment – specifically in a conservative manner. For example, if the concentration of oil was anomalously high given its distance from the well the potential presence of hydrocarbons derived from a natural seep were carefully considered using the other lines of evidence. A core's proximity to a known or apparent seep(s) was assessed through a combination of chemical fingerprinting of the core itself and nearby cores and proximity to Bureau of Ocean Energy Management (BOEM 2013) seismic amplitude anomalies representing active and formerly active seep areas. Proximity to former drill sites obtained from BOEM (2013) was also considered.

The mechanism(s) by which Macondo oil was deposited on the seafloor was, geologically-speaking, a discrete, short-term event. Near the well, the accumulation of impacted sediments could be many centimeters thick (see below). However, outside this immediate fallout zone (>~1 mile) the oil was deposited in a layer of oily floc at the seafloor surface. Thus, the hydrocarbon concentrations within the *carefully* collected high resolution cores (Payne and Driskell, 2015b) containing Macondo oil typically exhibited elevated hydrocarbons concentrations within the surface intervals (variously 0-1, 0-0.5, 0-1.5, and 0-2 cm). Below the surface sediment, much lower concentrations of background hydrocarbons were pervasively present in underlying intervals (see below).

Cores taken within or proximal to known or apparent seep locations exhibited variable hydrocarbon concentration profiles. Many such cores exhibited higher hydrocarbon concentrations at depth (>2 cm) or more uniformly from "top-to-bottom" (0-10 cm). Such profiles, after considering other components, were generally easily recognized as being impacted by seeped oil (not Macondo). Some apparent seep-impacted cores, however, also exhibited higher hydrocarbon concentrations only at the surface, in which case additional lines of evidence (absolute concentrations, chemical fingerprint, proximity to other cores/seeps) were necessary to distinguish the impact of seeped oil *versus* Macondo oil. If uncertainty remained, equivocal cores were conservatively attributed to apparent seeps rather than Macondo oil.

Consideration of Nearby Samples: Many cores were collected using a multi-corer tool in which multiple (2 to 4) sediment cores were collected within a few meters of one another at a given location. The forensic assessment of these "co-located" cores often benefited from an assessment of the features evident in one core to aid in the assessment of a proximal core. The heterogeneity sometimes evident among co-

located cores testified to the fact that Macondo oil (oily floc) was not uniformly deposited as a "blanket" but rather as particles of oily floc that were heterogeneously distributed upon their deposition, or perhaps were remobilized and accumulated in certain "pockets" on the seafloor. Similarly, heterogeneity sometimes evident among co-located cores in a known or apparent seep area often varied indicating natural seeps did not necessarily pervasively impact the seafloor in a given area; rather, only localized areas or depth intervals attributed to migration of seep oil along preferred pathways were impacted. Regardless, in some co-located cores the features of one core could be beneficial in assessing more equivocal features in a nearby core.

In addition, some of the cores collected on some NRDA cruises also had supernatants and slurp gun filters to aid in the forensic assessment of the core's sediment (Table 1). The chemical fingerprinting character of the supernatant and slurp gun filters, both of which could contain a predominance of oily floc particles (if present), were sometimes more clearly impacted with Macondo oil than the associated core's surface sediment, and thereby aid in the forensic assessment of the sediment.

Results and Discussion

Conceptual Model for Seafloor Deposition of Macondo Oil

The presentation of the 2010/2011 sediment results (below) is best achieved after describing the conceptual model that was revealed based upon the relationship between chemical fingerprints, concentrations, and the location of seafloor samples containing Macondo oil (and seeped oil). This is practical since the character of Macondo oil, and thereby the basis for recognizing its presence in deep-sea sediments varied depending upon where the sample was collected.

Figure 2 illustrates the conceptual model depicting the general processes by which Macondo oil was deposited on the deep-seafloor. As described briefly above (and in more detail below), sediments collected within about ~1 mile of the wellhead exhibit chemical characteristics that were readily recognized as Macondo oil or SBM associated with direct fallout from the Macondo well. However, beyond ~1 mile from the wellhead the surface sediments commonly contained a wax-rich, severely weathered Macondo oil with distinctive chemical fingerprints. Nonetheless, this wax-rich, severely weathered oil could still be recognized as Macondo oil for multiple reasons, including (1) the degree of weathering of the oil tends to increase with increasing distance from the well, (2) the concentration of the oil in surface sediment intervals is highest closer to the wellhead and generally decreases away from the well, (3) the concentration of severely weathered oil is many times higher in the surface sediment intervals (0-1 and 1-3 cm) near the well than in the deeper sediment intervals, and (4) near the wellhead the severely weathered oil sometimes co-occurs at comparably high concentrations with less weathered Macondo oil (and with SBM), sometimes even appearing "sandwiched" between or above sediment layers containing fresher Macondo oil.

These facts indicate that the wax-rich, severely weathered oil found on the seafloor surface away from the well (> 1 mile) was formed by severe and rapid weathering (dissolution and biodegradation) of the Macondo oil as it moved within the deep-sea. These processes were apparently "super-activated" within the (chemically and naturally) dispersed oil droplets within the deep-sea plume and proliferation of bacteria. As noted above, this super-activity was likely promoted by the small droplet size of the oil within

the deep-sea plume, which having a large surface area to mass ratio, allowed for accelerated dissolution and biodegradation (Payne and Driskell, 2015a,c). Notably, Prince et al. (2013) demonstrated the severity to which chemically-dispersed crude oil could be biodegraded at low concentrations in seawater in the laboratory.

Oil particles within the deep-sea plume eventually reached the seafloor through (1) scavenging and agglomeration with bacteria-rich, marine snow formed in the deep-sea plume (supplemented by marine snow descending from the surface) and (2) by impingement on bathymetric obstacles, including the continental slope (Fig. 2). In some instances the wax-rich, severely weathered Macondo oil settled atop sediments already impacted by crude oil from naturally-occurring seeps. The severe weathering of the Macondo oil during its transport within the deep-sea allowed it to be distinguished from naturally-seeped oil, which although sometimes severely weathered itself, had not experienced the same effects of weathering that the transported Macondo oil had. Specifically, seep oils retain many compounds that the Macondo oil had lost.

Since 2010/2011, the amount and extent Macondo oil still recognizable on the seafloor has declined through continued weathering (biodegradation), or perhaps mixing with underlying background sediments during bioturbation or resuspension/redistribution events. As such, in 2014 the concentrations of PAHs attributable to Macondo oil were an order of magnitude lower than were observed in 2010/2011.

In the following sections, the chemical fingerprint characteristics of representative sediment samples and concentration trends exemplifying and justifying the *Conceptual Model* described above (Fig. 2) are presented in detail. The results are presented in various sections in a progressive manner so that the *Conceptual Model* is logically demonstrated:

- Character of Macondo Oil within 1 Mile of the Wellhead – 2010/2011
- Weathering of Macondo Oil near the Wellhead – 2010/2011
- Character of Macondo Oil 1 to 5 Miles from the Wellhead – 2010/2011
- Wax-Rich, Severely Weathered Macondo Oil Beyond 5 Miles – 2010/2011
- Distinguishing Wax-Rich, Severely Weathered Macondo Oil from Seeps – 2010/2011
- Concentration Spatial and Depth Trends – 2010/2011
- Background PAH in the Study Area
- Summary of Forensic Classifications – 2010/2011
- Summary of Forensic Classifications – 2014

<u>Character of Macondo Oil within 1 Mile of the Wellhead – 2010/2011</u>
Forty-three (43) cores were collected within 1 mile of the wellhead. All but three of these contained surface (0-1 cm) sediments impacted with Macondo oil and varying amounts of (including no) SBM, the latter exemplified by the varying amounts of C_{15} to C_{18} olefin clusters (Fig. 3B and C; see also Stout, 2015b.) The three other cores contained Macondo oil in the 1-3 cm interval but not on the surface. In most cores the impact is restricted to the upper 3 cm of the core but in multiple locations, Macondo oil and/or SBM was present in the 5-10 cm intervals (i.e., the deepest intervals studied) indicating significant thicknesses of oil and SBM (perhaps even > 10 cm) had been deposited on the seafloor in some areas around the well.

The Macondo oil that was present in about half of the sediment cores within 1 mile of the wellhead was only slightly weathered compared to the fresh oil (Fig. 3A) and could be easily recognized by the distribution of *n*-alkanes ranging from about n-C_{10} to n-C_{40} and a broad unresolved complex mixture (UCM) hump (Fig. 3B-C). Losses among the lower molecular weight fraction of the crude oil (<~n-C_{15}) and corresponding increase in the UCM are attributable to a combination of dissolution and incipient biodegradation (as, obviously, evaporation did not affect oil in the deep-sea). Payne and Driskell (2015a) observed similar dissolution losses of n-alkanes (up to C_{12}) in water samples collected at depth that contained particulate oil droplets. Minor losses of lower molecular weight PAHs were also evident. This slightly weathered Macondo oil within ~1 mile of the well and often in association with SBM (e.g., Fig. 3B-C) is believed to represent oil that was quickly deposited on the seafloor due to direct fallout (likely aided by its association with SBM) after exiting the wellhead (Fig. 2).

Twenty-three (23) of the cores within ~1 mile of the wellhead contained Macondo oil that exhibited an increasingly weathered character lead to a distinctive "wax-rich, severe weathering of Macondo oil". Recognizing the progressive changes in the chemical fingerprints from slightly weathered oil (Fig. 3B-C) to the wax-rich, severely weathered oil (as described in the *Conceptual Model* above and exemplified below) was critical in recognizing the impact of Macondo oil on deep-sea sediments outside of the immediate (~1 mile radius) area around the well. This was because the wax-rich, severely weathered oil was the overwhelming form of Macondo oil that was found beyond ~1 mile from the well (Fig. 2; and results below). The chemical fingerprinting changes due to this progression in weathering are described in the next section.

Weathering of Macondo Oil near the Wellhead – 2010/2011

The range in weathering of the Macondo oil found in sediments near the well in 2010-2011 is demonstrated by the four surface sediment samples' chemical fingerprints shown in Figures 4 to 6. These four samples are not unique as many other surface sediments within 1 to 2 miles of the wellhead exhibit comparable or intermediate features to those shown here. These four samples, however, exemplify the progression in weathering ultimately leading to the "wax-rich, severely biodegraded oil" that was present within the oily floc deposited throughout the deep-sea (after having been transported laterally and increasingly weathered within the deep-sea plume; Fig. 2).

A combination of dissolution and biodegradation while in the water column (with the latter perhaps continuing in sediment) is likely responsible for the formation of the wax-rich, severely weathered oil. The basis for concluding that much of the weathering occurred within the water column as part of the deep-sea plume is that there is an overall increase in weathering with distance from the well (see next section). In addition, analysis of water samples from the deep-sea revealed the severe effects of dissolution that was attributed, at least in part, to the effects of dispersant injection at the wellhead (Payne and Driskell, 2015a,c). In addition, beyond 1 mile from the well there is remarkable consistency in the fingerprint of the wax-rich, severely weathered oil. If weathering occurred predominantly in sediment a greater degree of heterogeneity would be anticipated. Since this was not observed, it is more likely that most weathering (observed in 2010/2011) occurred within the water column. (Of course, additional weathering observed in 2014 must have occurred while the oil was in the sediment; see below.)

The severely weathered Macondo oil's wax-rich appearance is based on the progressive loss of shorter-chain n-alkanes (Fig. 4A-C), ultimately producing an oil containing an abundance of longer-chain n-alkanes spanning from ~n-C_{25} to n-C_{44} with a maximum ~ n-C_{33} (Fig. 4D). These longer-chain n-alkanes compounds are being preferentially *preserved* as the oil weathers, they are not being formed or absolutely enriched to the weathered oil (e.g., by some sort of wax-precipitation mechanism; see Fig. 7 described below). The preferential loss of n-alkanes below ~n-C_{30} is reasonably attributable to intense biodegradation, which can preserve longer chain n-alkanes as shorter chain n-alkanes are preferentially degraded (Prince, 2002). However, under the circumstances of this particular spill, some loss of shorter-chain n-alkanes might also be attributed to dissolution (Fu et al., 2015), despite these compounds limited (but extant) solubility. As noted above, Payne and Driskell (2015a) observed similar dissolution losses of n-alkanes (up to C_{12}) and lower molecular weight PAH in particulate (filtered) oil droplets sampled from the water column at depth. As noted above, both processes were likely to have been "super-activated" within the very small (chemically and physically) dispersed oil droplets (with high surface area to volume ratios) that existed within the deep-sea plume (Prince et al., 2013). It is also important to note that the wax-rich, severely weathered Macondo oil (e.g., Fig. 4D) was already present in surface sediments collected in June 2010. This indicates that the rate at which weathering affected the oil in the deep-sea was remarkably fast, perhaps another reason that the loss of these compounds likely occurred within the water column.

Accompanying the loss of n-alkanes was the progressive loss of isoprenoids (e.g., pristane and phytane) and the bulk of unresolved and resolved compounds within the C_{10} to C_{25} range, commonly referred to as diesel range organics (DRO; Fig. 4). This loss in DRO can be seen in the reduction in the size of the unresolved complex mixture (UCM) in the DRO range – and corresponding retention of the compounds within the residual range oil (RRO; C_{25}+; Fig. 4). The progressive loss in DRO compounds is also reasonably attributed to the combined effects of dissolution and biodegradation of the Macondo oil, which would be predicted to remove these lower molecular weight DRO compounds in preference to the higher molecular RRO compounds. Prince et al. (2013) observed a comparable reduction in DRO range hydrocarbons due to biodegradation in laboratory experiments of chemically-dispersed oil.

The preferential loss of lower molecular weight compounds in the TPH (Fig. 4) is clearly evident upon inspection of the PAHs for these four representative surface sediment samples (Fig. 5). The PAH histograms also show a progressive loss of increasingly heavier PAHs during weathering of the Macondo oil near the well, which is also attributable to a combination of dissolution and biodegradation. It is particularly notable that the wax-rich, severely weathered oil had commonly lost all of the decalins and benzothiophenes, and nearly all of its lower molecular weight PAHs (naphthalenes, fluorenes, phenanthrenes, and dibenzothiophenes; e.g. Fig. 5D). Similar abiotic dissolution losses of these PAH were noted in water samples containing oil droplets captured at depth in close proximity to the wellhead, where the losses were attributed to *in situ* effects of dispersants (Payne and Driskell, 2015c). This feature is also one to note because it contrasts with most seep oils, which did not experience the same degree of dissolution/biodegradation (having not been transported as small droplets within the water column; see below.)

The remaining higher molecular weight PAHs (fluoranthenes/pyrenes, naphthobenzothiophenes, benz(a)anthracenes/chrysenes) in the wax-rich, severely

weathered Macondo oil are also significantly reduced from the fresh Macondo oil (despite these PAHs' low aqueous solubilities). (Discussion of the measured percent depletion of individual PAHs and $TPAH_{50}$ relative to hopane is discussed later in this report.) Thus, severe weathering of Macondo oil in the deep-sea progressively removed nearly all of the lower molecular weight compounds and a significant portion of the higher molecular weight PAHs that were originally present in the Macondo oil (Fig. 5). Analysis of water samples collected from the deep-sea plume confirmed that at least some of these "lost" compounds were present within the dissolved phase of the deep-sea water column (Payne and Driskell, 2015a).

Further inspection of Figure 5 reveals that each of the PAH homologue groups were progressively skewed toward the more highly alkylated homologues, e.g., C_3- and C_4-benz[a]anthracenes/chrysenes (BC3 and BC4) ultimately becoming the most abundant PAHs present in the wax-rich, severely weathered oil (Fig. 5D). This pattern is not unexpected as both solubility and susceptibility to biodegradation decreases with increasing degree of alkylation (Elmendorf et al., 1994). Payne and Driskell (2015c) observed a comparable PAH pattern in which some water samples containing particulate oil showed losses of the parent- and C1 through C3 alkylated PAH homologues at least through the dibenzothiophenes, with a benz[a]anthracene/chrysene homologue pattern dominated by the C_3- and C_4 alkylated homologues. Because n-alkanes were preserved this change in the PAH distribution was attributed to the effects of dispersant injection at depth that accelerated the abiotic dissolution. Prince et al. (2013), however, observed the same depletion of 2- and 3-ring PAHs and relative enrichment of the more highly alkylated benz[a]anthracene/chrysene homologues in laboratory biodegradation experiments of chemically-dispersed crude oil. Thus, the combined effects of dissolution and biodegradation were likely working together to produce the observed PAH pattern in the wax-rich, severely weathered Macondo oil.

The petroleum biomarkers in the Macondo oil also exhibited some progressive changes upon weathering as exemplified in Figure 6. These changes were very important to recognize since biomarkers are sometimes considered *recalcitrant* to weathering, not simply *resistant*. Biomarker degradation under different environmental conditions is extremely complex and can be difficult to predict *a priori*. Therefore, only after recognizing/documenting the progressive changes in the Macondo oil biomarkers (among samples found close to the wellhead) could the altered biomarker fingerprint of the wax-rich, severely weathered Macondo oil found further from the well be confidently attributed to Macondo oil.

The data indicate that the distributions of triterpane biomarkers remained fairly consistent during weathering of the Macondo oil in the deep-sea in 2010/2011. There is some evidence that degradation of 17α(H),21β(H)-homohopane homologues (T33-T35; Fig. 6) was sometimes evident (Fig. 6D), as was also observed in some Macondo oil that had reached the surface (Aeppli et al., 2014). Also, at lower Macondo oil concentrations the contribution (interference) of naturally-occurring triterpenoids derived from recent organic matter (e.g., algal or microbial biomass) that occurs as "modern" background throughout the deep-sea sediments (Simoneit, 1986; Hood et al. 2002; Dembicki, 2010) are often recognized to artificially increase the relative abundance of T20, T26, and T30 (e.g., Fig. 6C-D). The largest of these occurs at T20 (moretane; Fig. 6) and is likely due to the co-elution of 17β(H),21β(H)-30-norhopane, a naturally-occurring triterpane, which can be prominent in recent marine sediments (Kennicutt and Comet, 1992). Thus,

interferences among several triterpane biomarkers were important to recognize in Macondo oil deposited further from the wellhead.

Steranes, on the other hand, exhibited multiple changes due to weathering (*viz.*, biodegradation). The most notable of which was a marked reduction in the relative abundances of 13β(H),17α(H)-diacholestane epimers (S4 and S5) and 14β(H),17β(H)-cholestane epimers (S14 and S15; Fig. 6). A reduction is also evident in the S12/S13 and S17/S18 (Fig. 6), peaks that include co-eluting epimers of 14α(H),17β(H)-cholestane and 13β(H),17α(H)-diaethylcholestane epimers (Table 2). The preferential biodegradation of 13β(H),17α(H)-diacholestanes and 14β(H),17β(H)-cholestanes was previously observed in spilled oil, although over much longer time scales (Wang et al. 2001; Prince et al., 2002) and *in vitro* (Diez et al. 2005). As was the case for other hydrocarbons (see above), the rapid biodegradation of these steranes in the Macondo oil over a short period of time is likely due to the finely dispersed nature of the oil droplets in the deep-sea plume, which promoted their biodegradation. Notably, a comparable loss of 13β(H),17α(H)-diacholestanes and 14β(H),17β(H)-cholestanes was also reported by White et al. (2012) in floc on deep-sea coral samples collected from northeast Biloxi Dome in later 2010. These researchers hypothesized this was due to biodegradation, a hypothesis that is confirmed herein after observing sterane biodegradation in samples close to the Macondo well (Fig. 6). Similarly, sediment trap particulates collected from the deep-sea just east of Biloxi Dome in the months following the *Deepwater Horizon* oil spill also exhibited sterane biodegradation, which further indicates sterane biodegradation likely occurred in oil particles while still within the water column (Stout and Passow, 2015).

Finally, the wax-rich, severely weathered oil near the well showed evidence for some reduction in the amount of triaromatic steroids (TAS) compared to fresh Macondo oil (Fig. 6D). This incipient loss of TAS in oil near the wellhead is notable because (as will be shown below), the loss of TAS generally increased in wax-rich, severely weathered Macondo oil found in sediments further from the well. TAS are markedly reduced in Macondo oil that reached the surface due primarily to photo-oxidation (Aeppli et al. 2014; Stout, 2015d). Obviously however, photo-oxidation could not have affected the TAS in oil that remained in the deep-sea. Thus, the reduction of TAS in Macondo oil found in deep-sea sediments must be due to dissolution or biodegradation. TAS are conventionally thought to be resistant to biodegradation, and therefore dissolution of these aromatic biomarkers (despite their limited solubility; ~ 1 to 5 x 10^{-6} mg/L; Aeppli et al. 2014) most likely caused the slight decrease observed (Fig. 6D). The loss of TAS from deep-sea Macondo oil is notable since natural seep oils, having not been transported through water generally do not exhibit TAS loss (see below).

Character of Macondo Oil 1 to 5 Miles from the Wellhead – 2010/2011

Eighty-eight (88) cores were collected between 1 and 3 miles from the wellhead and 48 cores were collected between 3 and 5 miles from the wellhead in 2010/2011. Many of the surface sediments from the cores between 1 and 5 miles exhibited relatively high concentrations of the wax-rich, severely weathered Macondo oil consistent with what was observed nearer the wellhead (resembling Fig. 4D, 5D, and 6D). However, some additional weathering is evident in these sediments, which further aids in recognizing Macondo oil's presence in sediments beyond 5 miles from the wellhead. Excluded from this assessment are 47 cores between 3 and 5 miles from the wellhead that were collected from locations along the margins of Mitchell, Gloria, and Biloxi Domes (Fig.

1A). These 47 cores are not described in this section due to the potential influence of seeps on the sediment fingerprints in these areas; see below.

Before discussing this additional weathering of the wax-rich, severely weathered Macondo oil, it should be noted that a few sediment cores from this area contained other evidence of impact by the *Deepwater Horizon* disaster. First, chemical fingerprinting revealed a few cores between 1 and 1.5 miles southwest of the wellhead contained SBM at their surface indicating it had been transported beyond 1 mile from the well in a southwesterly direction (see Stout, 2015b). Second, weathered diesel fuel was present in near surface sediments (0-1 and 1-3 cm) at one location approximately 1.8 miles north of the wellhead.[1] The origin of this diesel fuel is uncertain although it is presumed to be associated with fuel released from the sunken *Deepwater Horizon* drill rig. Third, less weathered Macondo oil occurred in three cores ~2 miles north of the wellhead[2] that were attributed to sunken *in situ* burn residues (Stout and Payne, 2015).

However, as noted above, many of the cores between 1 to 3 miles (n=26) and 3 to 5 miles (n=20) from the wellhead (and not located along salt dome margins) exhibited relatively high concentrations of the wax-rich, severely weathered oil at the surface consistent with what was observed nearer the wellhead (resembling Fig. 4D, 5D, and 6D). Samples from these locations were given forensic classifications of "A" or "B", often depending upon concentration (Table 3). Other cores contained lower concentrations of oil at their surface, but with more equivocal fingerprints (forensic class "C") or did not appear to be impacted by any Macondo oil (forensic class "D"; Table 3).

The knowledge gained from understanding the progression in weathering observed closer to the well (Figs. 4-6) assured that the observed wax-rich, severely weathered oil found in sediments 1 to 5 miles from the well (excluding any seep areas) was undoubtedly derived from Macondo oil. Establishing this, in turn, further aided in developing the *Conceptual Model* described above (Fig. 2). The results also revealed that the degree of weathering of the wax-rich, severely weathered oil generally increased from what was observed closer to the well. This observation also contributed to the *Conceptual Model* described above, *viz.*, weathering (dissolution and biodegradation) progressed during the Macondo oil's transport within the deep-sea plume (Fig. 2) and perhaps after deposition on the seafloor.

To demonstrate this progression in weathering, the average chemical fingerprints of the wax-rich, severely weathered oil in surface sediments collected between 1 to 3 miles (n=26) and 3 to 5 miles (n=20) were determined and compared to each other and to wax-rich oil observed less than 1 mile from the well. Figures 7, 8, and 10 show the hopane-normalized average distributions of n-alkanes, PAHs, and biomarkers in these three sample groups, respectively. Figure 9 provides the percent depletion results (*Eq. 1*) for PAHs in these samples. These figures are described in the following paragraphs.

Figure 7 shows that most n-alkanes are indeed markedly depleted in the wax-rich, severely weathered Macondo oil. Of course, by definition, only the wax-rich samples are included here so it is expected that longer-chain n-alkanes (>n-C_{25}) are preserved. It is also clear, however, that these longer-chain n-alkanes are not *enriched* relative to fresh

[1] SB9-65-B0603-S-NF011-HC-1681 and -1682.
[2] HSW6_FP10188_B0827_H_0071; HSW6_FP10188_B0827_H_0072; SB9-65-B0603-S-NF011-HC-1758.

Macondo oil, they are only *preserved*. Notably, closer to the well there is some evidence of SBM present in some samples as exhibited by the relative abundances of n-C_{16} and n-C_{18} (Fig. 7A-B), which is caused by co-elution of SBM-derived olefins with these n-alkanes).

Figure 8 shows the changes in the relative abundance and distributions of PAHs in the wax-rich, severely weathered Macondo oil with increasing distance from the well. The average absolute concentrations observed within these sediments are given in Table 5. Within 1 mile of the well the PAHs exhibit some depletions relative to fresh Macondo oil, although decalins, naphthalenes and other lower molecular weight PAHs are still clearly present (Fig. 8A). Between 1 to 3 miles and 3 to 5 miles from the well, however, decalins and low molecular weight PAHs become increasingly reduced (Fig. 8B-C). Higher molecular weight PAHs also become reduced between 0 to 1 mile and 1 to 3 miles (Fig. 8A-B), but then do not show much additional reduction beyond 3 miles (Fig. 8C). Decalins and naphthalenes, however, are (on average) virtually absent in the wax-rich, severely weathered Macondo oil beyond 3 miles from the wellhead (Fig. 8C; Table 5).

Figure 9 provides more details on the depletion of individual and total PAH ($TPAH_{50}$) evident in the wax-rich, severely weathered Macondo oil found in surface sediments within 5 miles of the well (calculated per *Eq. 1*). $TPAH_{50}$ depletions within 1 mile of the well averaged 86 ± 8% (Fig. 9A), indicating most PAHs present in the oil that remained in the deep-sea were not deposited on the seafloor, but were instead lost to the deep-sea water column via dissolution and/or biodegradation. As noted above, the depletion of decalins and lower molecular weight PAHs was greater than higher molecular weight PAHs (e.g., fluoranthene/pyrenes and benz[a]anthracenes/chrysenes; Fig. 9A).

Additional depletion of PAHs occurred beyond 1 mile from the well, wherein the $TPAH_{50}$ depletions between 1 to 3 miles increased to 94 ± 3% (Fig. 9B). Additional depletion of decalins and both lower and higher molecular weight PAHs advanced also. Between 3 to 5 miles from the well, however, there was only minor additional depletion of decalins and PAHs, leading to only a slight increase in $TPAH_{50}$ depletion to 95 ± 1% (Fig. 9C). This indicates that there was no significant additional loss of PAHs from the wax-rich, severely weathered Macondo oil beyond 3 to 5 miles from the well. This is likely due to inability of deep-sea weathering processes (dissolution and biodegradation) to further reduce the high(est) molecular weight PAHs (prior to sampling). These compounds were simply too insoluble and too resistant to biodegradation to be further depleted. This observation is notable since it indicates that the PAH character of wax-rich, severely weathered Macondo oil deposited beyond 5 miles from the well is unlikely to have been much more weathered compared to what was found 3 to 5 miles from the wellhead (Fig. 8C).

Figure 10 shows that the biomarkers present in the wax-rich, severely weathered Macondo oil deposited on the seafloor were much less affected than the n-alkanes or PAHs. As noted above, some triterpane interferences are evident due to pre-existing, naturally-occurring triterpenoids in deep-sea sediments (e.g., T20 and T26 in particular; Fig. 10). Extended homohopanes (T31 to T35) are also slightly reduced in oil deposited more than 1 mile from the wellhead owing to biodegradation (Fig. 9B-C). The marked depletion of the 13β(H),17α(H)-diacholestanes (S4 and S5), 14β(H),17β(H)-cholestanes (S14 and S15), and co-eluting 14α(H),17β(H)-cholestanes and 13β(H),17α(H)-

diaethylcholestanes (S12/S13 and S17/S18) observed in the wax-rich, severely weathered oil deposited close to the well (Fig. 6 and Fig. 10A) advanced only slightly beyond 1 mile from the well (Fig. 10B) and then remained stable 3 to 5 miles from the well (Fig. 10C). Similarly, TAS were slightly reduced between 1 and 3 miles from the well (Fig. 10B) but then remained stable between 3 to 5 miles from the well (Fig. 10C). Thus, like the PAHs, the biomarkers within the wax-rich, severely weathered Macondo oil deposited beyond 5 miles from the well are unlikely to have been much further weathered compared to what was found 3 to 5 miles from the wellhead (Fig. 10C).

Wax-Rich, Severely Weathered Macondo Oil Beyond 5 Miles – 2010/2011

The knowledge gained from the progression in chemical fingerprints evident within 5 miles of the wellhead provided the basis to assess whether sediments further than 5 miles from the wellhead (and also cores within 5 miles but along the margins of Mitchell, Gloria, or Biloxi Domes) contained Macondo oil. Thus, sediments in all 503 cores collected beyond 5 miles in 2010/2011 were compared to the average wax-rich, severely weathered Macondo oil found in sediments 3 to 5 miles from the well, as represented in Figures 7C, 8C and 10C. These oils were expected to have a GC/FID fingerprint resembling that shown in Figure 4D.

For this report, two examples of cores containing wax-rich, severely weathered Macondo oil are given in order to demonstrate the forensic method employed. The two cores selected were located about 6.1 and 11.8 miles southwest of the well and their chemical fingerprinting and concentration results are summarized in Figures 11 and 12, respectively. These cores are located in the dominant direction of the deep-sea plume (Spier et al., 2013) and, as results show, contain Macondo-derived oily floc at their surfaces. The first of these cores was collected atop Biloxi Dome and the second was located about 3.5 miles west of the northwest portion of Biloxi Dome (Block 294), where natural seeps are recognized to exist (see below). These cores were selected as they demonstrate the deposition of Macondo-derived oily floc atop of Biloxi Dome and several miles beyond Biloxi Dome. (In the next section, the character of a core from northwest Biloxi Dome that contains seep oil is presented for comparison.)

The TPH in surface sediment (0-1 cm) of both cores exhibit GC/FID chromatograms dominated by long-chain n-alkanes and a RRO range UCM without any prominent DRO range UCM (Figs. 11A and 12A). In fact, the DRO range exhibits a downward-concave profile consistent with the loss of these lower boiling DRO range compounds comparable to what was observed closer to the well (e.g., Fig. 4D). Deeper sediment intervals in each core contain TPH that exhibit some trace of wax-rich oil in the 1-3 cm intervals, but none in deeper intervals (Figs. 11A and 12A). Those sediments below 3 cm in each core are, in fact, very typical of deeper (and unimpacted) sediments found throughout the study area, which are attributed to ambient (background) hydrocarbons present in deep-sea sediments.

The concentrations of PAHs at the surface (0-1 cm) interval in both of these cores are markedly enriched over deeper horizons (Fig. 11B and 12B). The core atop Biloxi Dome contains 1299 ng/g of $TPAH_{50}$ and the core collected 3.5 miles west of Biloxi Dome contains 1521 ng/g of $TPAH_{50}$. Deeper intervals in both cores contain only low concentrations of $TPAH_{50}$ (< 269 ng/g). The distribution of PAHs in the surface of both cores is dominated by C_3- and/or C_4-benz[a]anthracenes/chrysenes (BC3 and BC4) and exhibit an overall distribution consistent with the PAHs in the wax-rich, severely weathered oil found 3 to 5 miles from the well (Figs. 8C). Decalins are absent in both

core locations, which is consistent with their removal due to weathering that occurred closer to the well (Fig. 8C). The lower concentrations of PAH in the deeper intervals in both cores are comprised of a broader range of PAH than found in the surface sediments, including an abundance of pyrogenic (non-alkylated) PAHs (e.g., phenanthrene, fluoranthene, pyrene, etc.). Notably, the biogenic PAH perylene (Per; shaded green in Fig. 11B and 12B) is also relatively abundant in the deeper sediments, further testifying to the ambient (background) hydrocarbons present in these sediments. Some mixing of Macondo oil-derived PAHs and ambient PAHs is evident in the 1-3 cm interval of both cores.

Finally, the biomarkers present in both of these cores exhibit elevated concentrations at the surface (0-1 cm), as demonstrated by the concentrations of hopane (209 and 257 ng/g, respectively; Fig. 11C and 12C). Much lower concentrations of hopane are present in the deeper (3-5 and 5-7 cm) intervals (<26 ng/g). The distributions of biomarkers in the surface sediments closely match the severely weathered Macondo oil found 3 to 5 miles from the well (Fig. 10C), including the depletion of numerous steranes (S4, S5, S14, S15) and extended homohopanes (T32+; Fig. 11C and 12C). Interferences of naturally-occurring ambient (background) triterpenoids that are prominent in deeper sediment horizons (T20, T26, and T35) are also evident. Notably, the TAS are slightly reduced in both of the core's surface sediment relative to what was observed 3 to 5 miles from the well. This additional loss of TAS is attributed to continued weathering, likely dissolution, of these aromatic biomarkers during further transport of the oil within the deep-sea plume. A relative decrease in TAS was also observed in some deep-sea water samples containing particulate oil collected within 2-8 km of the wellhead in May and June 2010 (Payne and Driskell, 2015d).

A synthesis of these cores' chemical features – in light of all other results (including distance from known or apparent seeps; see below) – justified that each core's surface (0-1 cm) interval be given a forensic classification of "A" (per Table 3). The 1-3 cm intervals in each core were given a forensic classification of "C", owing largely to the low concentration and mixture of low concentration of oil and ambient hydrocarbons. The deeper intervals (3-5 and 5-7 cm) in each core were given a forensic classification of "D" as they were considered to contain only background (ambient) hydrocarbons.

Distinguishing Wax-Rich, Severely Weathered Macondo Oil from Seeps – 2010/2011

The existence of natural seeps in the Mississippi Canyon region is well established (e.g., Fugro 2011). The use of chemical fingerprinting alone to distinguish seeped oil from Macondo oil is difficult using a "conventional" PAH or biomarker diagnostic ratio approach due to the common features among South Louisiana Sweet crude oil family, wherein only subtle differences are present between relatively unweathered oily matrix samples (e.g., sheens collected above seeps; Stout, 2015a). Additional difficulties exist in distinguishing severely weathered Macondo oil from seep oils in deep-sea sediments due to background interferences. Thus, and in accordance with the forensic method used herein (see above), a weight of evidence approach was necessary to recognize sediments impacted by seeps.

In the 2010/2011 cores studied, 154 of the 729 were determined to contain hydrocarbons derived from a seep or an apparent seep (see Table 6 and the summary of forensic classifications given below). The difference between these two categories (seep and apparent seep) was typically based on (1) the presence of high concentrations and /or seep oil in multiple core intervals within a single core (i.e., seep)

or (2) low concentrations and/or seep oil within only a single interval (i.e., apparent seep). A map showing the locations of the cores containing seeps and apparent seeps within about 20 miles of the Macondo well is shown in Figure 13. Other seeps recognized 80 to 200 miles to the southwest of the Macondo well in the Atwater Valley and Green Canyon areas (Fig. 1) are not shown as these seeps are largely irrelevant to the *Deepwater Horizon* NRDA study. (Recall, all sediment sample forensic classifications are given in Attachment 1.)

It is notable that seeps recognized in cores almost exclusively occur along the margins of bathymetric features, e.g., salt domes or the edge of the continental slope (Fig. 13). This, of course, is consistent with the occurrence of fault-migration conduits located at these structural margins, along which oil can migrate from geologic depths to the seafloor. The locations of cores recognized to contain seep oil (Fig. 13) are highly consistent with seismic features associated with seafloor seeps (BOEM, 2013).

There was a variety of levels of weathering, namely biodegradation, among the seeps encountered in the sediment cores. This variation is not surprising since the rate of seepage is considered correlated to the rate of biodegradation, wherein higher rates of seepage lead to more biodegradation due to the proliferation of oil-degrading communities when oil concentrations are high, whereas oppositely, lower rates of seepage lead to less biodegradation (Wenger and Isakesen 2002; Hood et al. 2002). This relationship between level of biodegradation and oil concentration at seeps is interesting and may be extended to the *Deepwater Horizon* oil spill, viz., high concentrations of oil in the deep-sea, caused a proliferation of oil-degrading bacteria, which lead to an accelerated rate of biodegradation.

Some examples of the GC/FID chromatograms for several of the seeps observed are shown in Figure 14. The varying levels of biodegradation are evident in the relative abundance of resolved n-alkanes and isoprenoids (pristane and phytane) in the seep oils. Many cores collected in 2010-2011 contained a seep oil that was relatively undegraded and contained a nearly full suite of n-alkanes (e.g., Fig. 14A-C, E). This type of seep was "too fresh" to attribute to wax-rich, severely weathered Macondo oil transported and deposited beyond 3 to 5 miles from the well). Other seeps had retained isoprenoids while lower molecular weight n-alkanes were biodegraded (e.g., Fig. 14D-F, I, K, L). Still others contained no n-alkanes and no isoprenoids, and have been severely biodegraded (e.g. MC118 seep; Fig. 14G). These differences, as well as accompanying differences in PAHs and (sometimes) biomarkers, allowed many of the seep oils to be easily distinguished from wax-rich, severely weathered Macondo oil found beyond 3 to 5 miles from the well (e.g., Fig. 4D).

However, it is notable that some seeps also appear "wax-rich" and, in this one sense, resemble the wax-rich, severely weathered Macondo oil (e.g., Fig. 14H and J). The fact that longer-chain n-alkanes are preferentially preserved (or last to be degraded) is not surprising since, regardless of the oil's source, oil-degrading bacteria in the deep-sea will proceed similarly and biodegrade lower molecular weight n-alkanes preferentially. Thus, the presence of a wax-rich oil (e.g., Fig. 14H or J) is not alone an indication of Macondo oil.

However, a more distinctive feature of the TPH of *all* seeps (alluded to previously) is the presence of a significant mass of unresolved hydrocarbons within the DRO range (C_{10}-C_{25}) of the oil. As can be seen in Figure 14, all of these seep oils contain a prominent

DRO range UCM that is not present in the wax-rich, severely weathered Macondo oil found beyond 3 to 5 miles from the well (e.g., Fig. 4D) or cores containing Macondo oil at their surface (Fig. 11A and 12A). This difference in the TPH DRO abundance was one of the key features used in distinguishing "wax-rich" oil from seeps versus Macondo oily floc.

This difference is envisioned to be caused by the fact that seep oils have not experienced the same degree of weathering as the wax-rich, severely weathered Macondo oil found in the oily floc deposited "far" from the well. Per the *Conceptual Model* described above (Fig. 2), and represented by sediment samples collected at increasing distance from the well (Fig. 4), the Macondo oily floc was severely weathered during its transport within the deep-sea plume through the combined effects of dissolution and biodegradation. These processes combined to significantly reduce the DRO range hydrocarbons retained by the Macondo-derived oily floc beyond 3 to 5 miles from the well (Fig. 4D). Seep oils, on the other hand, did not experience this type of transport (as small oil droplets within the water column). Seep oils slowly reached the seafloor from the deep subsurface via migration along faults over long periods of time. As they approach the surface they experience varying levels of biodegradation (Fig. 14) dependent upon the rate of seepage (Wenger and Isakesen 2002; Hood et al. 2002). The seep oils found in seafloor sediments were never subjected to the intense dissolution or biodegradation as small oil droplets within the water column, because instead they ascended from a deep geologic formation to the seafloor. As a result, seep oils retain much more of the DRO originally present in the oil while plume-transported, Macondo-derived oily floc does not (Fig. 2).

Numerous previous studies of northern Gulf of Mexico seeps in which comparable chromatographic data were provided (Brooks et al. 1986; Kennicutt et al. 1988; Sassen et al. 1994; 2006; MacDonald et al. 2002; Wenger et al. 2002; Hood et al. 2002; Song et al. 2008), also show that seep oils in sediments exhibit a UCM hump that spans both the DRO and RRO ranges even when heavily biodegraded. These studies support the observations herein that seep oils in sediment (e.g., Fig. 14-16) do not exhibit the same loss of DRO range hydrocarbons that the dispersed Macondo oil does (Fig. 4D).

This difference in weathering is also expressed in PAHs and (sometimes) biomarkers within the seep oils. Figure 15 shows the results for a core collected from MC338 in northwest Biloxi Dome about 8.1 miles from the wellhead. This core obviously contained a wax-rich, weathered oil in the upper 5 cm (Fig. 15A). However, as described in the previous paragraph, this wax-rich oil contains a prominent UCM mass within the DRO range, which is distinct from the wax-rich, severely weathered oil attributed to Macondo oil found beyond 3 to 5 miles from the well (Fig. 4D) or in cores with Macondo-derived oily floc at their surface (Fig. 11A and 12A).

The PAHs in this MC338 core also contain an abundance of lower molecular weight decalins and other PAHs that significantly exceed the amounts typical for the wax-rich, severely weathered Macondo oil transported beyond 3 to 5 miles from the wellhead (Fig. 15B) or cores containing Macondo-derived oily floc at their surface (Fig. 11B and 12B). As with DRO, the decalins and lower molecular weight PAHs are retained in the seep oil because it has not experienced the intense dissolution and biodegradation that the Macondo oil had experienced during its transport within the deep-sea plume. This difference further allowed for a distinction between seep oil and Macondo-derived oily floc.

Finally, Figure 15C shows that biomarkers in the oil in this MC338 core are less weathered than is expected for Macondo oil transported more than 3 to 5 miles from the well or cores containing Macondo-derived oily floc at their surface. The seep oil (Fig. 15C) contains homohopanes (T33+) and 13β(H),17α(H)-diacholestanes (S4 and S5), 14β(H),17β(H)-cholestanes (S14 and S15), and co-eluting 14α(H),17β(H)-cholestanes and 13β(H),17α(H)-diaethylcholestanes (S12/S13 and S17/S18) that exceed the abundances found in Macondo oil transported beyond 3 to 5 miles (Fig. 10C) or cores containing Macondo-derived oily floc at their surface (Fig. 11C and 12C). This indicates that the seep oil did not experience the same degree of biodegradation while ascending to the seafloor that the Macondo oil experienced while within the deep-sea plume. The seep oil also contained an excess of TAS compared to Macondo-derived oily floc (Figs. 15C versus Figs 10C, 11C, and 12C).

In addition to the chemical fingerprinting differences described above, the high concentrations of $TPAH_{50}$ and hopane in multiple depth intervals in this core (Fig. 15B-C), given this core's location (~8.1 miles from the well; see further discussion below), provided additional evidence that this MC338 core contained a seep oil, not Macondo oil. Collectively, then the 0-5 cm intervals were each given forensic classifications of "E", while the 5-10 cm interval was given a forensic classification of "D" (i.e., background, per Table 3). A comparable process to that described for this core was used to recognize the other 153 cores ultimately recognized to contain seep oil (Fig. 13).

The MC338 core shown in Figure 15 provides an opportunity to point out that not all seep-impacted cores exhibit evidence of seep oil at all depth intervals within a core (i.e. from "top-to-bottom"). For example, this particular core does not indicate seep oil is present in the 5 to 10 cm depth interval. Some seep-impacted cores exhibited only one depth interval consistent with seep oil (i.e., the apparent seeps). This serves to emphasize that seep oil does not necessarily permeate the entire top 10 cm of the seafloor. Instead it is apparent that seep oil moves through small "zones" within the uppermost seafloor sediment. This is important to recognize since sometimes co-located cores do and do not show the presence of seep oil. This indicates that a seep's impact on sediments can be very highly localized. This is important since it argues that seeps do not universally impact the sediment throughout a given seep zone and do not widely impact sediment far beyond the actual seep, i.e., on the scale of these 10 cm cores they are highly localized features.

One more example of a core containing a seep oil is given in Figure 16. This shows the results for a core collected from the well-studied MC118 (gas hydrate) seep area (e.g., Sassen et al. 2006) about 10.8 miles north of the wellhead (Fig. 13). The seep oil found in multiple cores at this location are all significantly biodegraded and devoid of n-alkane or isoprenoids. However, the MC118 core shown in Figure 16 shows the presence of long chain n-alkanes in the 0-1 cm interval (with trace also in 1-3 cm interval; Fig. 16A). Deeper intervals contain no n-alkanes. Thus, the uppermost part of this core appears *less* biodegraded than the deeper intervals, which is inconsistent with what would be expected from a seep oil alone. Was Macondo-derived oily floc deposited atop of the seep?

The answer to this question is *yes*. The PAHs profiles for intervals in this core clearly show the presence of decalins and PAHs in excess of typical wax-rich, severely weathered Macondo oil beyond 3 to 5 miles from the well. Thus, the PAH provide no

clear evidence, although the C_3- and C_4-benz[a]anthracenes/chrysenes typical of Macondo-derived oily floc (Fig. 8C) are present (Fig. 16B). However, the biomarker patterns are highly revealing. The deeper intervals within this core clearly show the presence of a severely biodegraded oil. One key piece of evidence of this is the prominence of the 17α(H)-diahopane in the deeper intervals (see component X, Fig. 16C). This diahopane is recognized as resistant to biodegradation in seep oil (e.g., Wenger and Isaksen, 2002) and its prominence over hopane (T19; Fig. 16C) in the deeper core intervals (below the 0-1 cm surface) is obvious. However, in the 0-1 cm surface interval diahopane is markedly reduced relative to hopane indicating the surface interval is *less* biodegraded than the deeper intervals. Similarly, the TAS are inexplicably reduced in the surface interval. The presence of a less weathered biomarker pattern at the surface is consistent with the addition of a *relatively* "fresher" Macondo oil atop this core.

Collectively, including the higher concentrations of $TPAH_{50}$ and hopane, the presence of long chain n-alkanes, altered biomarker pattern in the surface interval of this MC118 core indicates it contains a wax-rich, severely weathered Macondo oil that has been superimposed on the MC118 seep oil. This assessment resulted in the 0-1 cm interval of this core being given a forensic classification of "B", while the deeper intervals were classified as "E" (per Table 3).

This example serves to emphasize that Macondo-derived oily floc was sometimes deposited on top of sediment already containing seep oil – in a sufficient amount to be recognized. This observation is consistent with the *Conceptual Model* (Fig. 2). [Notably, the MC118 site is about 900 m deep (Fig. 13), i.e., ~100 m shallower than the top of the deep-sea plume. This suggests that either the deep-sea plume sometimes extended to shallower depths and impinged on this area, a less well developed shallower plume around 850-880 m reached this area, or perhaps marine oil snow from the surface also contributed oil to seafloor at this location.

Concentration Spatial and Depth Trends – 2010/2011

The fingerprinting changes in the Macondo oil deposited on the seafloor beyond 3 to 5 miles from the well – and the differences between it and seep oils – were critical in developing the *Conceptual Model* described above. However, in keeping with the three component forensic method used in this study (see above), hydrocarbon concentrations were also considered. (For example, the three core examples described above each made references to vertical concentration trends within each core.) In this section the trends in hydrocarbon concentrations in deep-sea sediments from 2010-2011 are discussed in a broader sense, which aided in the development of the *Conceptual Model* and the forensic classifications of all samples.

Spatial Trends: Although some variations are expected due to topographic and hydrodynamic processes, overall the *Conceptual Model* (Fig. 2) would predict higher concentrations of Macondo oil-derived hydrocarbons were likely deposited closer to the well and *vice versa*. Indeed, this overall spatial trend is revealed in Figure 17A, which shows the concentrations of $TPAH_{50}$ in surface sediments (0-0.5, 0-1, 0-1.5 and 0-2 cm) versus distance from the Macondo oil for the 724 cores collected in 2010/2011. The different symbols shown refer to the forensic classification ("A" to "E") that were given to each sample (per Table 3; Attachment 1). Figure 17B shows the same data but excludes those samples classified as "E" (seeps) and cores beyond 20 miles of the well.

Inspection reveals that those sediments recognized to contain Macondo oil ("A" or "B") show an overall decrease in $TPAH_{50}$ concentrations with increasing distance from the well with the highest concentrations of each occurring found less than 1 mile from the well. This overall trend is consistent with a localized source, *viz.*, the Macondo well, and the *Conceptual Model* of the lateral transport of oil away from this source.

The only exceptions among the overall trend are three Macondo oil samples ("A") collected around 2 miles from the well that contained exceptionally high concentration of $TPAH_{50}$ (Fig. 17). All three of these "sediment" samples are believed to have been impacted by discrete *in situ* burn residues that had sunk from the surface (Stout and Payne, 2015)[3] and therefore these three "A" sediments are not typical of the Macondo oily floc deposition resulting from the deep-sea plume and marine oil snow. The only other samples containing elevated concentrations of $TPAH_{50}$ that were located 3 or more miles from the well were recognized as being impacted by seep oil ("E"; Fig. 17; see also Fig. 13).

Not surprisingly, those surface sediment samples that were considered representative of background (i.e., "D" per Table 3) contain the lowest concentrations of $TPAH_{50}$ (Fig. 17; "background" concentrations are discussed further below). These background concentrations can be more easily seen in Figure 17B. Notably, within a few miles of the well, there is the co-occurrence of samples impacted by Macondo oil ("A" and "B") and samples containing background hydrocarbons ("D") that occur at about the same distances from the well. The presence/absence of Macondo oil within a few miles of the well serves to emphasize that the wax-rich, severely weathered Macondo oil was not uniformly deposited on the seafloor. This heterogeneity would seem consistent with its deposition as discrete particles of marine oil snow. While this type of particulate deposition will produce the overall trend observed (i.e., decreasing concentrations with increasing distance), it will also produce "scatter" among the absolute concentrations (Fig. 17). It is for this reason that the use of absolute "cut-off" (minimum) $TPAH_{50}$ concentration in surface sediment as a criterion by which to recognize the presence/ absence of Macondo oil was inappropriate in the forensic method. As noted above, spatial concentration trends were only one line of evidence considered in assessing any impact to sediments.

Depth Trends: Similarly the vertical concentration trends within each core were also considered in assessing impact at a given location. Figure 18A-C shows the $TPAH_{50}$ concentration profiles in those cores containing the wax-rich, severely weathered Macondo oil that were found 0 to 1, 1 to 3, and 3 to 5 miles from the well. These same populations of cores were used to develop the average concentrations and distributions of PAHs in Macondo oily floc (Table 5; Fig. 8.) These graphs show that cores in this area clearly contain higher concentrations of PAH at the surface (0-1 cm) than below the surface. Within 1 mile of the well some cores contained elevated concentration up to 10 cm deep, consistent with occasionally "thick" accumulations of oil near the well (Fig. 18A). The cores located 1 to 3 and 3 to 5 miles from the well only exhibit elevated concentrations in the surface sediments, which is consistent with the *Conceptual Model* in which oil was deposited at the surface only (Fig. 2).

[3] HSW6_FP10188_B0827_H_0071; HSW6_FP10188_B0827_H_0072; SB9-65-B0603-S-NF011-HC-1758.

The fact that the wax-rich, severely weathered oil was only present at the surface beyond ~ 1 mile from the well is consistent with its geologically-recent deposition. Even ignoring all other lines of evidence, this indicates the oil could only be reasonably attributed to the *Deepwater Horizon* oil spill and not with any pervasive background or geologically-long-lived seeps. As was also evident in Figure 17, the concentration of PAHs from oily floc are highest in surface sediments nearest the well (Fig. 18A) and decrease with increasing distance from the well (Figs. 18B-C), which again, is consistent with the *Conceptual Model* (Fig. 2).

Thus, cores beyond 5 miles that contained elevated $TPAH_{50}$ concentrations only at their surface beyond 5 miles could be impacted by Macondo oil. If chemical fingerprinting supported this conclusion these samples were given forensic classification of "A" or "B". If the fingerprinting was equivocal (due to low concentration and background interferences), but there was still an elevated concentration of $TPAH_{50}$ at the surface only, a forensic classification of "C" was justified.

Clearly impacted cores ("A" or "B") beyond 5 miles might be expected to contain $TPAH_{50}$ concentrations on the order of or lower than are observed within 5 miles of the well (~1000 to 5000 μg/kg; Fig. 18C), as generally less oil is expected to have reached further locations (Fig. 2). However, some variations in surface concentrations with distance are expected (Fig. 17) due to topographic and hydrodynamic processes which may have deposited (or accumulated) more Macondo oily floc particles in some locations than others. Of particular note in this regard are somewhat higher concentrations of hopane (and $TPAH_{50}$) observed in surface sediments along the continental slope north of the well, suggesting the effect of impingement of oil entrained in the deep-sea plume (Valentine et al. 2014; Stout et al., 2015). Similarly, an area beyond Biloxi Dome may have received additional deposition of Macondo-derived marine oil snow, perhaps due to preferential fallout (e.g., perhaps after reaching a certain level of weathering; Stout et al. 2015). Thus, as with the spatial concentration trend discussed above, there is no single "cut-off" (maximum) above which the presence of Macondo oil should be ruled out and seep presumed. As noted above, vertical concentration trends were only one line of evidence considered in assessing any impact to sediments.

Vertical concentrations at seeps were widely varying (Fig. 18D). Elevated PAH concentrations in surface sediments were only rarely observed in cores impacted by seeps. This is demonstrated by the scatter and elevated concentrations for 82 cores containing seeps and apparent seeps located within 20 miles of the well (Fig. 18D). Most of these cores contain elevated concentrations of $TPAH_{50}$ at multiple depths, sometimes being highest below the surface.

Background PAHs in the Study Area

The large number of deeper core intervals recognized to contain background hydrocarbons only ("D" per Table 3) provide information on the ambient concentration of PAHs in background sediments in the Mississippi Canyon area. (Some background biomarkers unrelated to seep oil are also present, as observed in earlier studies (Cole et al. 2001; Dembicki 2010), but these are not discussed herein.) The concentration of $TPAH_{50}$ in all 729 of the samples considered to represent background ("D", per Table 3) recognized between 3 and 10 cm deep and within 20 miles of the Macondo well are plotted in Figure 19. All samples at this depth contain no oil from Macondo, no oil from any other spilled/discharged oil (e.g., offshore oil production), and no oil directly

associated with natural seeps. These sediments instead contain only hydrocarbons associated with long-term, deep-sea deposition in the study area.

Inspection of Figure 19 shows that all background ("D") samples contained less than 1000 ng/g $TPAH_{50}$ and most contain less than 300 ng/g $TPAH_{50}$. The average and standard deviation concentration of $TPAH_{50}$ in these background sediments is 191 ± 102 ng/g (95^{th} percentile of 404 ng/g). There is quite a bit of variability in concentration, however, which indicates that a single background concentration of ambient PAHs does not exist. For this reason, kriging performed by Stout et al. (2015) developed depth- and site-specific background $TPAH_{50}$ (and hopane) concentrations throughout the study area.

Summary of Forensic Classifications for 2010/2011

Using the multiple lines of evidence forensic method described and demonstrated above, all 2782 sediments collected in 2010/2011 were classified into one of the five categories given in Table 3 (Attachment 1). Examples and various plots of these results were given above. In this section the results reported for surface sediments (<2 cm) are highlighted as, based upon the *Conceptual Model*, beyond ~1 mile from the well it was the surface sediments only that were impacted by Macondo oil. Within ~1 mile of the well the impact was greater due to thicker accumulations of oil and SBM that extended up to 10 cm (the deepest samples collected).

Table 6 contains an inventory of results for surface samples (mostly 0-1 cm, but up to 0-2 cm) obtained for 724 cores taken in 2010/2011. (Recall that five cores did not contain surface samples.) Inspection of these results shows that 197 of the cores contained Macondo oil at their surface (101 "A" and 86 "B"). Most of the "A" classified sediments were found within 5 miles of the well head, where the evidence of impact was (as might be predicted) greatest. Most of the "B" classified sediments were also found within 5 miles of the well although a significant number were also found 5 to 10 miles from the wellhead (Table 6). In total, only 15 (of the 317) sediment cores collected beyond 10 miles from the wellhead were determined to be impacted by Macondo oil. In this area (>10 miles) the number of cores impacted by natural oil seeps was greatest.

A map showing the results from Table 6 is given in Figure 20. The map shows that within 2 miles of the well Macondo oil was deposited in nearly all directions. However, between 2 and 5 miles from the well the oil appears to have been preferentially deposited to the north toward Whiting Dome and to the southwest toward Biloxi Dome. Deposition to the east is limited to the "valley" between Gloria and Mitchell Domes (Fig. 20). Beyond 5 miles from the well the dominant directions for deposition of the oil were to the west (toward the continental slope) and southwest (toward and beyond Biloxi Dome), with a single location to the northeast (north Mitchell Dome) also being evident (Fig. 20). The furthest surface sediments recognized to contain Macondo oil are located about 19 miles to the southwest of the well.

The spatial distribution of surface sediments recognized to contain Macondo oil reflects the varying directions of the oil's transport within the deep-sea plume. Clearly, the plume did not *only* transport oil in a southwesterly direction, although this was apparently the predominant direction based upon the sediment results described herein (Fig. 20). Independently, water sampling within the deep-sea plume and modeling had reached the same conclusion.

Specifically, although a persistent plume was observed to the southwest of the well (Camilli et al. 2010; Hazen et al. 2010; Payne and Driskell, 2015a; French-McKay et al. 2015), the deep-sea plume was also observed to extend in other directions from the well. Spier et al. (2013) calculated frequencies of hydrocarbon detections in water samples collected from the deep-sea plume in eight cardinal directions within ~28 miles of the wellhead. Their results are plotted Figure 21A. These researchers found that the deep plume was most frequently detected to the southwest and secondarily to the west, with much less frequency in the other directions. This independent finding is in complete agreement with the sediment results shown in Figure 20, which can be easily seen when the sediment and water results are superimposed in Figure 21B. Less frequent detections of the deep-sea plume, however, existed in all other directions but at lower concentrations (Fig. 21A; Spier et al. 2013). This too is consistent with the sediment results, which show less frequent and less far impacts in all directions (Fig. 21B).

As described in the forensic methods, the character of any oil present within the slurp gun filter samples and core supernatants collected with the 2010-2011 sediment cores were evaluated in assessing the character of any oil in associated sediments. Therefore it is not surprising that the forensic classification of these samples exhibit a comparable "footprint" as the surface sediments. These results are depicted in Figure 22, which as was observed in surface sediments (Fig. 20), shows evidence of Macondo-derived oily floc predominantly toward the southwest and west of the well. One difference to point out is the detection of Macondo oil in two slurp gun filter samples along the eastern margin of Whiting Dome (Fig. 22A) where an impact to surface sediments could not be recognized in the cores available there.

Summary of Forensic Classifications for 2014

Based upon the multiple lines of evidence, all 805 sediments from the 201 high resolution cores collected in 2014 (Table 1; Fig. 1B) also were classified into one of the five categories given in Table 3 (Attachment 1). The forensic method by which this was achieved was the same used to evaluate the 2010/2011 data (described in the preceding sections). Therefore, in this section only a summary of the results obtained in 2014 is provided. Table 7 provides an inventory of the surface sediment forensic results and Figure 23 shows maps of these results at variable scales.

0 to 1 Mile from Well: Results show that all 25 cores collected within 1 mile of the wellhead still contained Macondo oil and/or SBM four years after the spill ("A" or "B"; Table 7). As in 2010/2011, oil and/or SBM was typically still present both at the surface (0-1 cm) and depth (up to 10 cm). SBM was observed in 23 of the 24 cores collected within 1.5 miles of the well but exhibited a range of weathering, including some that still appeared "fresh" suggesting it may persist for many more years (Stout, 2015b). The oil present in sediments near the well in 2014 was also variably weathered, and although it was consistently more severely weathered than the oil present in 2010/2011, it could still be easily identified.

Figure 24 shows an example of the weathered Macondo oil found within 1 mile of the well in the 2014 sediments. These oils were universally biodegraded to the point where they had lost isoprenoids (e.g., pristane and phytane) and all n-alkanes below n-C_{25} and thereby exhibited a wax-rich appearance akin to the oily floc from 2010-2011 (Fig. 23A). [Note the trace of SBM residue can also still be seen in this sample; Fig. 23A]. Long-chain n-alkanes have (still) not been degraded testifying to their relative recalcitrance

under the conditions in these deep-sea sediments. Notably, the oil close to the well still exhibited a relatively prominent DRO range UCM, which has not been degraded (Fig. 24A). As was evident in 2010/2011, this DRO persists in oil deposited close to the well because these oils had not suffered the effects of transport within the deep-sea plume (wherein dissolution and biodegradation were "super-active"; see results and *Conceptual Model* discussed above).

Decalins were relatively abundant and naphthalenes and other lower molecular weight PAHs were variably preserved in the oiled sediments closest to the well in 2014; the C_3- and C_4-benz[a]anthracenes/chrysenes were increasingly prominent (Fig. 24B). Biomarkers exhibit the depletion of 13β(H),17α(H)-diacholestanes (S4 and S5) and 14β(H),17β(H)-cholestanes (S14 and S15; Fig. 24C) that was initiated in the oiled sediments in 2010/2011 (Fig. 6 and 10). This advancement in weathering of the oil in sediments nearest the well between 2010/2011 and 2014 indicates that favorable conditions existed in these sediments for oil-degrading microbes to continue to degrade the oil.

1 to 5 Miles from Well: Severe weathering was also evident in Macondo oil residues between 1 and 5 miles from the well in the sediments collected in 2014, in which 29 of 35 surface sediments contained residues of the wax-rich, severely weathered Macondo oily floc in relatively low concentrations (Table 7). These oils generally exhibited even more severe weathering than the oils present in 2010/2011 had, which has further altered their chemical fingerprints and overall reduced concentration (see below). Nonetheless, the presence of Macondo oil residues can still be recognized in sediments 1 to 5 miles, but owing to the lower concentrations and altered fingerprints warranted "B" forensic classifications (per Table 3).

Figure 25 shows an example of weathered Macondo oil found in surface sediment (0-1 cm) 1 to 5 miles from the wellhead in 2014. The oil is still wax-enriched and largely devoid of the DRO range hydrocarbons that were retained closer to the well (e.g., compare Fig. 25A and 24A). Long-chain n-alkanes have (still) not been degraded. Again, in keeping with the *Conceptual Model*, oils transported more than ~1 mile from the well within the deep-sea plume were increasingly weathered via dissolution and biodegradation, and therefore appeared wax-rich and severely weathered (including loss of most DRO) in 2010/2011 (Figs. 4D). The oil residues remaining in the sediments 1 to 5 miles from the well in 2014 still exhibit this same feature (Fig. 25A).

Decalins and lower molecular weight PAHs are mostly absent in oils 1 to 5 miles from the well in 2014 (Fig. 25B), which is also consistent with the 2010/2011 sediments (Fig. 8B-C). Again, this is consistent with the removal of these compounds due to weathering (dissolution and biodegradation) within the deep-sea plume in 2010. It is perhaps notable that the hopane-normalized abundance of PAHs in the 2014 sediments (e.g., Fig. 24B) is not lower than was observed in 2010/2011 (e.g., Fig. 8B-C). This seems inconsistent with the lower concentrations of PAHs present in 2014 versus 2010/2011 (see below). Thus, it is theorized that hopane may have been partly degraded over the past few years thereby preserving a comparable hopane-normalized abundance of PAHs in the 2010/2011 and 2014 sediments. Hopane degradation, which has been observed under laboratory conditions (Douglas et al. 2012) or prolonged natural exposure (Wang et al. 2001), is perhaps also reflected in the biomarkers in the 2014 sediments. For example, the biomarkers in most 2014 sediments' beyond 1 mile from the well biomarkers exhibit an excess of TAS (e.g., Fig. 25C) – whereas the 2010/2011

sediments had contained slightly less TAS (e.g., Fig. 10B-C). This difference could be explained if hopane was being degraded in sediments preferentially over TAS since 2010/2011. This same relative enrichment of TAS was observed in laboratory biodegradation studies in which hopane was degraded (Douglas et al. 2012).

Notably, the distribution of the four TAS congeners in these 2014 sediments is also altered compared to the fresh Macondo oil (Figs. 25C and 26C) and from Macondo-oiled sediments from 2010/2011 (Figs. 10, 11C, and 12C). Specifically, the C_{28} 20S-TAS congener has become the dominant TAS in the 2014 sediments (peak SC28TA; Figs. 25C-26C). This indicates that the other three TAS congener may be also experiencing biodegradation albeit slower than hopane and C_{28} 20S-TAS. The same relative resistance of the C_{28} 20S-TAS congener was observed in aggressive laboratory biodegradation experiments on crude oil (Douglas et al. 2012). Thus, even the highly resistant TAS appear to have been biodegraded in Macondo oil-impacted sediments between 2010/2011 and 2014.

Beyond 5 Miles from Well: Results show that Macondo oil was rarely recognized in sediment beyond 5 miles from the well in 2014. Only six of the 141 cores collected in 2014 indicated the presence of low concentrations of severely weathered Macondo oil (Table 7), and all six of these were found in cores collected than 11 miles from the well (Fig. 23B). As was also observed in the 2010/2011 results, the furthest recognized presence of Macondo oil in 2014 was found in cores toward the southwest (Fig. 23B), which is consistent with the predominant direction of deep-sea plume (Fig. 21A).

An example of the Macondo oil present in the six cores beyond 5 miles is shown in Figure 26. These oils had still retained the long-chain n-alkanes, and as expected given their distance from the well, were lacking the DRO hydrocarbons that were retained closer to the well (e.g. compared Fig. 26A and 24A). As noted multiple times, this is due to the dissolution and biodegradation experienced during transport of the Macondo oil within the deep-sea plume, and is one distinguishing feature between it and natural seep oils (which did not experience such transport and retain a prominent DRO; e.g., Figs. 14-16). For the same reason, the Macondo oil beyond 5 miles in the 2014 cores was also depleted in decalins, naphthalenes and other low molecular weight PAHs (Fig. 26B). The remaining PAHs appear even slightly more weathered than in 2010/2011 and increasingly enriched in C_3- and C_4-benz[a]anthracenes/chrysenes (Fig. 26B). Finally, the biomarker patterns in the sediments containing Macondo oil residues are increasingly influenced by "modern" background triterpenoids (T20, T26, and T35) derived from recent organic matter and low signal-to-noise owing to low concentrations of the oil. Despite these effects, the depleted character of the 13β(H),17α(H)-diacholestanes (S4 and S5) and 14β(H),17β(H)-cholestanes (S14 and S15 can still be recognized (Fig. 26C). In addition, the excess of TAS recognized in the Macondo oil 1 to 5 miles from the well – and likely attributed to hopane degradation since 2010/2011 (Fig. 25C) – is also exhibited by the Macondo oil residues found beyond 5 miles in 2014 (Fig. 26C).

Oil Concentrations in 2014: The increased difficulty of recognizing "fingerprintable" Macondo oil in the 2014 sediments owes itself to the overall lower concentrations of oil found in the 2014 sediments compared to 2010/2011, which can be visualized in Figure 27.

Figures 27A and 27B show the concentrations of $TPAH_{50}$ in surface sediments from the 201 cores collected in 2014 *versus* their distance from the well. The different symbols represent each sample's forensic classification (per Table 3). These results show the concentration of PAHs derived from Macondo oil ("A" and "B") are highest within 1 mile of the well but quickly decrease with increasing distance from the well. Those samples still recognized to contain Macondo oil in 2014 generally contained more than 300 ng/g $TPAH_{50}$ (Fig. 27A-B). This concentration is only slightly higher than the average regional background TPAH50 concentration determined from the 2010/2011 results (Fig. 19; 191 ± 102 ng/g). The concentration of $TPAH_{50}$ in sediments in which seeps were recognized ("E") were variable, but were generally higher than sediments containing Macondo oil. [It is notable that the 2014 cruises did not focus on sampling at known seeps (as some 2010/2011 cruises had), therefore the few seeps encountered in 2014 cores are likely "small" and very localized.]

When the $TPAH_{50}$ concentrations for sediments containing Macondo oil in the 2014 ("A" and "B" in Fig. 27A-B) are compared to those from 2010/2011 ("A" and "B" in Figure 27C-D), the markedly lower concentrations in 2014 are obvious. For example, with two exceptions, about half of the impacted sediments within 1 mile of the well collected in 2014 contained less than 1,000 ng/g $TPAH_{50}$ and the other half contained between 1,000 and 10,000 ng/g $TPAH_{50}$ (Fig. 27A-B). In 2010/2011, the samples within 1 mile of the well had contained approximately an order of magnitude higher concentrations of PAH, with about half of samples containing $TPAH_{50}$ concentrations less than 10,000 ng/g and the other half contained between 10,000 and 100,000 ng/g (or higher; Fig. 27C-D). For Macondo-impacted sediments beyond 1 mile from the well, all of the 2014 samples contained less than 1000 ng/g $TPAH_{50}$ (Fig. 27A-B), whereas in 2010/2011 most Macondo-impacted sediments had contained more than 1000 ng/g (Fig. 27C-D).

The approximately order of magnitude lower concentrations of Macondo-derived PAHs in sediments in 2014 (compared to 2010/2011) is at least in part due to the advancement in biodegradation of the oil over the past few years. This was also evidenced in the changes in chemical fingerprints described above. It is possible that bioturbation of the surface sediment over the past few years has contributed to the reduction by mixing (diluting) the oily floc deposited at the surface in 2010 with underlying (un-impacted) sediments. However, because some cores from 2014 still exhibit a maximum concentration of Macondo oil at the surface (0-1 cm), bioturbation cannot explain the universal reduction in concentration. Continued biodegradation of the oily floc deposited at the seafloor surface in 2010 seems more likely.

References

Atlas, R. M. and Hazen, T.C. (2011). "Oil biodegradation and bioremediation: A tale of the two worst spills in U.S. history." Environ. Sci. Technol. 45: 6709-6715.

Baelum, J. et al. (2012) "Deep-sea bacteria enrich by oil and dispersant from the Deepwater Horizon spill." Environ. Microbiol. 14(9): 2405-2416.

Bureau of Ocean Energy (2013). "Seismic water bottom anomalies map gallery". www.boem.gov/oil-and-gas-energy-program/mapping-and-data. Accessed Dec. 2013.

Brooks, J.M., H.B. Cox, W.R. Bryant, M.C. Kennicutt II, R.G. Mann, T.J. McDonald (1986). "Association of gas hydrates and oil seepage in the Gulf of Mexico". Org. Geochem. 10: 221-234.

Brooks, G.R. et al. (2015). "Sedimentation pulse in the NE Gulf of Mexico following the 2010 DWH blowout." PLoS ONE **10(7)**: e0132341. doi:10.1371/journal/pone.0132341.

Camilli, R., C. M. Reddy, D. R. Yoerger, B. A. S. Van Mooy, M. V. Jakuba, J. C. Kinsey, C. P. McIntyre, S. P. Sylva and J. V. Maloney (2010). "Tracking Hydrocarbon Plume Transport and Biodegradation at Deepwater Horizon." Science 330: 201-204.

Chanton, J., T. Zhao, B. E. Rosenheim, S. B. Joye, S. Bosman, C. Brunner, K. M. Yeager, A. Diercks and D. J. Hollander (2015). "Using natural abundance of radiocarbon to trace the flux of petrocarbon to the seafloor following the Deepwater Horizon oil spill." Environ. Sci. Technol. 49: 847-854.

Cole, G.A., Requejo, R., DeVay, J., Yu, A., Peel, F., Brooks, J., Bernard, B., Zumberge, J., Brown, S. (2001). Deepwater Gulf of Mexico piston coring: Seepage versus anomolies versus background and relationship to the Deepwater GoM petroleum system. Proc. Am. Assoc. Petrol. Geol., Denver, CO, Publ. No. 90906.

Continental Shelf Associates (CSA, 2009) "Effects of oil and gas exploration and development at selected continental slope sites in the Gulf of Mexico. Vol. 1: Executive Summary. Minerals Management Service, OCS Study MMS 2006-044. 45 p.

Crooke, E., Talukder, A.., Ross, A., Trefry, C., Caruso, M., Carragher, P., Stalves, C., Armand, S. (2015). Determination of sea-floor seepage locations in the Mississippi Canyon. Marine Pollut. Bull., 59: 129-135.

Dembicki, H. (2010) Recognizing and compensating for interference from sediment's background organic matter and biodegradation during interpretation of biomarker data from seafloor hydrocarbon seeps: An example from the Marco Polo area seeps, Gulf of Mexico, USA. Mar. Petrol. Geol. 27: 1936-1951.

Díez, S., Sabate, J., Vinas, M., Bayona, J. M., Solanas, A. M., Albaiges, J. (2005) The Prestige oil spill. I. Biodegradation of a heavy fuel oil under simulated conditions. Environ. Toxicol. Chem. 24: 2203-2217.

Douglas, G.D., J.H. Hardenstine, B. Liu, A.D. Uhler (2012) Laboratory and field verification of a method to estimate the extent of petroleum biodegradation in soil. Environ. Sci. Technol. 46: 8279-8287.

Elmendorf, D.L. et al. (1994) Relative rates of biodegradation of substituted polycyclic aromatic hydrocarbons. In: Bioremediation of Chlorinated and Polycyclic Aromatic Hydrocarbon Compounds, R.E. Hinchee et al. (Eds.), Boca Raton, FL: Lewis Publishers, pp. 188-202.

Fisher, C. R., P.-Y. Hsing, C. L. Kaiser, D. R. Yoerger, H. H. Roberts, W. W. Shedd, E. E. Cordes, T. M. Shank, S. P. Berlet, M. G. Saunders, ET AL. Larcom and J. M. Brooks (2014a). "Footprint of Deepwater Horizon blowout impact to deepwater coral communities." Proc. Nat'l. Acad. Sci. 111(32): 11744-11749.

Fisher, C.R., Demopoulos, A.W.J., Cordes, E.E., Baums, I.B., White, H.K., Bourgue, J.R. (2014b) Coral communities as indicators of ecosystem-level impacts of the Deepwater Horizon oil spill. BioScience 64(9): 796-807

French McCay, D.P, K. Jayko, Z. Li, M. Horn, Y. Kim, T. Isaji, D. Crowley, M. Spaulding, S. Zamorski, J. Fontenault, R. Shmookler, and J.J. Rowe, 2015a. Technical Reports for

Deepwater Horizon Water Column Injury Assessment – WC_TR.14: Modeling Oil Fate and Exposure Concentrations in the Deepwater Plume and Cone of Rising Oil Resulting from the *Deepwater Horizon* Oil Spill. RPS ASA, South Kingstown, RI, USA, August 2015.

Fu, J., Gong, Y., Zhao, X., O'Reilly, S.E., Zhao, D. (2014) "Effects of oil and dispersant on formation of marine oil snow and transport of oil hydrocarbons." Environ. Sci. Technol., 48(24): 14392-9.

Fugro (2011) Offshore seepage detection – Central Gulf of Mexico benchmarking. Fugro NPA Ltd. and references therein. Report commissioned by BP.

Garcia, O., MacDonalds, I., Silva, M., Shedd, W., Daneghar Asl, S., Schumaker, B. (2015). "Transience and persistence of natural hydrocarbon seepage in Mississippi Canyon, Gulf of Mexico. Deep-Sea Research II, on-line June 2015; doi:10.1016/j.dsr2.2015.05.011.

Graettinger George, Jamie Holmes, Oscar Garcia-Pineda, Mark Hess, Chuanmin Hu, Ira Leifer, Ian MacDonald, Frank Muller-Karger, Jan Svejkovsky, Gregg Swayze, 2015. Integrating data from multiple satellite sensors to estimate daily oiling in the northern Gulf of Mexico during the Deepwater Horizon oil spill. Draft report to DARP, Jan. 9, 2015. (J. Holmes, Stratus Consutling, corresponding author).

Hastings, D.W., Schwing, P.T., Brooks, G.R., Larson, R.A., Morford, J.L., Roeder, T., Quinn, K.A., Bartlett, T., Romero, I.C., Hollander, D.J. (2015) Changes in sediment redox conditions following the BP DWH blowout event. Deep-Sea Research II, published on-line, doi.org/0.1016/j.dsr2.2014.12.009.

Hazen, T.C., Dubinsky, E.A., DeSantis, T.Z., Andersen, G.L., Piceno, Y.M. et al. (2010). "Deep-sea oil plume enriches indigenous oil-degrading bacteria". Science 330: 204-208.

Hsing, P.-Y., B. Fu, ET AL. Larcom, S. P. Berlet, T. M. Shank, A. F. Govindarajan, A. J. Lukasiewicz, P. M. Dixon and C. R. Fisher (2013). "Evidence of lasting impact of the Deepwater Horizon oil spill on a deep Gulf of Mexico coral community." Elementa 1(doi: 10.12952/journal.elementa.000012).

Hood, K.C. et al. (2002) Hydrocarbon systems analysis of the northern Gulf of Mexico: Delineantion of hydrocarbon migration pathways using seeps and seismic imaging. In: Surface Exploration Case Histories, D. Schumacher and L.A. LeSchack, Eds., AAPB Studies in Geology, No. 48, and SEG Geophysical Ref. Series, No. 11: 25-40.

Kennicutt, M. C. and P. A. Comet (1992). Resolution of sediment hydrocarbons sources: Multiparameter approach. Organic Matter: Productivity, Accumulation, and Preservation in Recent and Ancient Sediments. J. K. Whelan and J. W. Farrington. New York, Columbia Univ. Press: 309-338.

Kennicutt, M.C., J.M. Brooks, R.R. Bidigare, G.J. Denoux (1988). "Gulf of Mexico hydrocarbon seep communities – I. Regional distribution of hydrocarbon seepage and associated fauna". Deep-Sea Res. 35(9): 1639-1651.

Kimes, N.E., Callaghan, A.V., Aktas, D.F., Smith, W., Sunner, J., Golding, B.T., Drozdowska, M., Hazen, T.C., Suflita, J.M., and Morris, P.J. (2013) Metagenomic analysis and metabolite profiling of deep-sea sediments from the Gulf of Mexico following the Deepwater Horizon oil spill. Frontiers in Microbiology, March 2013, 4: 1-17; doi: 10.3389/fmicb.2013.00050.

Kinner, N. E., L. Belden and P. Kinner, 2014. "Unexpected sink for Deepwater Horizon oil may influence future spill response". *EOS* **95**(21): 27.
Montagna, P. A., J. G. Baguley, C. Cooksy, I. Hartwell, L. J. Hyde, J. L. Hyland, R. D. Kalke, L. M. Kracker, M. Reuscher and A. C. E. Rhodes (2013). "Deep-sea benthic footprint of the Deepwater Horizon blowout." PLoS ONE 8(8): e70540. doi:70510.71371/journal.pone.0070540.

MacDonald, I.R., I. Leifer, R. Sassen, P. Stine, R. Mitchell, and N. Guinasso (2002). "Transfer of hydrocarbons from natural seeps to the water column and atmosphere". Geofluids 2: 95-107.

NOAA (2014) Analytical quality assurance plan, Mississippi Canyon 252 (Deepwater Horizon) natural resource damage assessment, Version 4.0. May 30, 2014.

OSAT-1 (2010) Summary report for sub-sea and sub-surface oil and dispersant detection: Sampling and monitoring. Operational Science Advisory Team, Dec. 17, 2010.

Passow, U. (2014). "Formation of rapidly-sinking, oil-associated marine snow." Deep-Sea Res. Part II, Top. Stud. Oceanogr.: doi: 10.1016/j.dsr1012.2014.1010.1001.

Passow, U., K. Ziervogel, V. Asper and A. Diercks (2012). "Marine snow formation in the aftermath of the Deepwater Horizon oil spill in the Gulf of Mexico." Environ. Res. Lett. 7: 11 p.

Payne, J.R. and W.B. Driskell. (2015a). 2010 DWH offshore water column samples – Forensic assessments and oil exposures. PECI Report to the Trustees in support of the DARP, August, 2015.

Payne, J.R. and W.B. Driskell. (2015b). Offshore adaptive sampling strategies. PECI Report to the Trustees in support of the DARP, August, 2015.

Payne, J.R. and W.B. Driskell. (2015c). Dispersant effects on waterborne oil profiles and behavior. PECI Report to the Trustees in support of the DARP, August, 2015.

Payne, J.R. and W.B. Driskell (2015d). Forensic fingerpringing methods and classification of DWH offshore water samples. PECI Report to the Trustees in support of the DARP, August, 2015.

Prince, R.C. (2002) Petroleum and other hydrocarbons, biodegradation of. In: Encyclopedia of Environmental Microbiology, Bitton, G., Ed., New York, J. Wiley, pp. 2402-2416.

Prince, R. C., D. L. Elmendorf, J. R. Lute, C. S. Hsu, C. E. Haith, J. D. Senius, G. J. Dechert, G. S. Douglas and E. L. Butler (1994). 17α(H),21β(H)-hopane as a conserved internal marker for estimating the biodegradation of crude oil. Environ. Sci. .Tech.. 28(1): 142-145.

Prince, R. C., E. H. Owens and G. A. Sergy (2002). "Weathering of an Arctic oil spill over 20 years: the BIOS experiment revisited." Marine Pollution Bulletin 44(11): 1236-1242.

Prince, R.C., K.M. McFarlin, J.D. Butler, E.J. Febbo, F.C.Y. Wang, T.J. Nedwed (2013) The primary biodegradation of dispersed crude oil in the sea. Chemosphere 90: 521-526.

Rowe, G.T. and Kennicutt, M.C. (2009) Northern Gulf of Mexico continental slope habitats and benthic ecology study – Final Report. Minerals Management Services, OCS Study, MMS 2009-039, July 2009.

Ryerson, Thomas B., Richard Camilli, John D. Kessler, Elizabeth B. Kujawinski, Christopher M. Reddy, David L. Valentine, Elliot Atlas, Donald R. Blake, Joost de Gouw, Simone Meinardi, David D. Parrish, Jeff Peischl, Jeffrey S. Seewald, and Carsten Warneke, 2012. "Chemical data quantify Deepwater Horizon hydrocarbon flow rate and environmental distribution." Proc. Nat'l. Acad. Sci. 109(50): 20246-20253.

Sassen, R., Brooks, J.M., Kennicutt, M.C., MacDonalds, I.R., Guinasso, N.L. (1993) "How oil seeps, discoveries relate in deepwater Gulf of Mexico. Oil & Gas J., April 19, 1993: 64-68.

Sassen, R., I.R. MacDonald, A.G. Requejo, N.L. Guinasso, M.C. Kennicutt II, S.T. Sweet, and J.M. Brooks (1994). "Organic geochemistry of sediments from chemosynthetic communities, Gulf of Mexico slope". Geo-Marine Letters 14: 110-119

Sassen, R., Roberts, H.H., Jung, W., Lutken, C.B., DeFreitas, D.A., Sweet, S.T., Guinasso, N.L. (2006) The Mississippi Canyon 118 gas hydrate site: A complex natural system. Proc. Offshore Techn. Conf., Houston, May 1-4, 2006, OCT No. 18132, 6 p.

Schrope, M. 2013. "Dirty blizzard buried Deepwater Horizon oil." Nature News. Jan. 26, 2013. Doi:10.1038/nature.2013.12304.

Schwing, P.T., Romero, I.C., Brooks, G.R., Hastings, D.W., Larson, R.A., Hollander, D.J. (2015) A decline in benthic foraminifera following the Deepwater Horizon event in the northeastern Gulf of Mexico. PLoS ONE 10(3): e0120565. doi:10.1371/journal.pone.0120565.

Simoneit, B. R. T. (1986). Cyclic terpenoids of the geosphere. Biological Markers in the Sedimentary Record. R. B. Johns. Amsterdam, Elsevier: 43-59.

Socolofsky, S. A., E. E. Adams and C. R. Sherwood (2011). Formation dynamics of subsurface hydrocarbon intrusions following the *Deepwater Horizon* blowout. Geophys. Res. Letters **38**(L09602, doi:10.1029/2011GL047174): 6 p.

Song, Z., L. Wang, J. Liu, C. Wang, D. Chen (2008). Characterizing organic matter in marine sediments associated with gas hydrate and oil seepage from the Gulf of Mexico. Geofluids 8: 293-300.

Spier, C., W. T. Stringfellow, T. C. Hazen and M. Conrad. 2013. Distribution of hydrocarbons released during the 2010 MC252 oil spill in deep offshore waters. *Environmental Pollution* **173**:224-230.

Stout, S.A. (2015a) Chemical fingerprinting methodology and the classification of oily matrices used in the *Deepwater Horizon* NRDA. NewFields Technical Report to the Trustess in support of the DARP. August 2015.

Stout, S.A. (2015b) Composition of Olefin-Based Synthetic Mud(s) used by BP and its Occurrence and Persistance in Deep-Sea Sediments near the Macondo well. NewFields Technical Report to the Trustess in support of the DARP. August 2015.

Stout, S.A. (2015c) Chemical Composition of Fresh Macondo Crude Oil. NewFields Technical Report to the Trustess in support of the DARP. August 2015.

Stout, S.A. (2015d) Range in Composition and Weathering among Floating Macondo Oils during the *Deepwater Horizon* Oil Spill. NewFields Technical Report to the Trustess in support of the DARP. August 2015.

Stout, S.A. and C. German (2015). Characterization and flux of marine oil snow in the Viosca Knoll (*Lophelia* Reef) area due to the *Deepwater Horizon* oil spill. NewFields Technical Report to DARP, August 2015.

Stout, S.A. and U. Passow (2015). Character and Sedimentation Rate of "Lingering" Macondo Oil in Deep-Sea up to One Year after the Deepwater Horizon Oil Spill. NewFields Technical Report to DARP, August 2015.

Stout, S.A. and J.R. Payne, (2015) Chemical Composition of Floating and Sunken In-Situ Burn (ISB) Residues from the Deepwater Horizon Oil Spill. NewFields Technical Report to DARP, August 2015.

Stout, S.A., Rouhani, S., Liu, B., Oehrig, J. (2015). Spatial Extent ("Footprint") and Volume of Macondo oil found on the deep-sea floor following the Deepwater Horizon oil spill. NewFields Technical Report to DARP, August 2015.

Valentine, D.L., Kessler, J.D., Redmond, M.C., Mendes, S.D., Heintz, M.B. et al. (2010) Propane respiration jump-starts microbial response to a deep oil spill. Science 330: 208-211.

Valentine, D. L., G. Burch Fisher, S. C. Bagby, R. K. Nelson, C. M. Reddy, S. P. Sylva and M. A. Woo (2014). "Fallout plume of submerged oil from Deepwater Horizon." Proc. Nat'l. Acad. Sci. 10.1073/pnas.1414873111: 6 p.

Wade, T.L. et al. (2008) Trace elements and polycyclic aromatic hydrocarbons (PAHs) concentrations in deep Gulf of Mexico sediments. Deep Sea Research II, 55: 2585-2593.

Wang, Z. et al. (2001) Long-term fate and persistence of the spilled Metula oil in a marine salt marsh environment. Degradation of petroleum biomarkers. J. Chrom. A. 926: 275-290.

Wenger, L.M. and Isaksen, G.H. (2002). Control of hydrocarbon seepage intensity on level of biodegradation in sea bottom sediments. Org. Geochem. 33: 1277-1292.

White, H. K. et al. (2012). "Impact of the Deepwater Horizon oil spill on a deep-water coral community in the Gulf of Mexico." Proc. Nat'l. Acad. Sci. 109(50): 20303-20308.

Table 1: Inventory deep-sea samples evaluated herein from 729 high-resolution cores collected in 2010-2011 and 201 high-resolution cores collected in 2014.

Study ID	Dates	Sediment	Slurp Gun Filter	Supernatant
2010-2011 Surveys*		**2782**	**222**	**442**
HOS Davis Cruise 03**	Sept. 8-28, 2010	142		
Pisces Cruise 06	Sept. 25-Oct. 4, 2010	13		
Atlantis Cruise	Dec. 4-15, 2010	45		
HOS Davis Cruise 05***	Dec. 4-18, 2010	190		34
HOS Sweetwater Cruise 01	Mar. 10-13, 2011	18		
HOS Sweetwater Cruise 02	Mar. 23-Apr. 24, 2011	612	85	168
Sarah Bordelon Cruise 09	May 23-Jun. 13, 2011	456		
HOS Sweetwater Cruise 04	Jul. 14-Aug. 7, 2011	366	58	96
HOS Sweetwater Cruise 6 Leg 1	Aug. 24-Sept. 02, 2011	168	31	43
Holiday Chouest Cruise 01	Aug. 25-Sept. 13, 2011	112		
Holiday Chouest Cruise 02	Sept. 15-30, 2011	84		
HOS Sweetwater Cruise 6 Leg 2	Sept. 29-Oct. 21, 2011	414	48	101
Holiday Chouest Cruise 03	Oct. 1-25, 2011	162		
2014 Surveys		**805**		
Irish Cruise 01 Leg 1	May 28-Jun. 11, 2014	356		
Irish Cruise 01 Leg 2	Jun. 14-28, 2014	449		
Grand Total		**3587**	**222**	**442**

* 47 low resolution cores collected from Nancy Foster Cruises (Jul. 21-30, 2010, Aug. 1-10, 2010), Cape Hatteras Cruise (Sept. 20-Oct. 3, 2010, and Ron Brown Cruise (Oct. 16-Nov. 3, 2010) were excluded

** 4 low resolution cores (n=12) were excluded

*** 1 low resolution core (n=3) was excluded

Table 2: Inventory of PAH and biomarker analytes with abbreviations used in figures.

Abbrev.	Compound
D0	cis/trans-Decalin
D1	C1-Decalins
D2	C2-Decalins
D3	C3-Decalins
D4	C4-Decalins
BT0	Benzothiophene
BT1	C1-Benzo(b)thiophenes
BT2	C2-Benzo(b)thiophenes
BT3	C3-Benzo(b)thiophenes
BT4	C4-Benzo(b)thiophenes
N0	Naphthalene
N1	C1-Naphthalenes
N2	C2-Naphthalenes
N3	C3-Naphthalenes
N4	C4-Naphthalenes
B	Biphenyl
DF	Dibenzofuran
AY	Acenaphthylene
AE	Acenaphthene
F0	Fluorene
F1	C1-Fluorenes
F2	C2-Fluorenes
F3	C3-Fluorenes
A0	Anthracene
P0	Phenanthrene
PA1	C1-Phenanthrenes/Anthracenes
PA2	C2-Phenanthrenes/Anthracenes
PA3	C3-Phenanthrenes/Anthracenes
PA4	C4-Phenanthrenes/Anthracenes
RET	Retene
DBT0	Dibenzothiophene
DBT1	C1-Dibenzothiophenes
DBT2	C2-Dibenzothiophenes
DBT3	C3-Dibenzothiophenes
DBT4	C4-Dibenzothiophenes
BF	Benzo(b)fluorene
FL0	Fluoranthene
PY0	Pyrene
FP1	C1-Fluoranthenes/Pyrenes
FP2	C2-Fluoranthenes/Pyrenes
FP3	C3-Fluoranthenes/Pyrenes
FP4	C4-Fluoranthenes/Pyrenes
NBT0	Naphthobenzothiophenes
NBT1	C1-Naphthobenzothiophenes
NBT2	C2-Naphthobenzothiophenes
NBT3	C3-Naphthobenzothiophenes
NBT4	C4-Naphthobenzothiophenes
BA0	Benz[a]anthracene
C0	Chrysene/Triphenylene
BC1	C1-Chrysenes
BC2	C2-Chrysenes
BC3	C3-Chrysenes
BC4	C4-Chrysenes
BBF	Benzo[b]fluoranthene
BJKF	Benzo[jk]fluoranthene
BAF	Benzo[a]fluoranthene
BEP	Benzo[e]pyrene
BAP	Benzo[a]pyrene
PER	Perylene
IND	Indeno[1,2,3-cd]pyrene
DA	Dibenz[a,h]anthracene
GHI	Benzo[g,h,i]perylene

Abbrev.	Compound
T4	C23 Tricyclic Terpane
T5	C24 Tricyclic Terpane
T6	C25 Tricyclic Terpane
T6a	C24 Tetracyclic Terpane
T6b	C26 Tricyclic Terpane-22S
T6c	C26 Tricyclic Terpane-22R
T7	C28 Tricyclic Terpane-22S
T8	C28 Tricyclic Terpane-22R
T9	C29 Tricyclic Terpane-22S
T10	C29 Tricyclic Terpane-22R
T11	18α(H)-22,29,30-Trisnorneohopane-T_S
T11a	C30 Tricyclic Terpane-22S
T11b	C30 Tricyclic Terpane-22R
T12	17α(H)-22,29,30-Trisnorhopane-T_M
T14a	17α/β & 21β/α 28,30-Bisnorhopane
T14b	17α(H),21β(H)-25-Norhopane
T15	17α(H),21β(H)-30-Norhopane
T16	18α(H)-30-Norneohopane-C29Ts
X	17α(H)-Diahopane
T17	17β(H),21α(H)-30-Normoretane
T18	18α(H)&18β(H)-Oleananes
T19	17α(H),21β(H)-Hopane
T20	17β(H),21α(H)-Moretane
T21	30-Homohopane-22S
T22	30-Homohopane-22R
T26	30,31-Bishomohopane-22S
T27	30,31-Bishomohopane-22R
T30	30,31-Trishomohopane-22S
T31	30,31-Trishomohopane-22R
T32	Tetrakishomohopane-22S
T33	Tetrakishomohopane-22R
T34	Pentakishomohopane-22S
T35	Pentakishomohopane-22R
S4	13b(H),17a(H)-20S-Diacholestane
S5	13b(H),17a(H)-20R-Diacholestane
S8	13b,17a-20S-Methyldiacholestane
S12/S13	14a(H),17a(H)-20S-Cholestane + 13b(H),17a(H)-20S-Ethyldiacholestane
S17/S18	14a(H),17a(H)-20R-Cholestane + 13b(H),17a(H)-20R-Ethyldiacholestane
S18x	Unknown sterane
S19	13a(H),17b(H)-20S-Ethyldiacholestane
S20	14a(H),17a(H)-20S-Methylcholestane
S24	14a(H),17a(H)-20R-Methylcholestane
S25	14a(H),17a(H)-20S-Ethylcholestane
S28	14a(H),17a(H)-20R-Ethylcholestane
S14	14b(H),17b(H)-20R-Cholestane
S15	14b(H),17b(H)-20S-Cholestane
S22	14b(H),17b(H)-20R-Methylcholestane
S23	14b(H),17b(H)-20S-Methylcholestane
S26	14b(H),17b(H)-20R-Ethylcholestane
S27	14b(H),17b(H)-20S-Ethylcholestane
RC26/ SC27TA	C26,20R- +C27,20S- triaromatic steroid
SC28TA	C28,20S-triaromatic steroid
RC27TA	C27,20R-triaromatic steroid
RC28TA	C28,20R-triaromatic steroid

Table 3: Forensic classification of deep-sea sediments.

Sample's Forensic Classification	Description	Practical Conclusion to NRDA
A	Chemical fingerprints and core characteristics are consistent with Macondo oil or differences can unequivocally be explained by external factors*; SBM is present near wellhead; co-occurs with slurp-gun filter or core supernatant classified as "A"	Macondo crude oil is present
B	Chemical fingerprints and core characteristics preclude unequivocal match but differences can be reasonably explained by external factors*; often lower concentrations than "A"	
C	Chemical fingerprints and core characteristics are equivocal but other lines of evidence** suggest possible presence of Macondo oil; Concentrations often low	Equivocal; Macondo crude oil is possibly present
D	Chemical fingerprints and core characteristics are inconclusive and no other classification is justified; most often due to a very low hydrocarbon concentrations	No spill or seep oil is present, only "background"
E	Chemical fingerprints and core characteristics are inconsistent with Macondo oil and cannot be explained by external factors*	Macondo oil is absent; a different petroleum (seep) is present

*For example, weathering, mixing, low(er) concentrations, and/or interferences

**co-occurrence with or proximity to of A or B samples; slightly elevated hydrocarbon concentration at surface.

Table 4: Diagnostic ratios (DRs) considered in comparing deep-sea sediment samples to Macondo oil. See Table 2 for compound abbreviations.

DR#	*PAH Ratios*	*Definitions using peak IDs*
1	DBT2/(DBT2+PA2)	DBT2/(DBT2+PA2)
2	DBT3/(DBT3+PA3)	DBT3/(DBT3+PA3)
3	NBT2/(NBT2+BC2)	NBT2/(NBT2+BC2)
4	NBT3/(NBT3+BC3)	NBT3/(NBT3+BC3)
	Triterpane Ratios	
5	Ts/(Ts+Tm)	T11/(T11+T12)
6	H29Ts/(H29Ts+H29)	T16/(T16+T15)
7	X/(X+H29)	X/(X+T15)
8	X/(X+H30)	X/(X+T19)
9	H31-22S/(22S+22R)	T21/(T21+T22)
10	H32-22S/(22S+22R)	T26/(T26+T27)
11	te24/(te24+H30)	T6a/(T6a+T19)
12	te24/(te24+t26)	T6a/(T6a+T6b+T6c)
13	(t28+t29)/(t28+t29+H30)	(T7+T8+T9+T10)/(T7+T8+T9+T10+T19)
14	BNH/(BNH+H30)	T14a/(T14a+T19)
15	H29/(H29+H30)	T15/(T15+T19)
16	OL/(OL+H30)	T18/(T18+T19)
17	M30/(M30+H30)	T20/(T20+T19)
18	H34/(H34+H30)	(T32+T33)/(T32+T33+T19)
	Sterane Ratios	
19	aa29S/(aa29S+aa2920R)	S25/(S25+S28)
20	(bb29RS)/(bb29RS+aa29RS)	(S26+S27)/(S26+S27+S25+S28)
21	Ster/(Ster+Hop)	(S12+S17+S18+S25+S28+S22+S23+S26+S27)/(S12+S17+S18+S25+S28+S22+S23+S26+S27+T11+T12+T15+T19)
22	(d27RS)/(d27RS+aa27RS+d29RS)	(S4+S5)/(S4+S5+S12+S13+S17+S18)
23	C27bb/bbTotal	(S14+S15)/(S14+S15+S22+S23+S26+S27)
24	C28bb/bbTotal	(S22+S23)/(S14+S15+S22+S23+S26+S27)
25	C29bb/bbTotal	(S26+S27)/(S14+S15+S22+S23+S26+S27)
	Triaromatic Steroid Ratios	
26	(C2620R+C2720S)/(C2620R+C2720S+C2720R+C2820R)	(RC26+SC27)/(RC26+SC27+RC27+RC28)
27	C2820S/(C2820S+C2820R)	SC28/(SC28+RC28)
28	C2820S/(C2820S+C2720R)	SC28/(SC28+RC27)
29	Total TAS/(tTAS+H30)	(RC26+SC27+RC27+RC28)/(RC26+SC27+RC27+RC28+T19)

	0 to 1 Mile (n=23)		1 to 3 Miles (n=26)		3 to 5 Miles (n=20)	
	Avg.	σ	Avg.	σ	Avg.	σ
D0	689	1500	5	10	1	1
D1	2191	4614	26	46	10	18
D2	3168	6097	54	84	18	47
D3	2140	3875	42	68	15	39
D4	2457	4291	67	88	25	66
BT0	3	6	nd	nd	0.03	0.2
BT1	50	88	nd	nd	nd	nd
BT2	58	92	2	4	3	4
BT3	151	257	5	12	10	14
BT4	164	303	1	4	nd	nd
N0	35	58	9	4	8	3
N1	130	205	12	7	9	4
N2	952	1852	21	13	17	9
N3	1942	3806	34	39	18	11
N4	1886	3437	48	60	21	30
B	52	71	5	3	4	2
DF	28	40	2	1	2	2
AY	22	34	3	1	2	1
AE	25	54	1	2	0.1	0.3
F0	71	131	3	3	2	1
F1	486	899	11	11	5	4
F2	1305	2350	33	43	16	25
F3	1495	2571	42	66	29	59
A0	43	75	4	15	1	1
P0	340	627	14	11	10	3
PA1	1570	3102	35	40	20	14
PA2	2568	4817	79	92	52	56
PA3	2039	3748	88	75	67	74
PA4	1031	1766	79	55	60	62
RET	1	4	0.3	1	nd	nd
DBT0	54	91	3	2	2	1
DBT1	378	743	9	8	8	6
DBT2	776	1432	31	28	24	24
DBT3	818	1432	37	34	26	39
DBT4	514	861	31	23	22	26
BF	54	93	4	16	1	1
FL0	57	79	8	3	9	3
PY0	207	241	13	8	13	10
FP1	622	896	64	38	52	30
FP2	1141	1692	147	72	121	61
FP3	1424	2115	212	105	189	87
FP4	1209	1739	206	109	192	89
NBT0	122	209	7	8	5	6
NBT1	436	721	31	18	27	25
NBT2	716	1104	83	39	83	49
NBT3	645	861	148	77	144	61
NBT4	485	621	128	70	126	54
BA0	53	65	8	18	5	3
C0	424	636	69	43	56	31
BC1	926	1516	123	69	106	61
BC2	1303	2049	206	116	190	89
BC3	1492	2107	378	206	375	150
BC4	952	1268	314	176	314	147
BBF	75	87	13	10	11	6
BJKF	31	33	8	10	7	4
BAF	9	11	1	3	1	2
BEP	174	191	49	28	44	20
BAP	78	77	14	12	11	6
PER	46	34	14	6	13	3
IND	50	46	10	7	9	4
DA	34	39	9	5	8	4
GHI	81	78	17	10	15	6
Hopane	870	998	320	185	294	130
$TPAH_{50}$	31360		2902		2540	

Table 5: Average and standard deviation of PAH and hopane concentrations (ng/g dry) in surface sediments containing the wax-rich, severely weathered Macondo oil 0-1, 1-3, and 3-5 miles from the wellhead.

Table 6: Summary of forensic classification results for surface sediments (< 2 cm, mostly < 1 cm) in the high-resolution cores collected in 2010-2011. For classification A to E, see Table 3.

Distance from Macondo Well	A	B	C	D	E	Total
≤ 1 mile	39	1	2	1	0	43
1-3 miles	29	31	21	7	0	88
3-5 miles	18	13	29	11	24	95
5-10 miles	12	29	70	22	48	181
>10 miles	3	12	43	177	82	317
Total	101	86	165	218	154	724

Table 7: Summary of forensic classification results for surface sediment (0-1 cm) in the high resolution cores collected in 2014. For classifications A to E, see Table 3.

Distance from Macondo Well	A	B	C	D	E	Total
≤ 1 mile	24	1	0	0	0	25
1-3 miles	2	20	5	0	0	27
3-5 miles	0	7	0	1	0	8
5-10 miles	0	4	6	1	1	12
>10 miles	0	2	35	84	8	129
Total	26	34	46	86	9	201

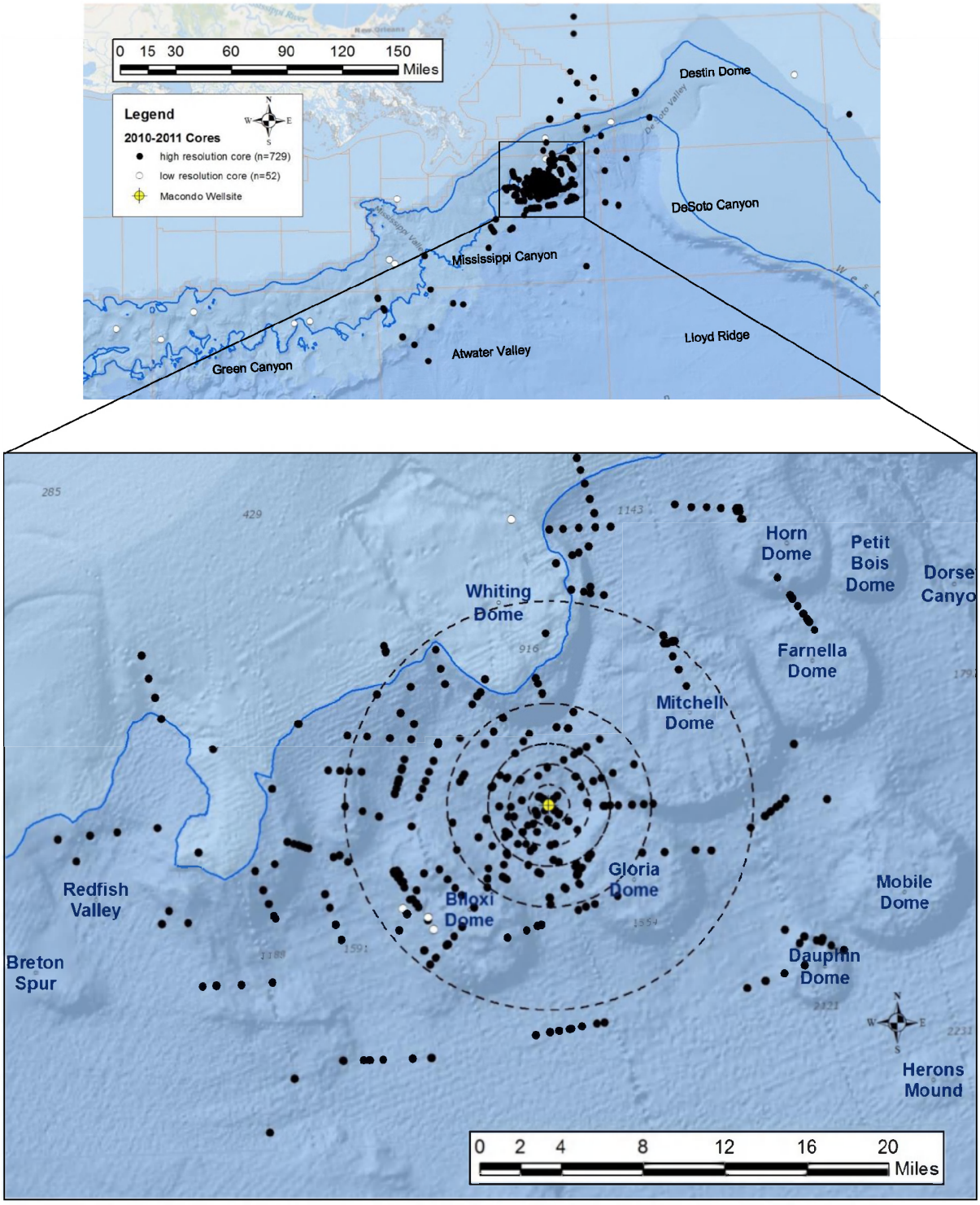

Figure 1A: Maps showing the locations of sediment cores collected in 2010-2011 considered in this review (729 high-resolution per Table 1 and 47 low-resolution). Top figure shows relevant BOEMRE lease regions and bottom shows major topographic features. Radii of circles show 1, 2, 3, 5 and 10 miles from wellhead.

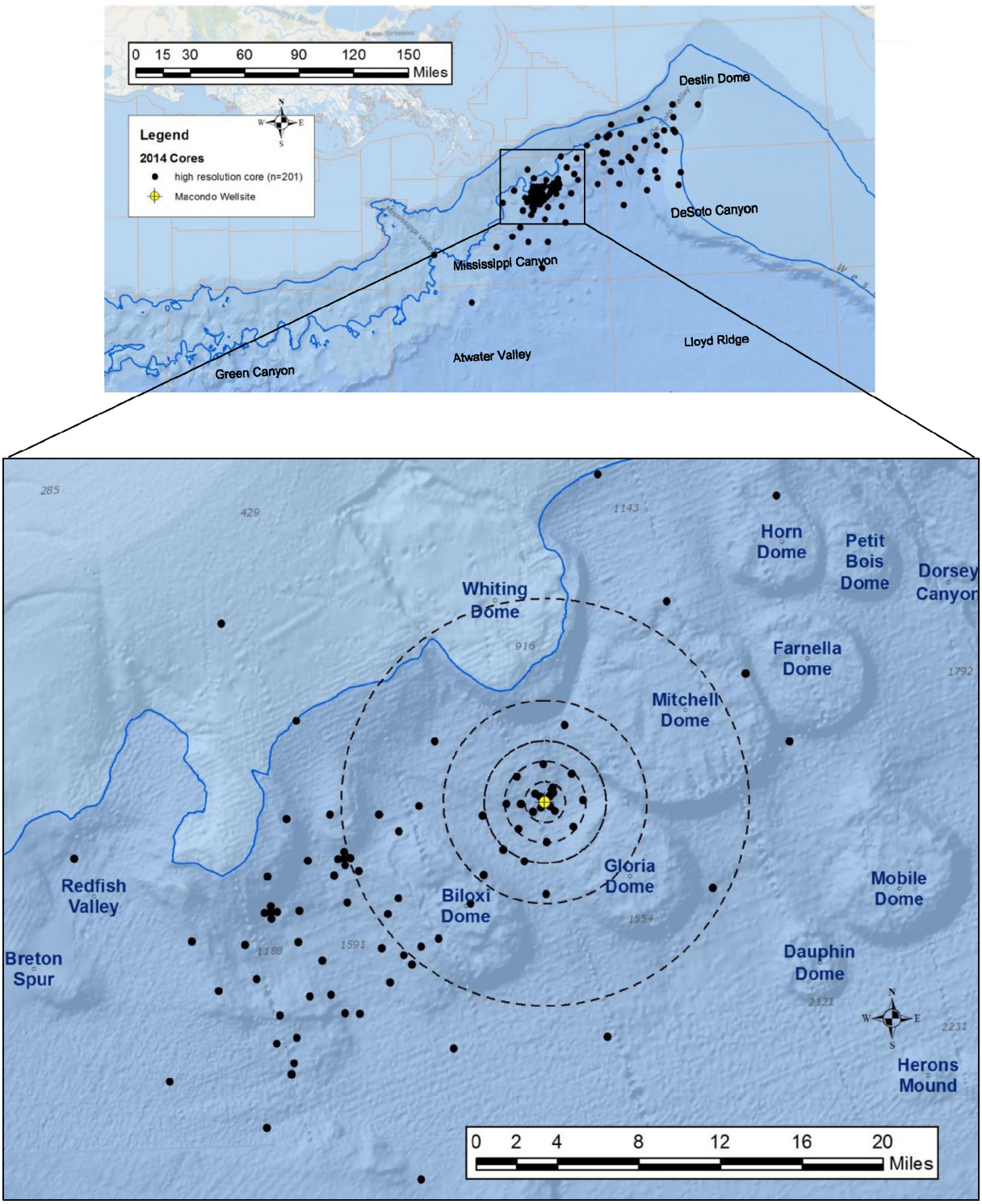

Figure 1B: Maps showing the locations of sediment cores collected in 2014 considered in this review (201 high-resolution per Table 1). Top figure relevant BOEMRE lease regions and bottom shows major topographic features. Radii of circles show 1, 2, 3, 5 and 10 miles from wellhead.

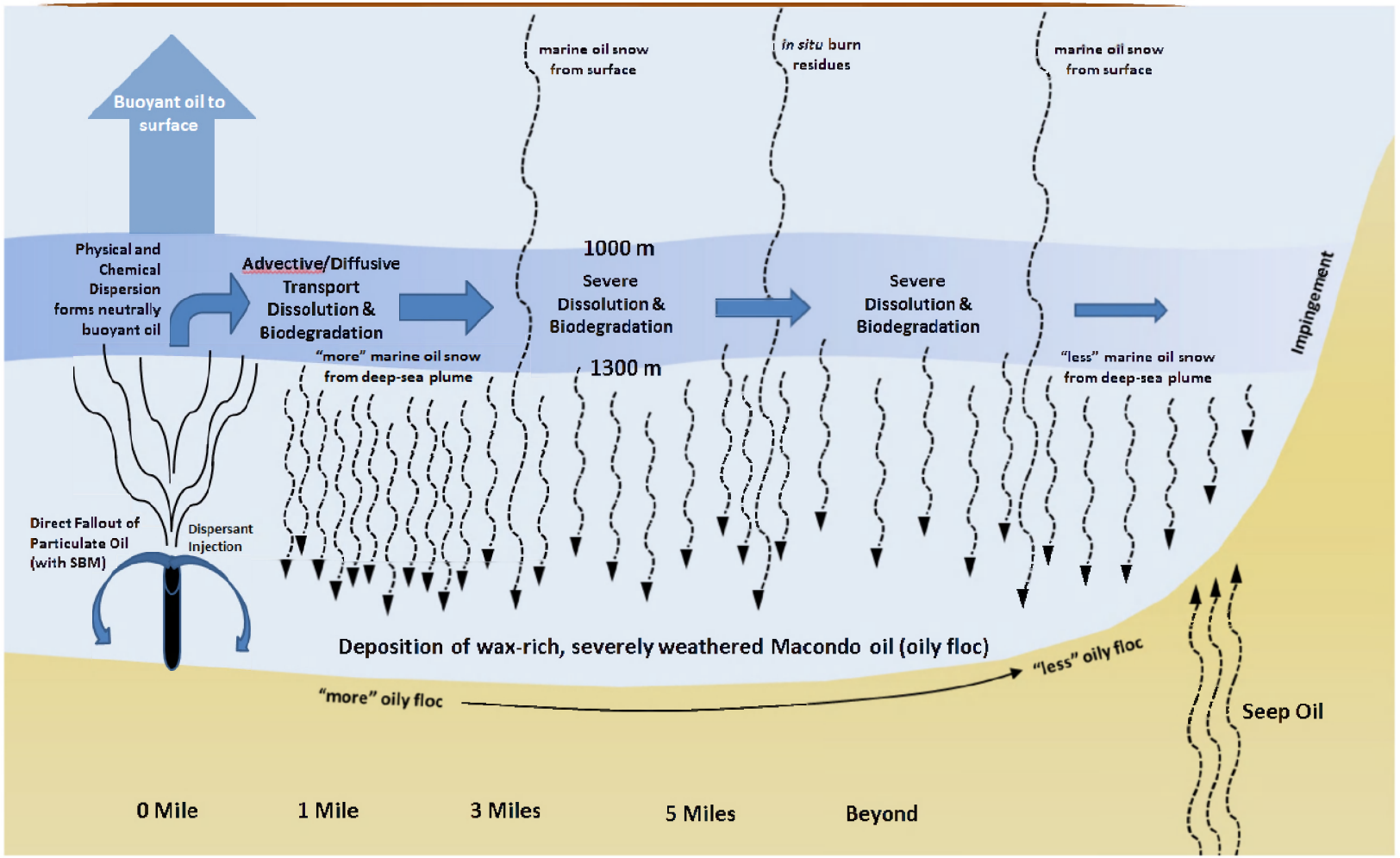

Figure 2: Conceptual model for Macondo oil deposition on the deep-sea floor.

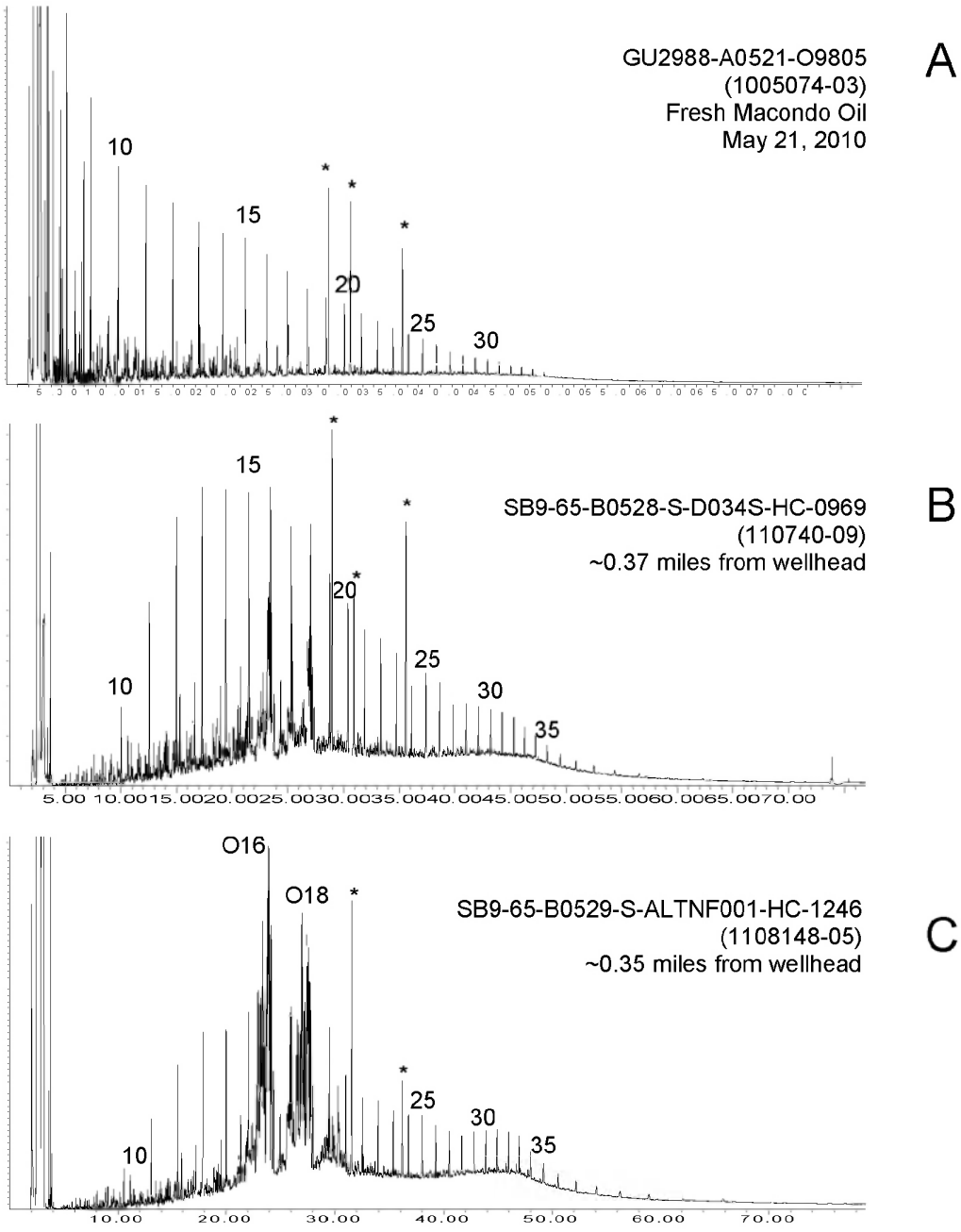

Figure 3: GC/FID chromatograms exemplifying the weathering and range of mixing (oil with synthetic based drilling mud) among surface (0-1 cm) sediments near the wellhead in May 2011. (A) fresh Macondo oil, (B) a sediment containing minimally weathered Macondo oil with minor synthetic-based mud, and (C) a sediment containing synthetic-based mud with a minor amount of a minimally weathered Macondo oil. # - n-alkane carbon number; O# - olefin cluster carbon number; * - internal standard.

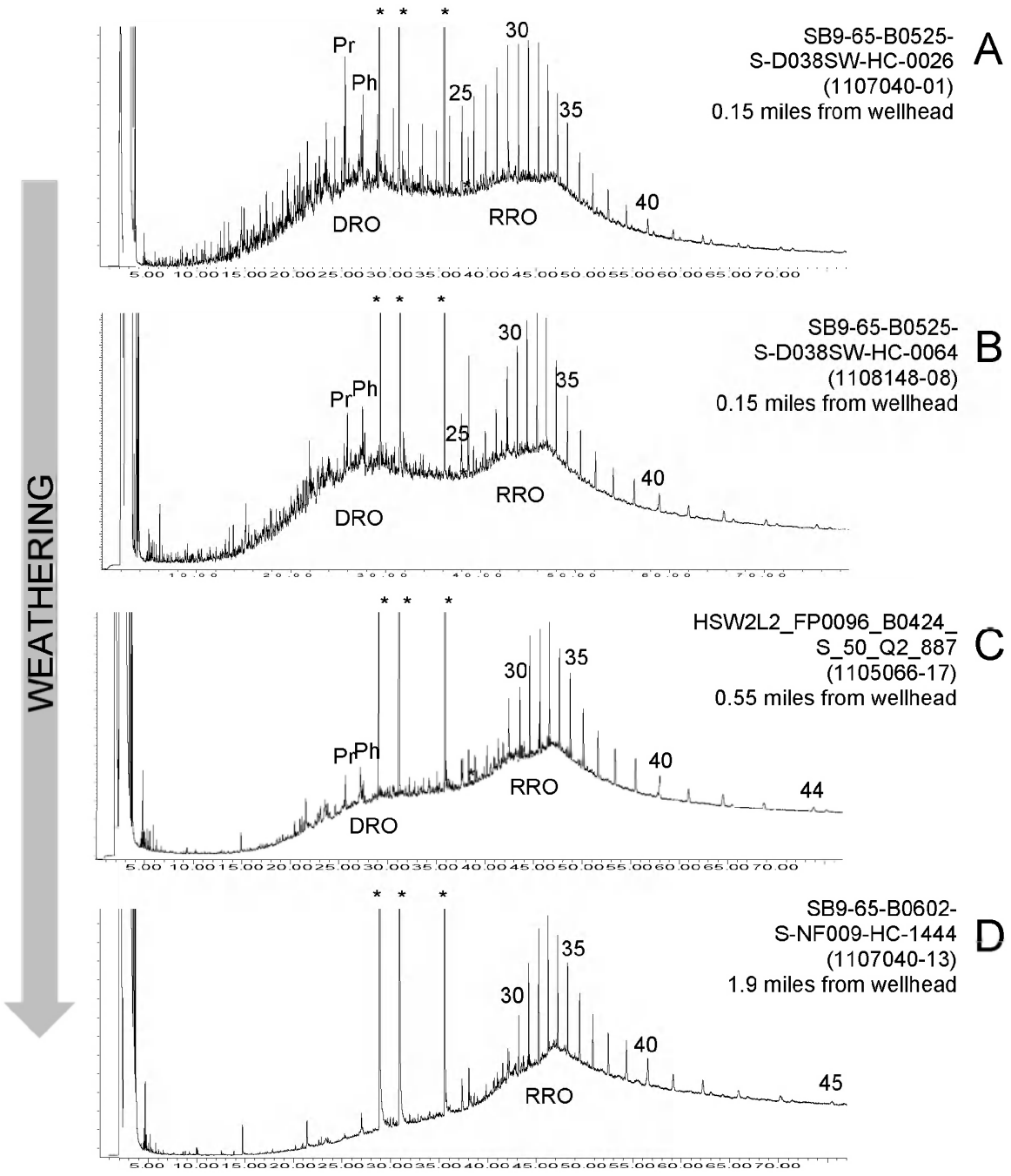

Figure 4: GC/FID chromatograms of surface sediments (0-1 cm) from four cores proximal to the wellhead in 2011 that exemplify the range of weathering of Macondo oil. (A) partially weathered and wax-rich oil, (B) intermediately weathered and wax-rich oil, (C) highly weathered and wax-rich oil, and (D) severely weathered wax-rich oil Pr-pristane; Ph-phytane; # - n-alkane carbon number; * - internal standard. DRO – diesel range organics; RRO – residual range organics.

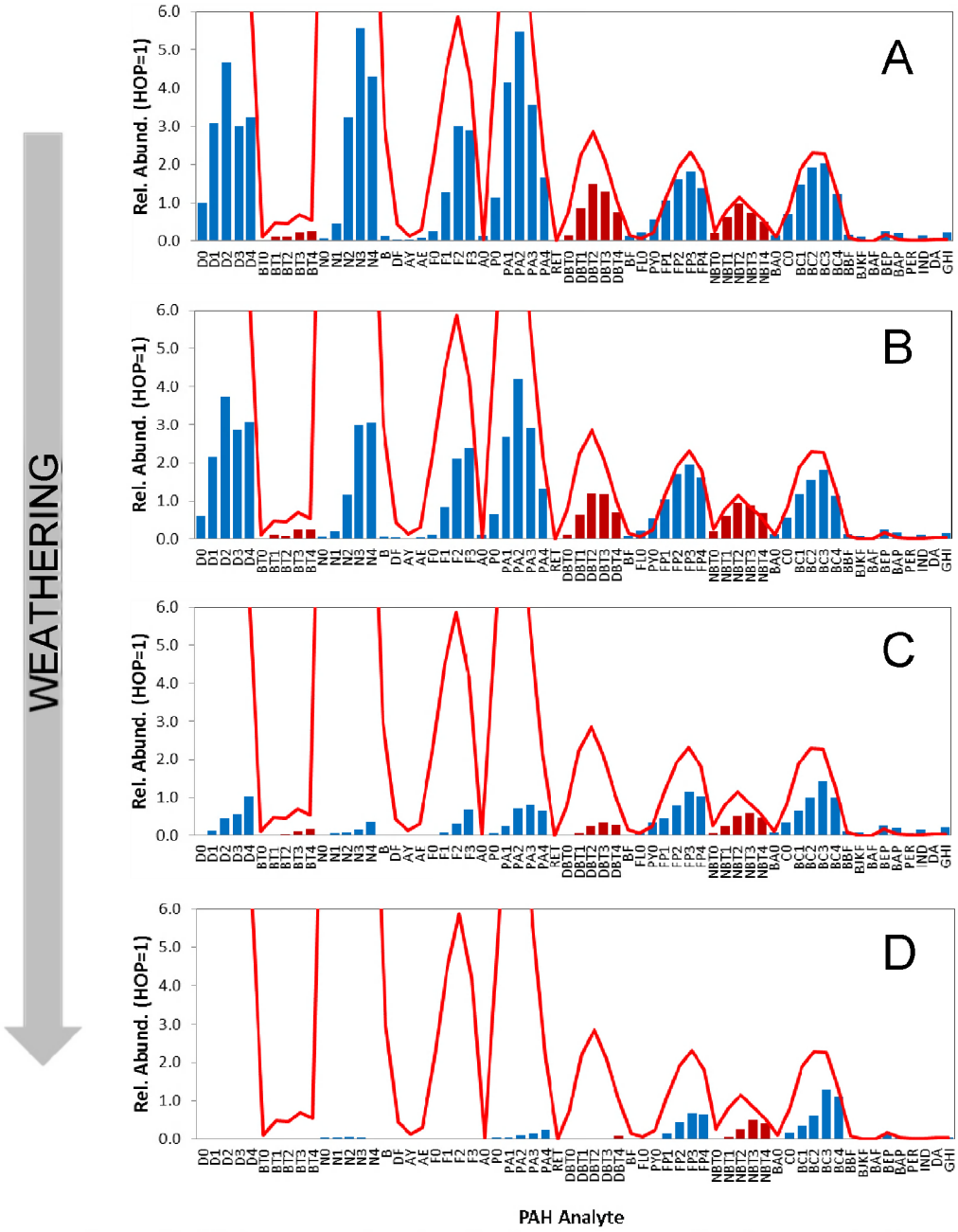

Figure 5: Histograms showing the hopane-normalized concentrations of PAH analytes in surface sediments (0-1 cm) from four cores proximal to the wellhead in 2011 that exemplify the range of weathering of Macondo oil. (A) partially weathered and wax-rich oil, (B) intermediately weathered and wax-rich oil, (C) highly weathered and wax-rich oil, and (D) severely weathered wax-rich oil Red line represents the average hopane-normalized concentrations of PAHs in fresh Macondo oil (Stout, 2015c). Red bars represent sulfur-containing aromatics, viz., benzothiophenes (BT#), dibenzothiophenes (DBT#) and naphthobenzothiophenes (NBT#). See Table 2 for compound abbreviations.

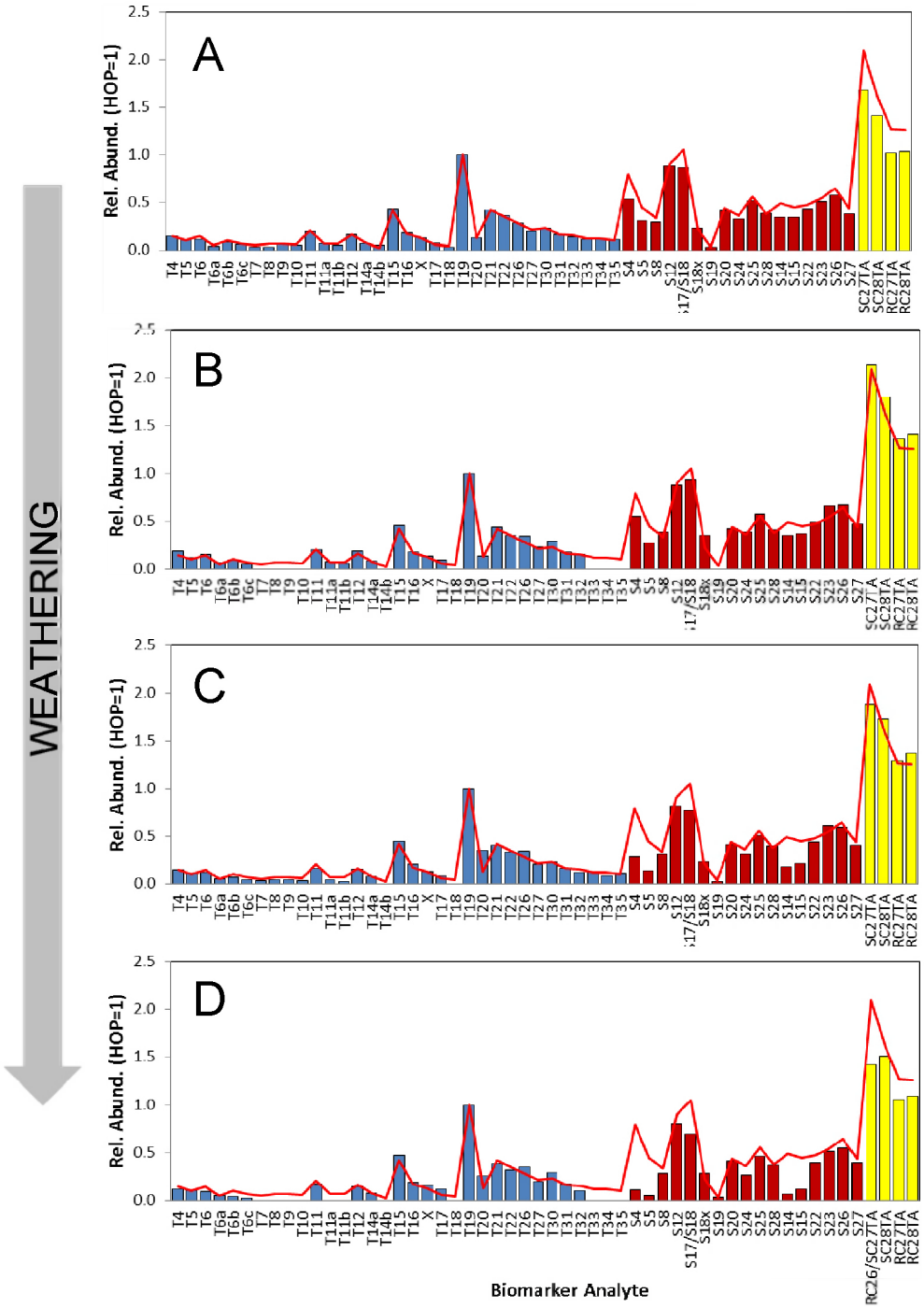

Figure 6: Histograms showing the hopane-normalized concentrations of PAH analytes in surface sediments (0-1 cm) from four cores proximal to the wellhead in 2011 that exemplify the range of weathering of Macondo oil. (A) partially weathered and wax-rich oil, (B) intermediately weathered and wax-rich oil, (C) highly weathered and wax-rich oil, and (D) severely weathered wax-rich oil Red line represents the average hopane-normalized concentrations of PAHs in fresh Macondo oil (Stout, 2015c). Triterpanes (blue; T#), steranes (red; S#) and aromatic steroids (yellow; RC#) Note the progressive depletion of C27 diasteranes (S4 & S5) and C27-ββ steranes (S14 & S15). See Table 2 for compound abbreviations.

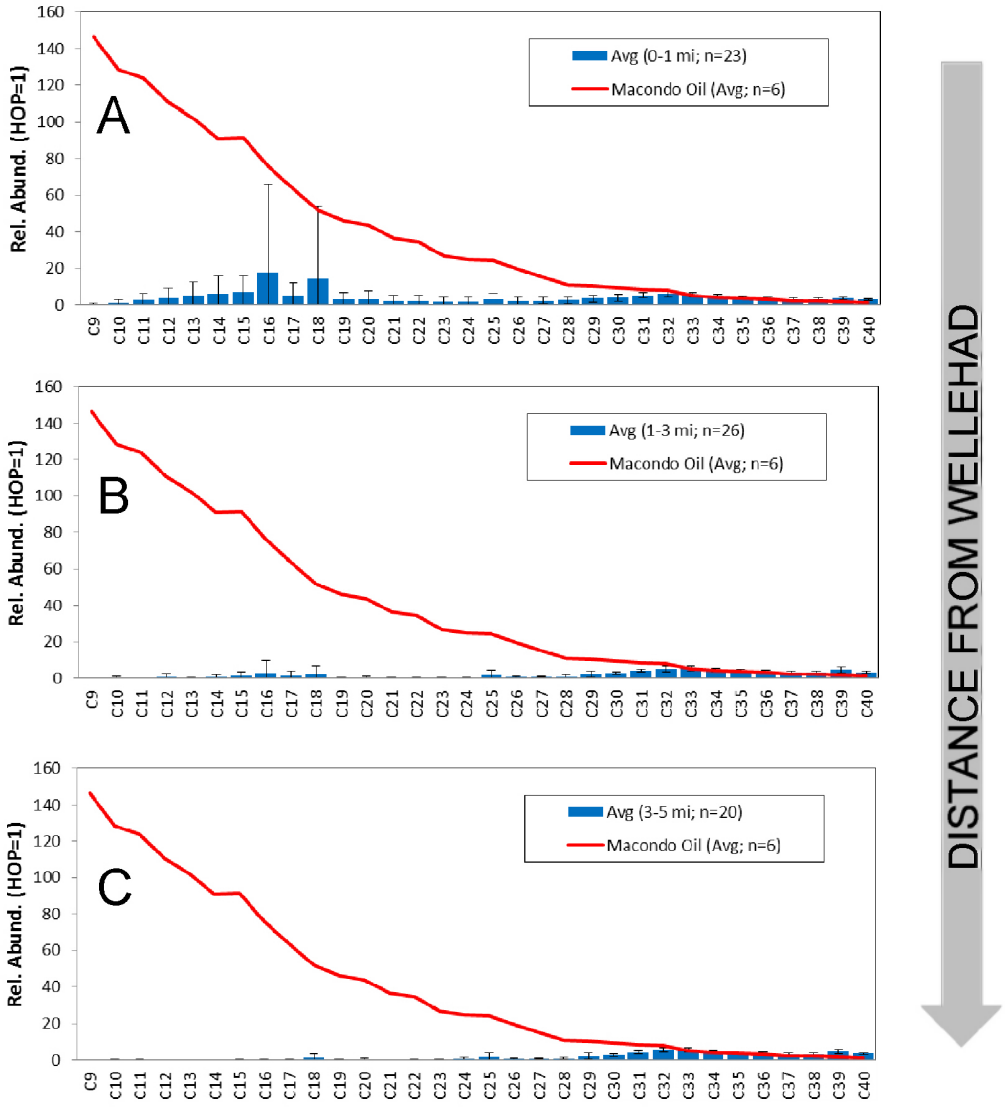

Figure 7: Histograms showing the average hopane-normalized concentrations of n-alkanes in severely weathered Macondo oil in surface sediments (0-1 cm) from 2010-2011: (A) 0 to 1 mile from wellhead, (B) 1 to 3 miles from wellhead, and (C) 3 to 5 miles from wellhead. Red line represents the average hopane-normalized concentrations of n-alkanes in fresh Macondo oil (Stout, 2015c). Error bars = 1σ.

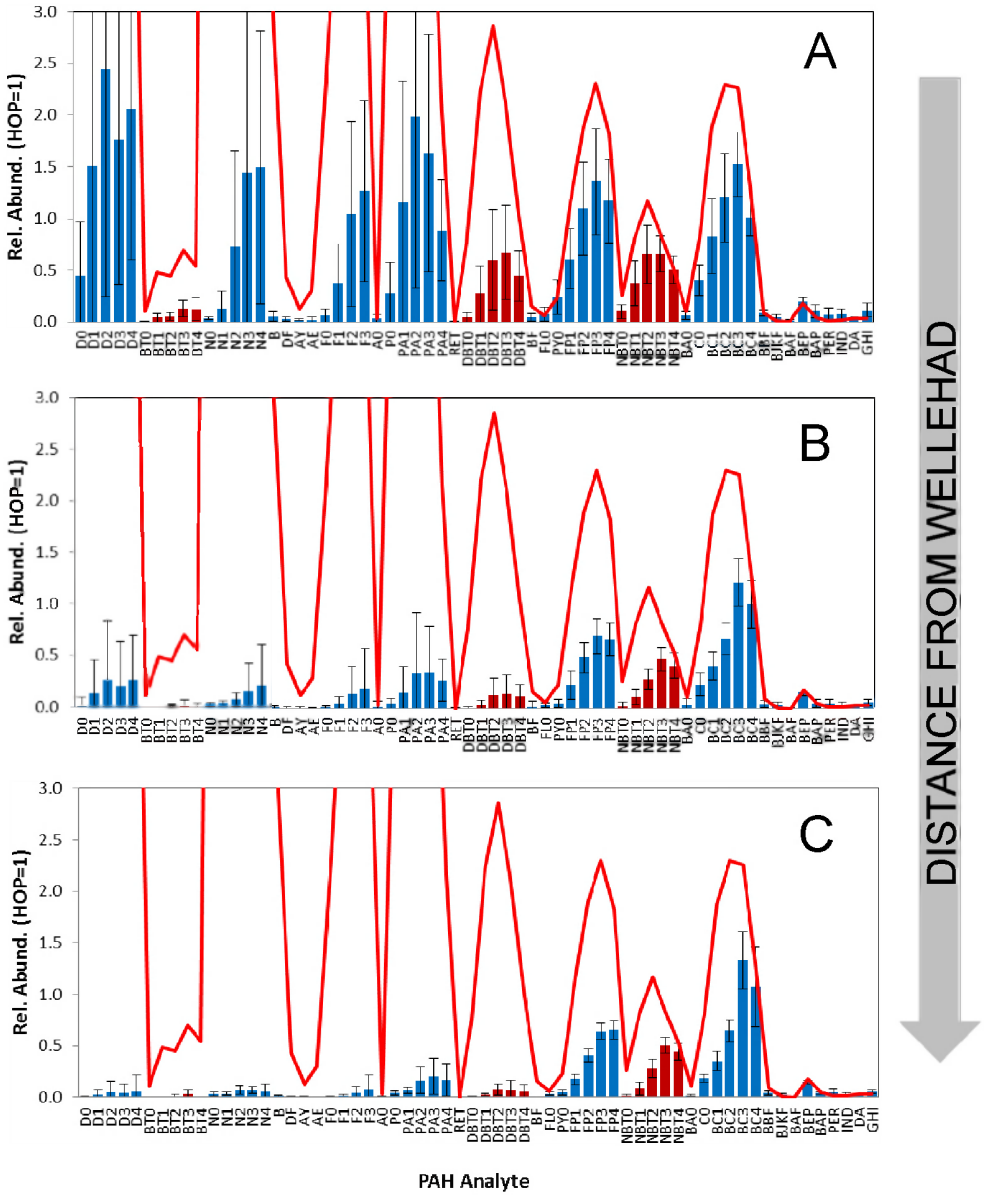

Figure 8: Histograms showing the average hopane-normalized concentrations of PAHs in severely weathered Macondo oil in surface sediments (0-1 cm) from 2010-2011: (A) 0 to 1 mile from wellhead (n=23), (B) 1 to 3 miles from wellhead (n=26) and (C) 3 to 5 miles from wellhead (n=20). Red line represents the average hopane-normalized concentrations of PAHs in fresh Macondo oil (Stout, 2015c). Error bars = 1σ. See Table 2 for compound abbreviations.

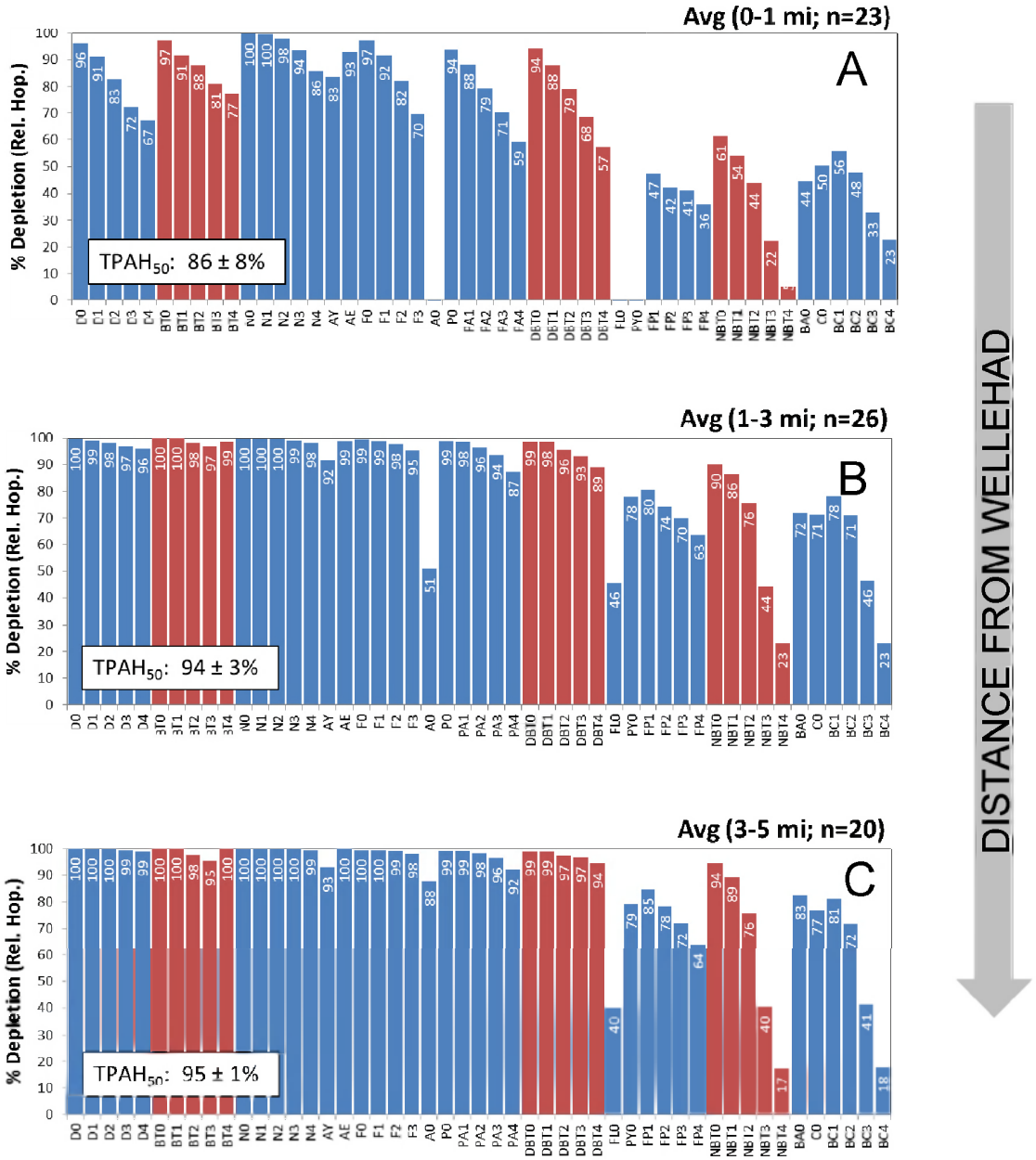

Figure 9: Histograms showing the average percent depletion of PAH homologues in severely weathered Macondo oil in surface sediments (0-1 cm) from 2010-2011: (A) 0 to 1 mile from wellhead (n=23), (B) 1 to 3 miles from wellhead (n=26) and (C) 3 to 5 miles from wellhead (n=20). Individual and TPAH50 percent depletions calculated per Eq. 1). See Table 2 for compound abbreviations.

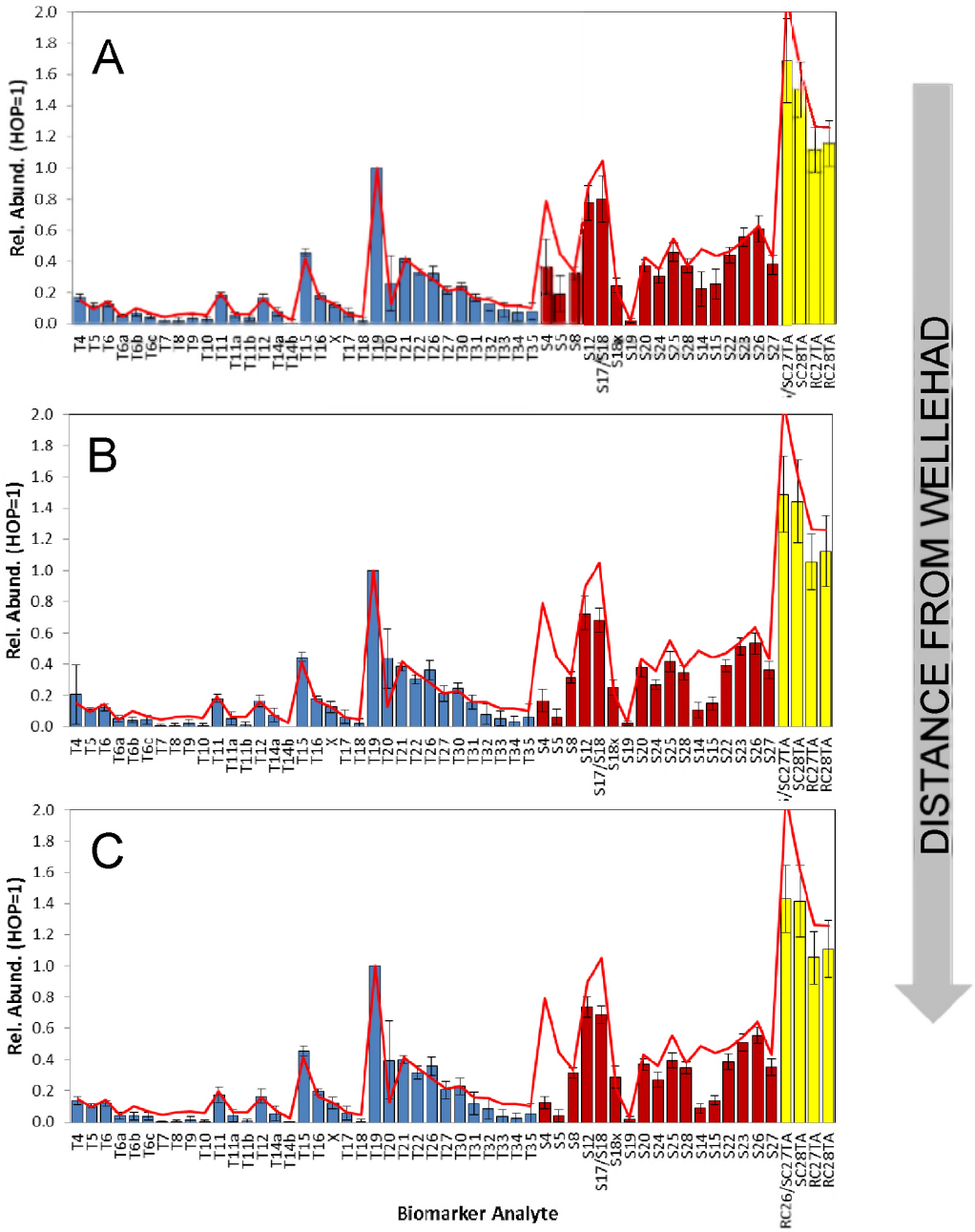

Figure 10: Histograms showing the average hopane-normalized concentrations of biomarkers in severely weathered Macondo oil in surface sediments (0-1 cm) from 2011: (A) 0 to 1 mile from wellhead (n=23), (B) 1 to 3 miles from wellhead (n=26) and (C) 3 to 5 miles from wellhead (n=20). Red line represents the average hopane-normalized concentrations of biomarkers in fresh Macondo oil (Stout, 2015c). Error bars = 1σ. See Table 2 for compound abbreviations.

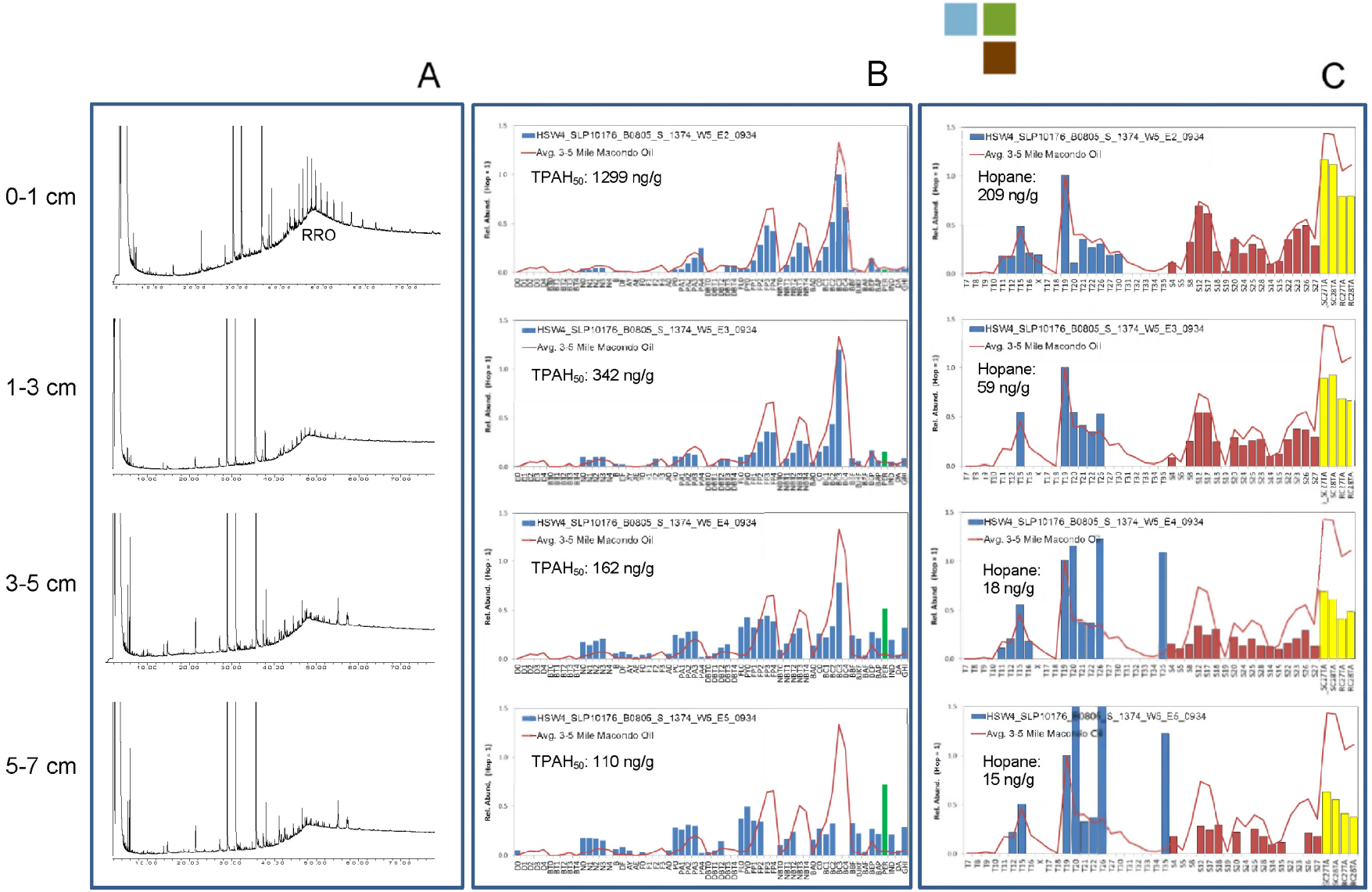

Figure 11: (A) GC/FID chromatograms and hopane-normalized (B) PAH and (C) biomarker distributions for sediment samples from the HSW4_SLP10176_B0805_1374_W5_E_934 core taken atop Biloxi Dome (6.1 miles from wellhead). The 0-1 cm interval contains wax-rich, severely weathered Macondo oil consistent with that observed in sediments 3-5 miles from wellhead (red lines) and was classified as an "A" (Table 3). The 1-3 cm interval may contain trace of Macondo oil ("C" per Table 3) while the deeper intervals are consistent with ambient (background) hydrocarbons ("D" per Table 3). See Table 2 for compound abbreviations.

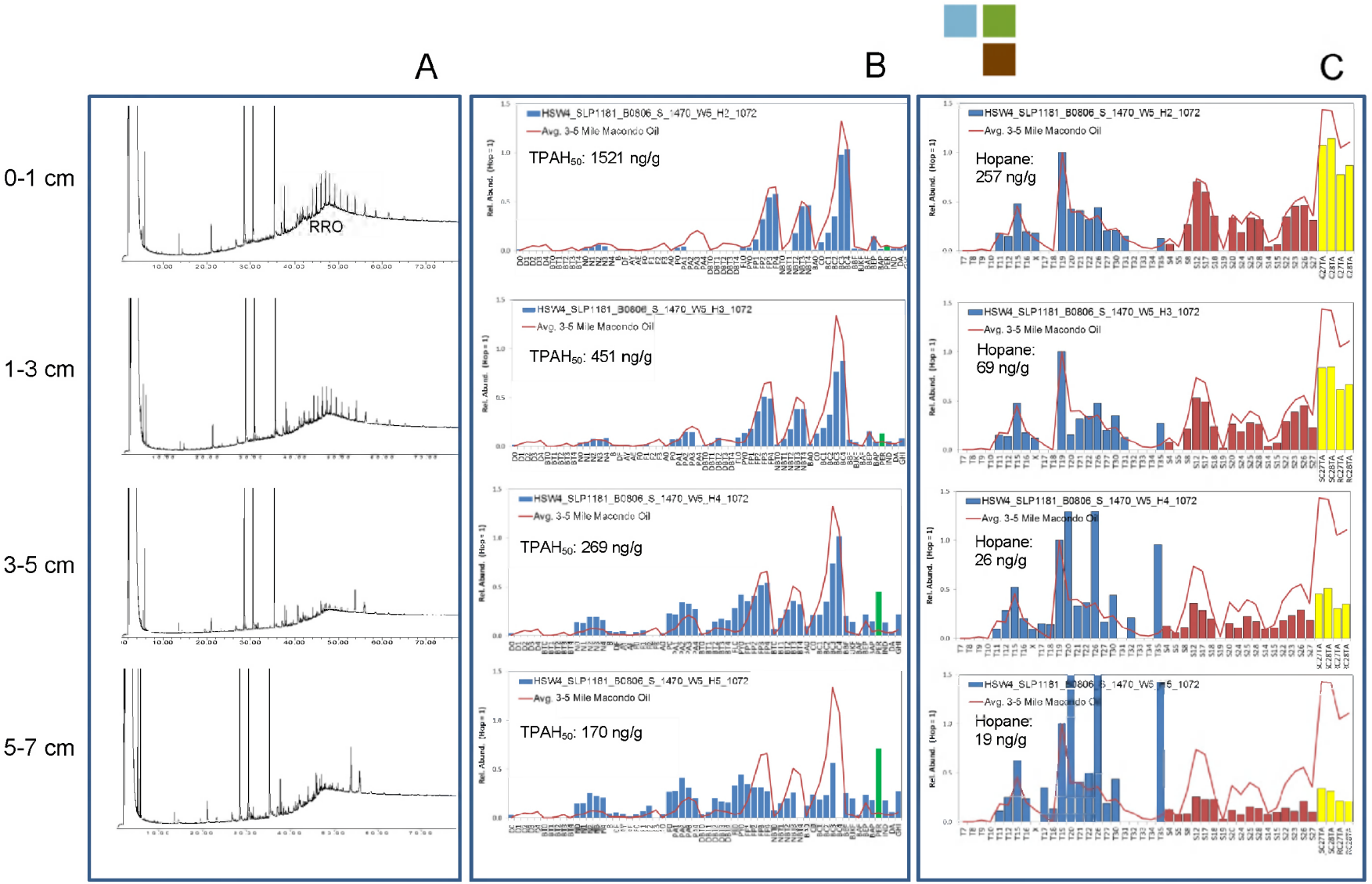

Figure 12: (A) GC/FID chromatograms and hopane-normalized (B) PAH and (C) biomarker distributions for sediment samples from the HSW4_SLP1181_B0806_1470_W5_H_1072 core taken west of Biloxi Dome (11.8 miles from wellhead). The 0-1 cm interval contains wax-rich, severely weathered Macondo oil consistent with that observed in sediments 3-5 miles from wellhead (red lines) and was classified as an "A" (Table 3). The 1-3 cm interval may contain trace of Macondo oil ("C" per Table 3) while the deeper intervals are consistent with ambient (background) hydrocarbons ("D" per Table 3).

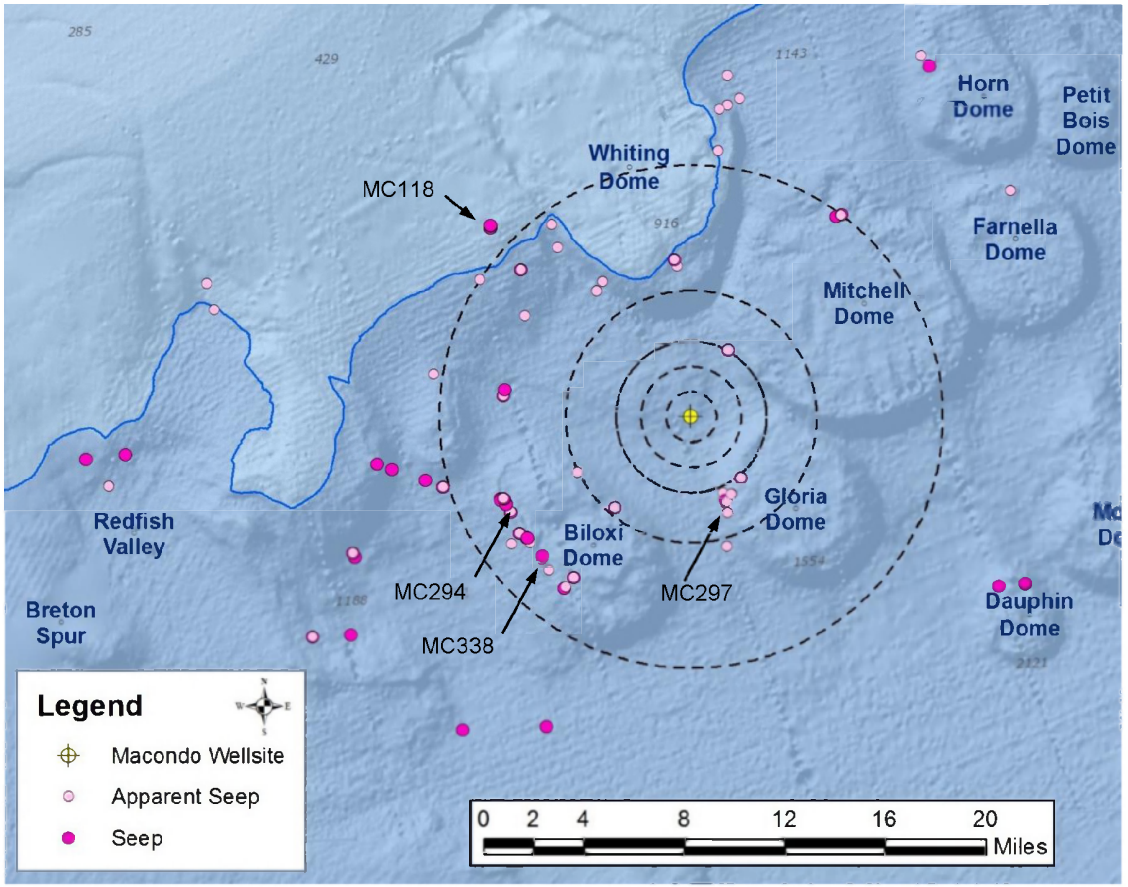

Figure 13: Locations of seeps or suspected seeps based upon core results (2010-2011). At least one interval from these cores was classified as "E" (per Table 3). Some seep locations still have Macondo oil present at the surface (e.g., Fig. 17 from MC118 area). A few prominent seeps locations are indicated and referred to by the BOEM OCS Block in which they occur. Radii of circles show 1, 2, 3, 5 and 10 miles from wellhead.

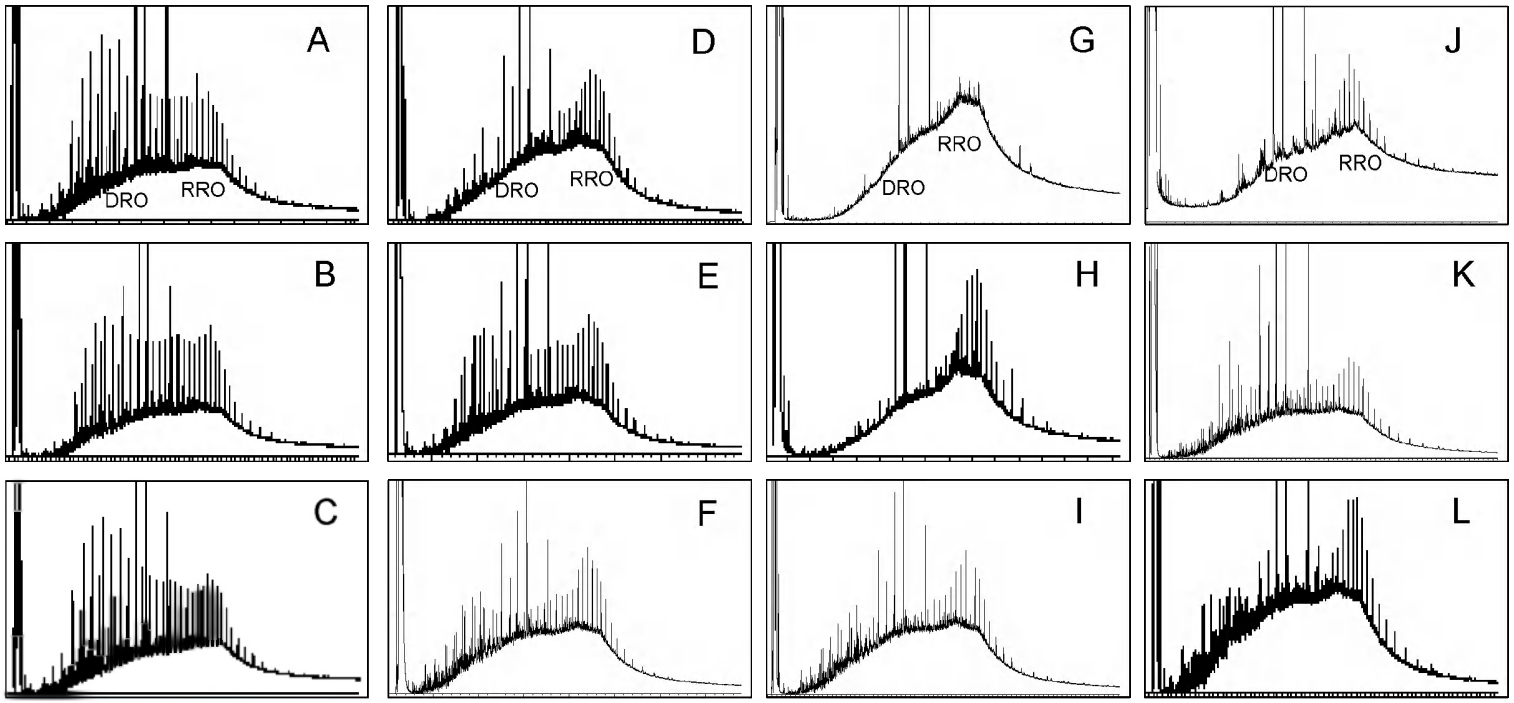

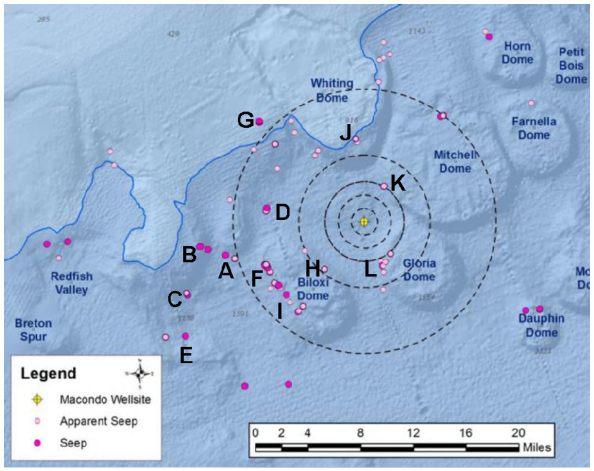

Figure 14: GC/FID chromatograms for a variety of seeps showing varying degrees of weathering. Map shows approximate locations by letter code. DRO-diesel range organics; RRO –residual range organics. Three off-scale peaks are internal standards.

A: HSW2L2_BRD055B_B0413_S_50_E2_464
B: HSW2L2_BRE056A_B0414_S_50_A2_485
C: HSW2L2_BRD051_B0412_S_50_D2_427
D: HSW6L2_FP6223_B0111_S_1392_50_G2_0083
E: HSW6L2_SLP12242_B1015_S_1376_50_H2_0309
F: HSW6L2_TWG254_B1018_S_1361_50_B2_0465
G: HC3_B1021_S_E8_MC11824_HC_020
H: SB9-65-B0605-S-LBNL4-HC-2548
I: HSW6L2_SLP3230_B1012_S_1385_50_P2_0158
J: HSW2_HSW2017_B0331_S_W5_E2_131
K: HSW6_FP10189_B0828_S_1469_50_D2_0092
L: HSW6_SEP8250L_B01017S_1558_50_T2_0421

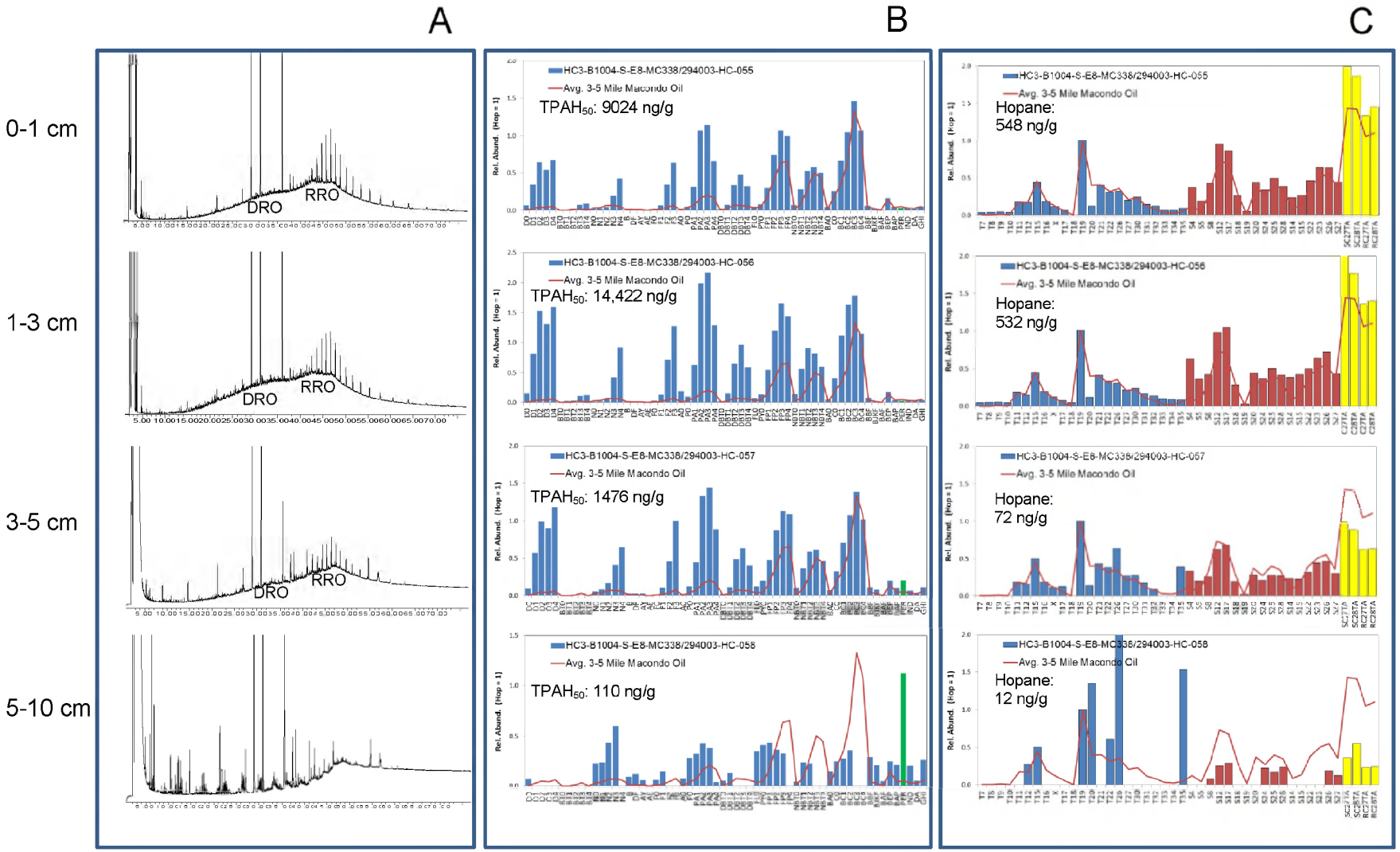

Figure 15: (A) GC/FID chromatograms and hopane-normalized (B) PAH and (C) biomarker distributions for sediment samples from the HC3-B1004-S-E8-MC338_294003-HC-055-058 core taken in northwest Biloxi Dome (MC338; 8.1 miles from wellhead). The 0-5 cm intervals contains wax-rich oil with a prominent DRO, as evidenced in prominent decalins, naphthalenes and phenanthrenes. A seep oil is present in 0-5 cm intervals ("E" per Table 3) while the 5-10 cm interval is consistent with ambient (background) hydrocarbons ("D" per Table 3). See Table 2 for peak identifications.

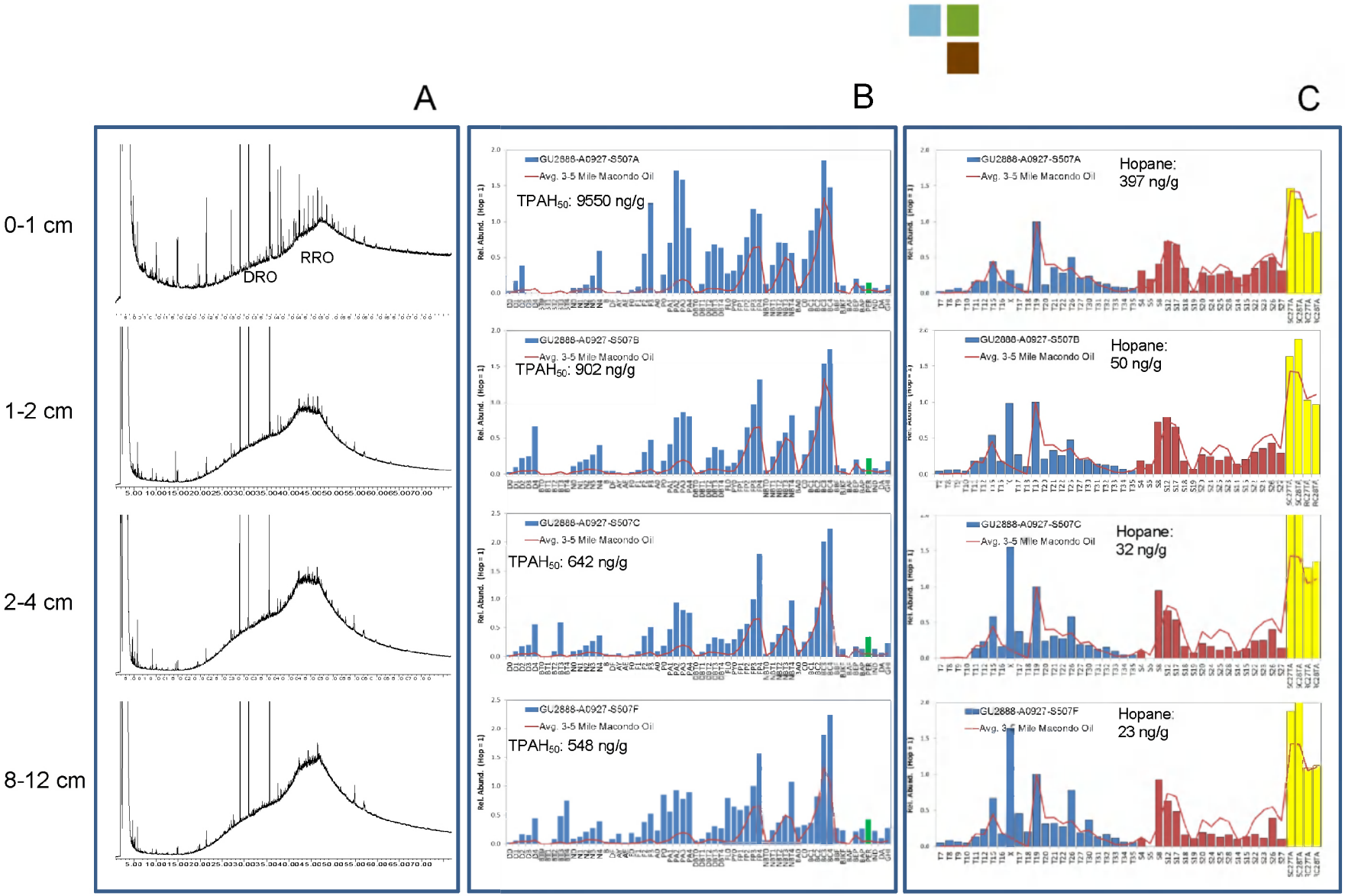

Figure 16: (A) GC/FID chromatograms and hopane-normalized (B) PAH and (C) biomarker distributions for sediment samples from the GU2888-A0927-S507 core taken in MC118 area (10.8 miles northwest of the wellhead). A seep oil is present throughout the core, however, the surface (0-1 cm) also contains a wax-rich, severely weathered Macondo oil component; see text. The 0-1 cm is considered a "B" (per Table 3). All other intervals are "E" (per Table 3). See Table 2 for peak identifications.

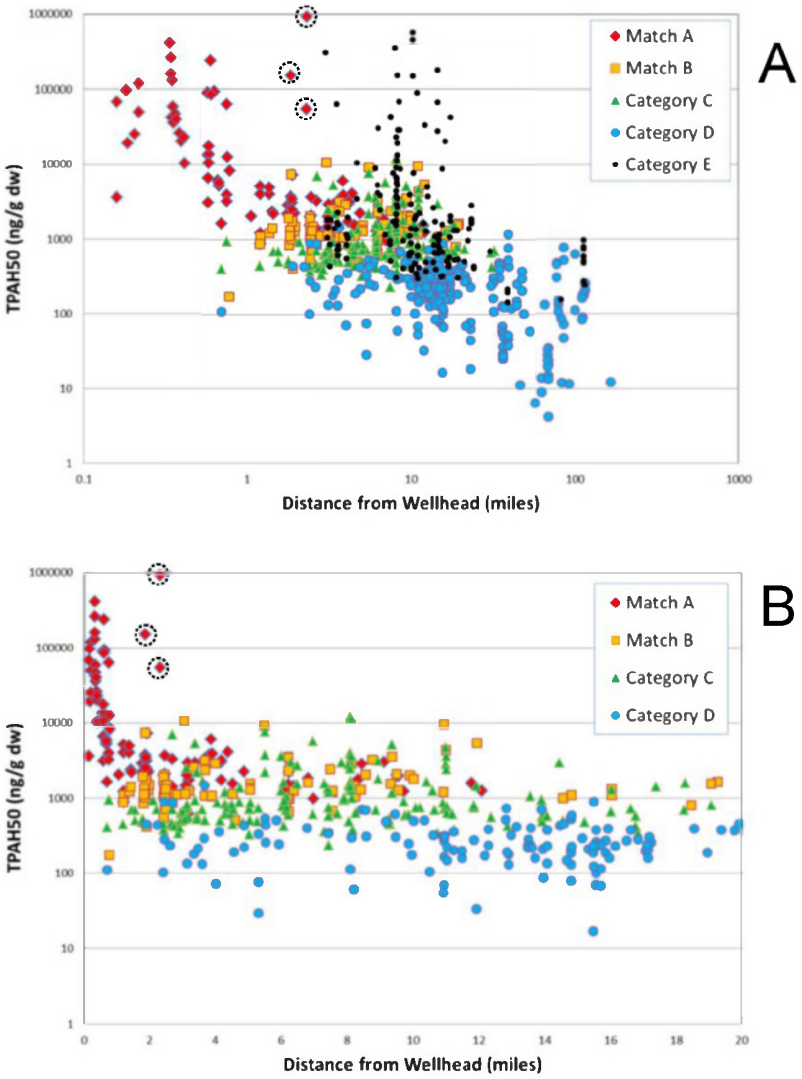

Figure 17: Graphs showing the concentrations of $TPAH_{50}$ in surface sediments (n=725) in cores versus distance from the Macondo well by forensic category ("A" to "E"; per Table 3). (A) all results and (B) all results excluding all "E" samples and all samples beyond 20 miles. All data from Appendix 1. Dashed circles indicate sediments impacted by sunken *in situ* burn residues.

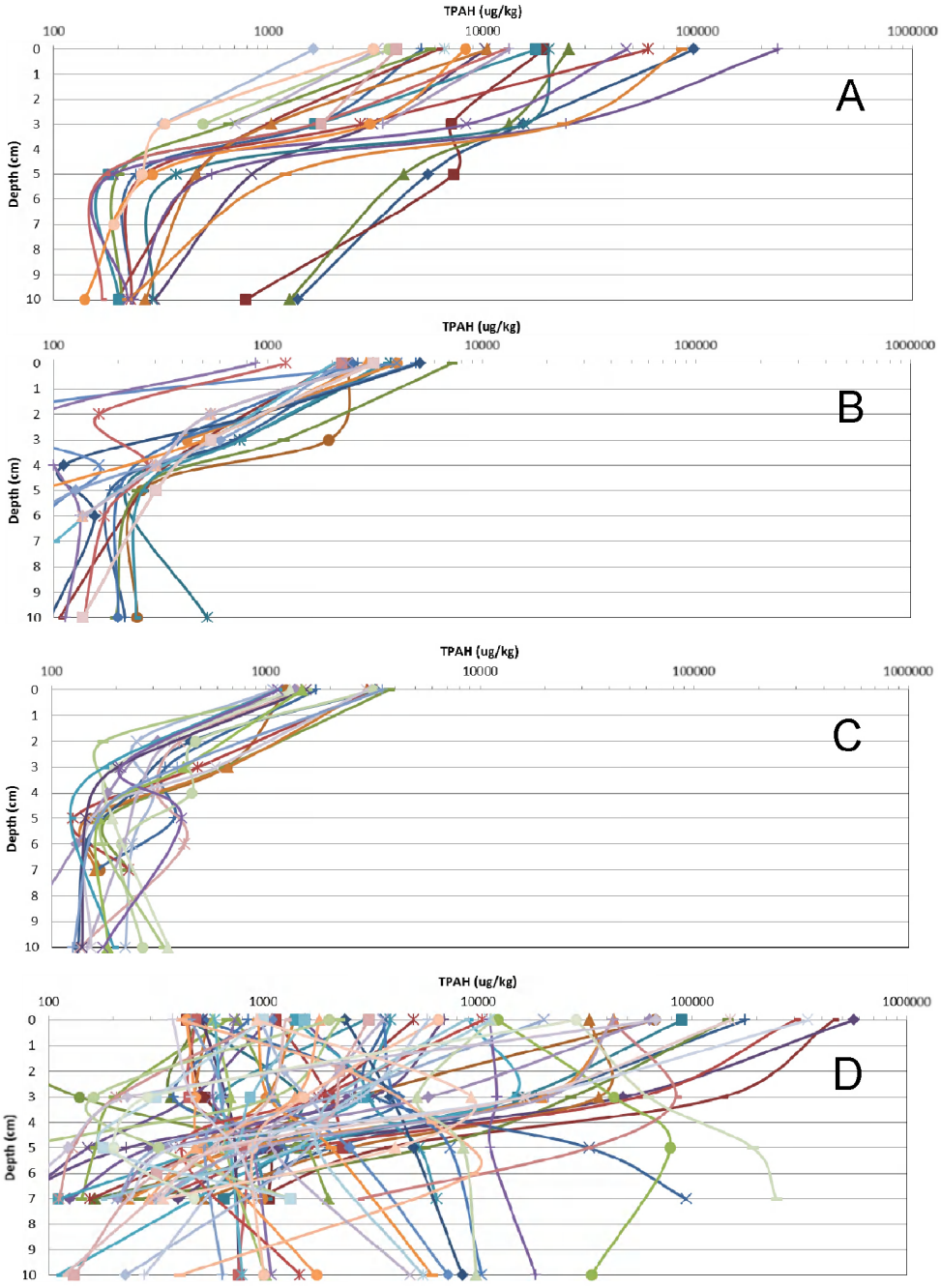

Figure 18: Graphs showing the concentrations of $TPAH_{50}$ cores *versus* sediment depth for cores (2010/2011) containing wax-rich, severely weathered Macondo oil (A) 0 to 1 mile (n=23), (B) 1 to 3 miles (n=26), and (C) 3 to 5 miles (n=20). (D) shows all cores within 20 miles of the well containing seeps or apparent seeps ("E" per Table 3). Top depths of each interval are plotted on y-axes.

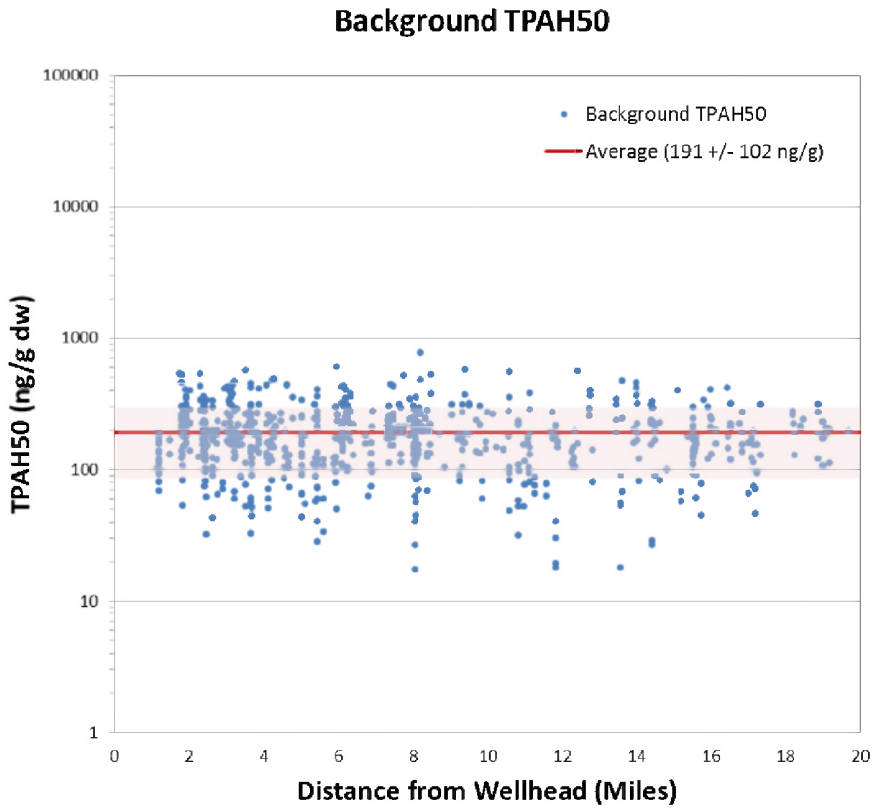

Figure 19: Graphs showing the concentrations of $TPAH_{50}$ in all (n=729) sediment samples > 3 cm deep (2010/2011) 1 to 20 miles of the Macondo well considered to contain only background (ambient) PAHs (i.e., not impacted by Macondo oil or seep oil). Average (191 ng/g; red line) and 1s (±102; pink shading) are indicated. Variability indicates variable (site-specific) background exist in the study area, though 95% are below 404 ng/g $TPAH_{50}$.

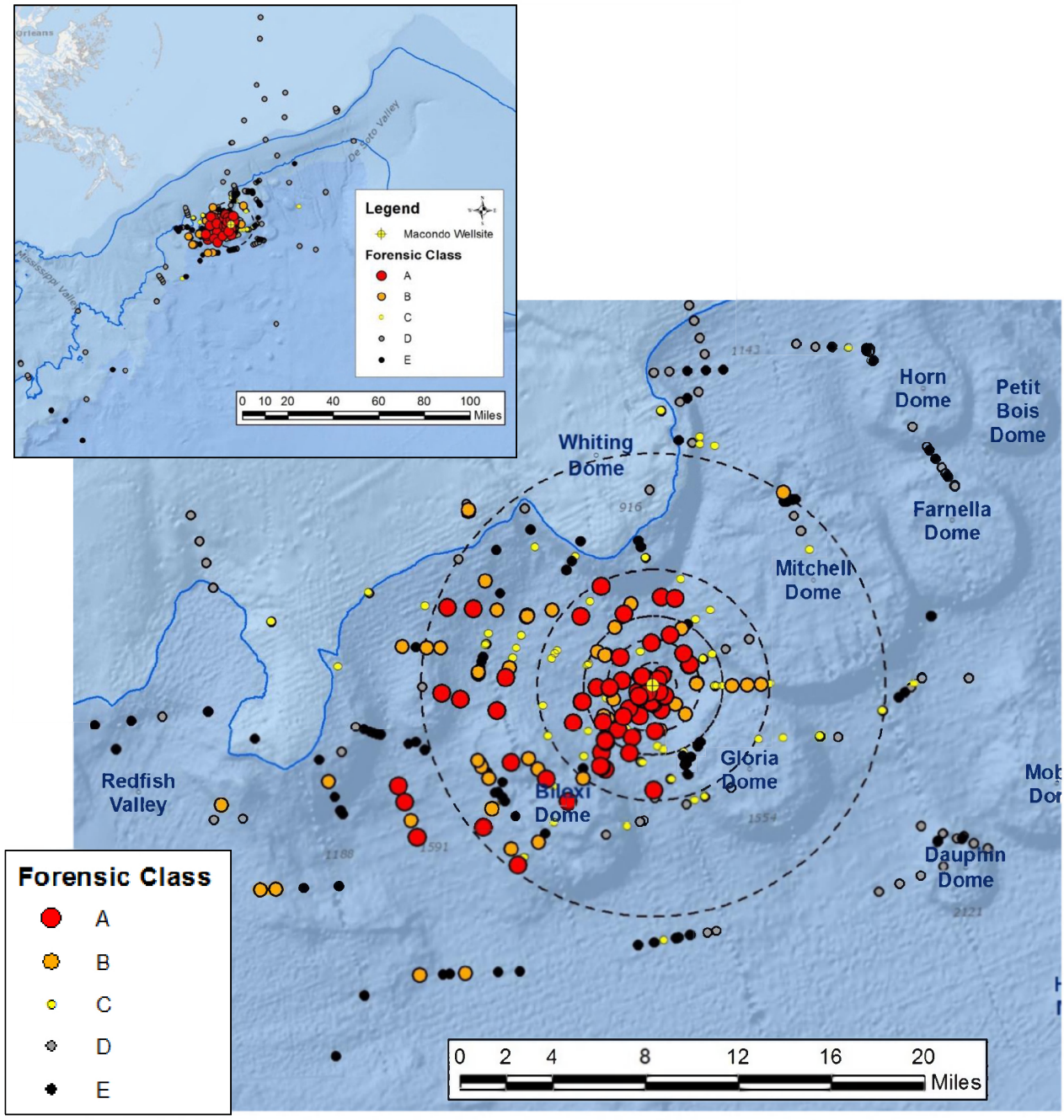

Figure 20: Maps showing the forensic classifications for 725 surface sediment samples collected in 2010-2011. Radii of circles show 1, 2, 3, 5 and 10 miles from wellhead.

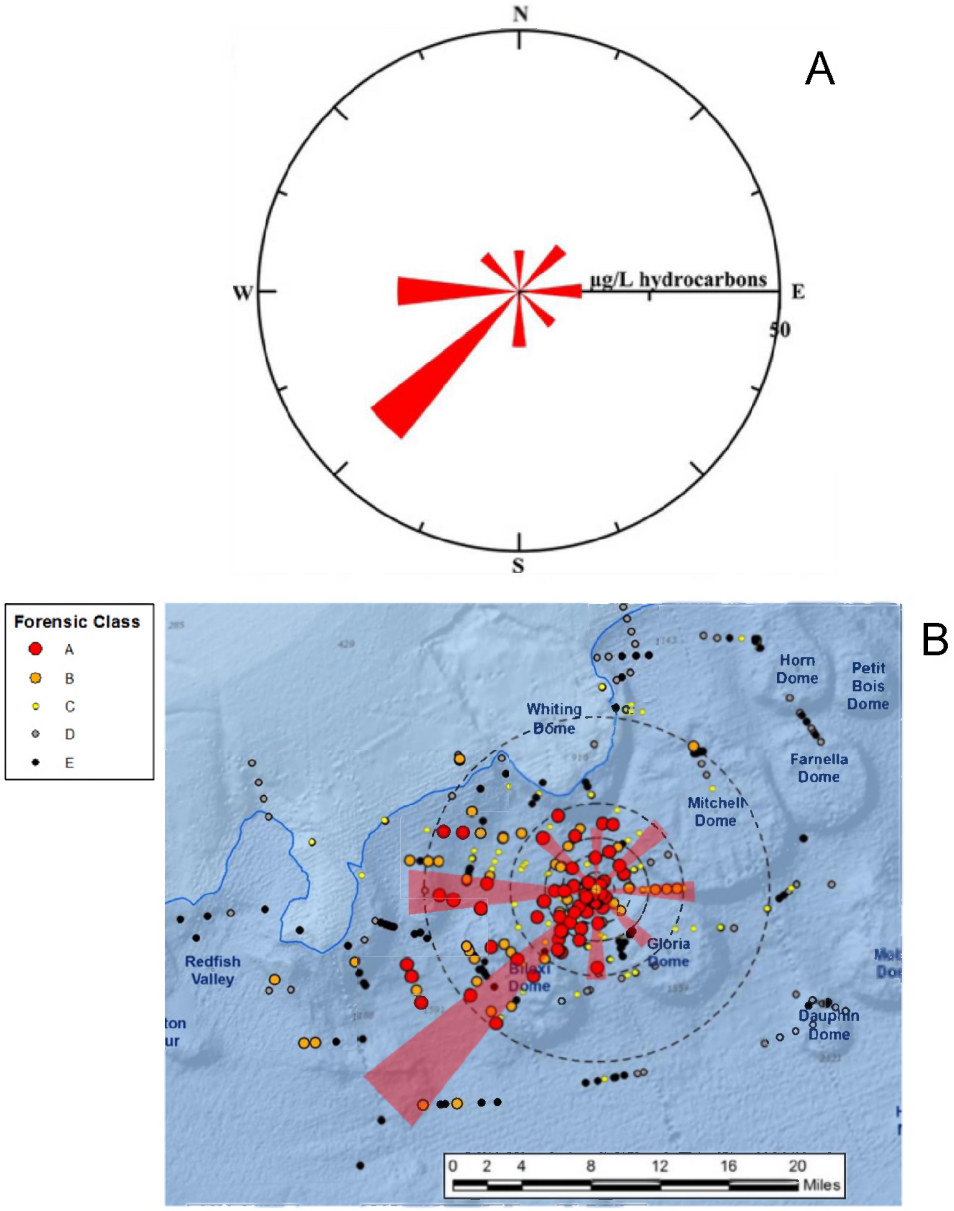

Figure 21: (A) Percent detectable concentrations of hydrocarbons in each of eight directions from the wellhead measured in water samples from the deep-sea plume (1050-1300 m) in 2010. Reproduced from Spier et al. (2013; Fig. 3D). (B) Data from (A) superimposed on the surface sediment forensic map (from Figure 20). Note the dominant directions (southwest and west) of oil in the deep-sea plume were also the dominant directions of oil found in surface sediments.

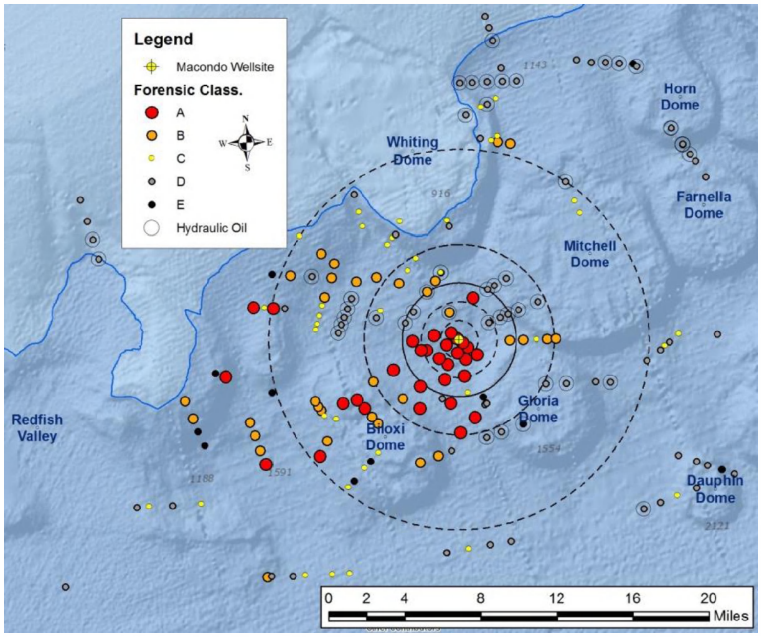

A

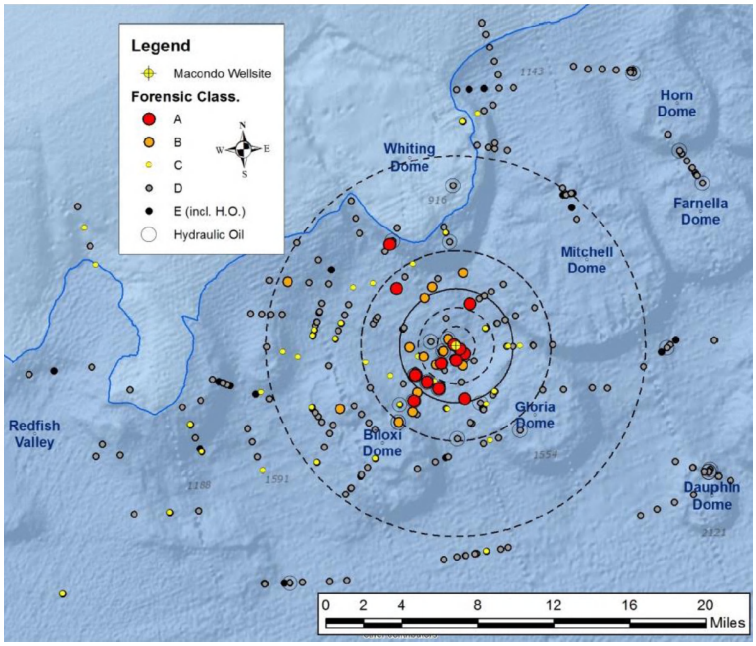

B

Figure 22: Maps showing the forensic classifications for (A) slurp gun filter samples and (B) core supernatant samples collected in 2010-2011. Radii of circles show 1, 2, 3, 5 and 10 miles from wellhead. Note that some samples were impacted by trace amounts of hydrocarbons derived from hydraulic oil that is presumed to have leaked from the ROV in use on selected cruises. These are indicated by the circled samples. This had minimal effect on the ability to classify these samples.

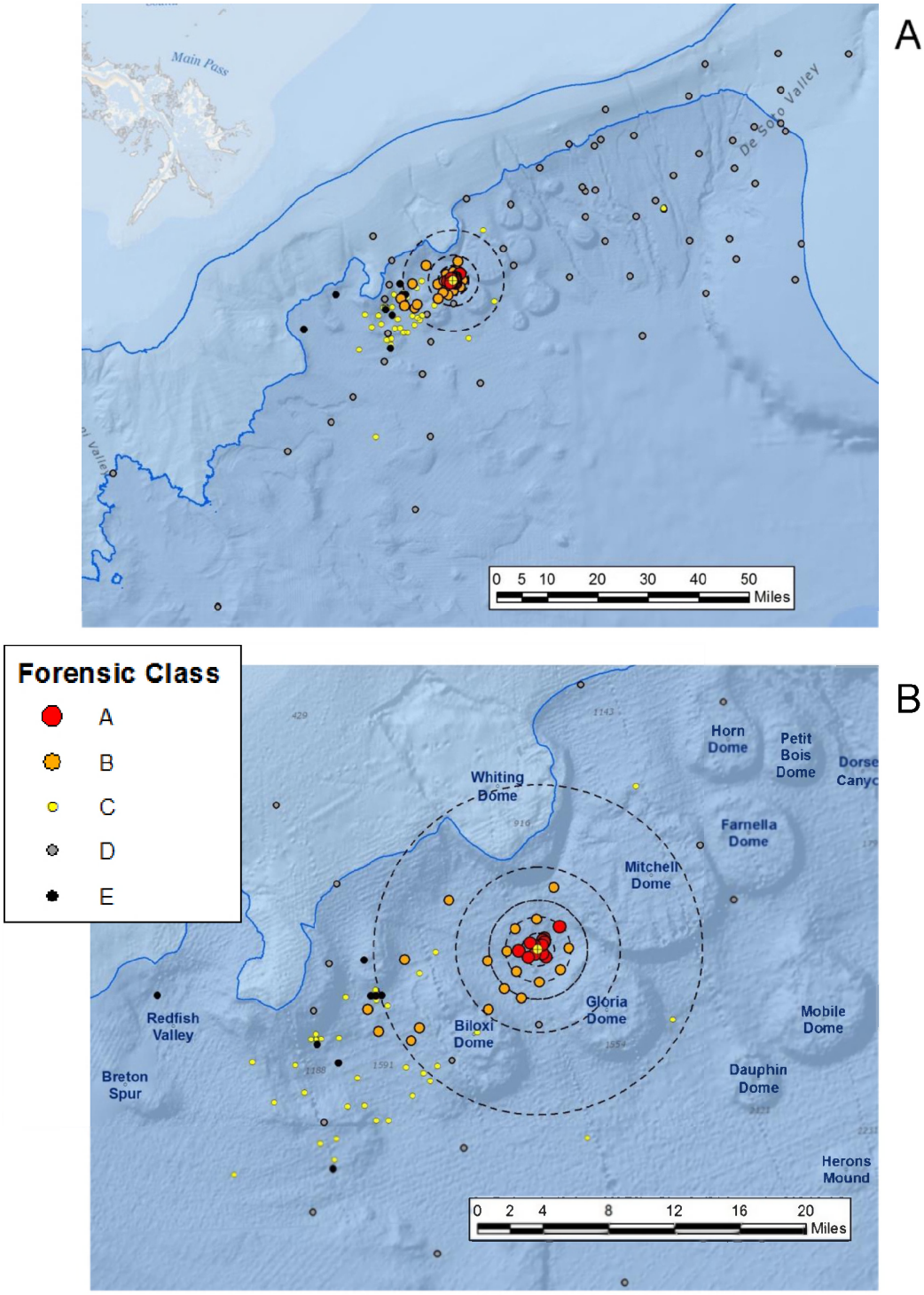

Figure 23: Maps showing the forensic classifications for 201 surface sediment samples collected in 2014. (A) regional scale and (B) basinal scale. Radii of circles show 1, 2, 3, 5 and 10 miles from wellhead.

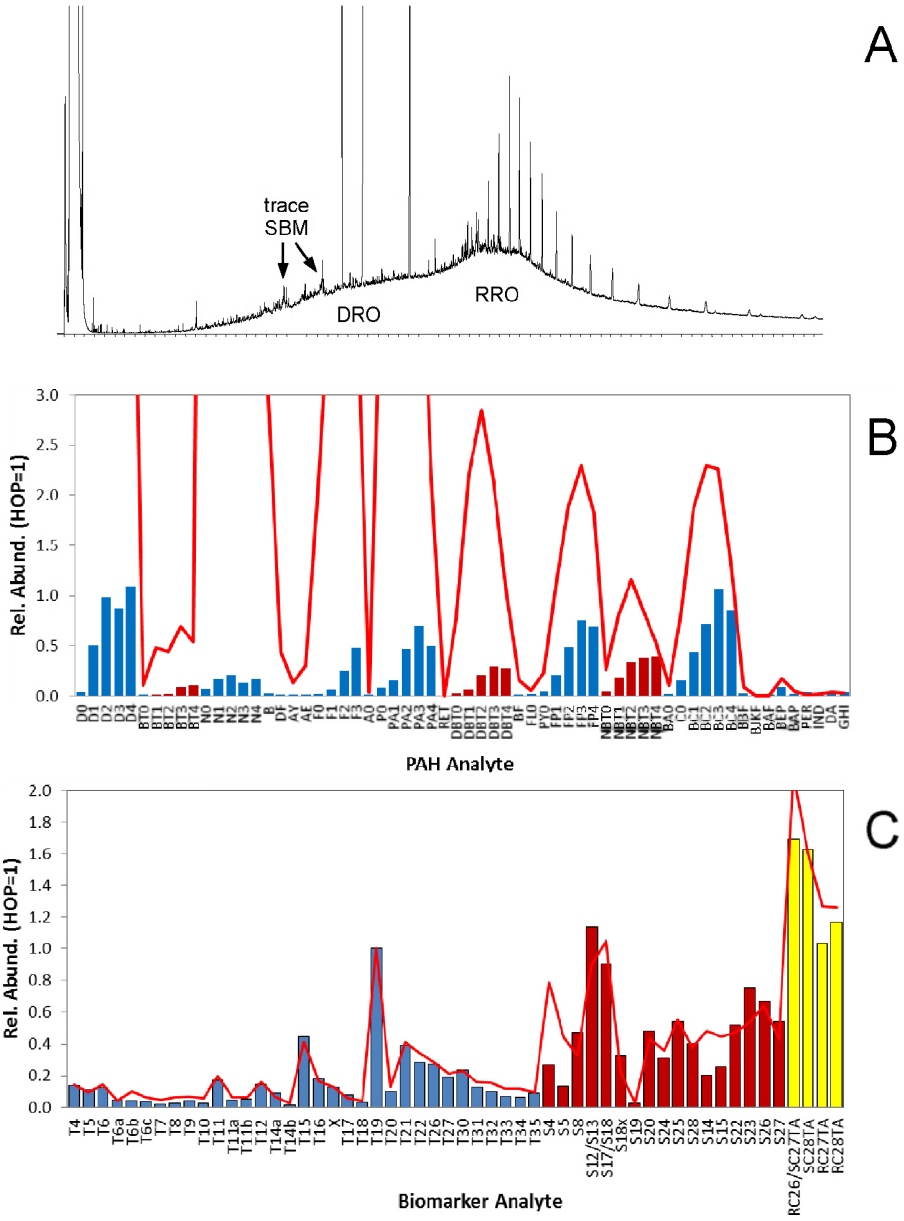

Figure 24: Representative features of the oil found in a surface sediment less than 1 mile from the well in 2014; RH1-65-E0603-S-D031S-HC-0559. (A) GC/FID chromatogram, (B) hopane-normalized PAHs, (C) hopane-normalized biomarkers. See Table 2 for compound abbreviations. DRO-diesel range hydrocarbons; RRO-residual range hydrocarbons. Red line reflects distribution in unweathered Macondo oil (Stout, 2015c). Three large peaks in (A) are internal standards.

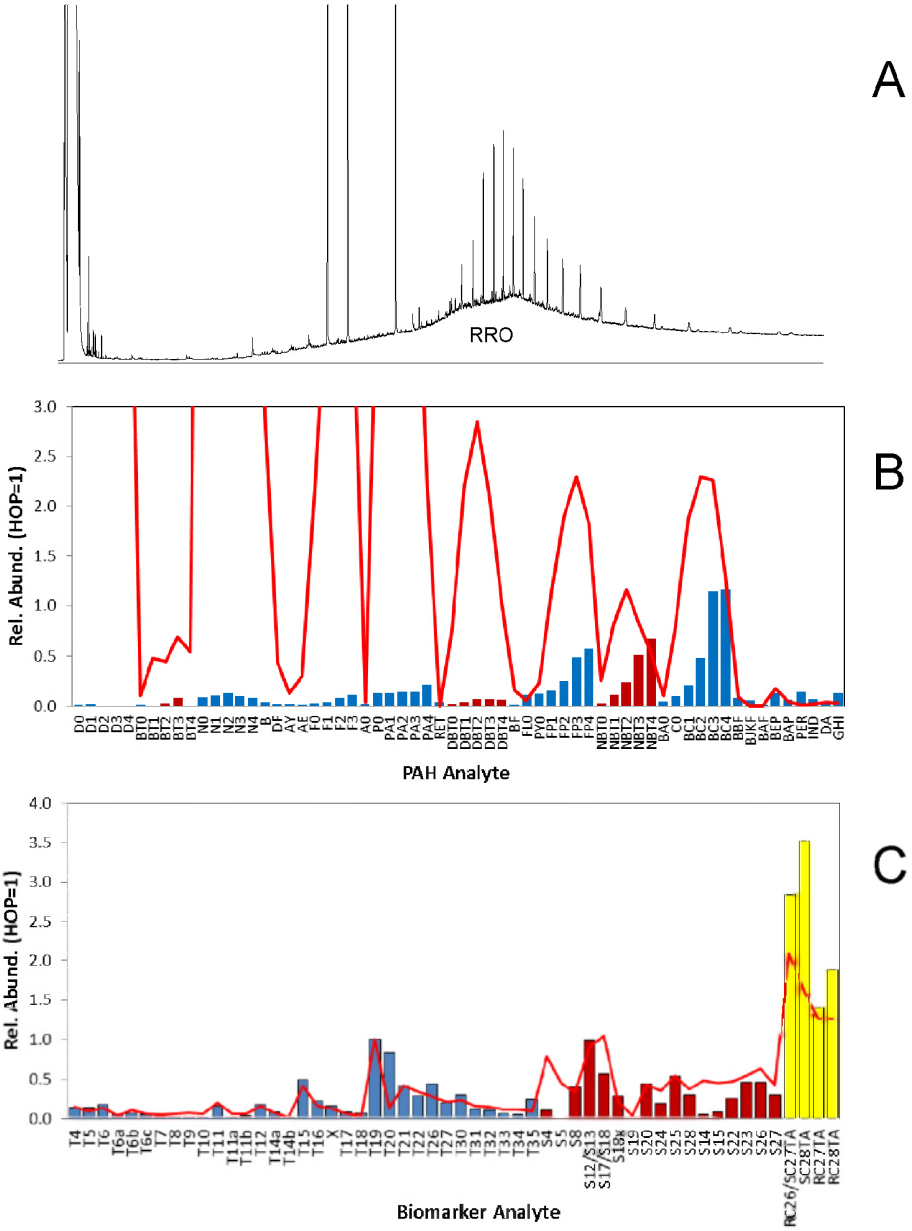

Figure 25: Representative features of the oil found in a surface sediment 1 to 5 miles from the well in 2014; RH1-65-E0605-S-NF009-HC-1268. (A) GC/FID chromatogram, (B) hopane-normalized PAHs, (C) hopane-normalized biomarkers. See Table 2 for compound abbreviations. RRO-residual range hydrocarbons. Red line reflects distribution in unweathered Macondo oil (Stout, 2015c). Three large peaks in (A) are internal standards.

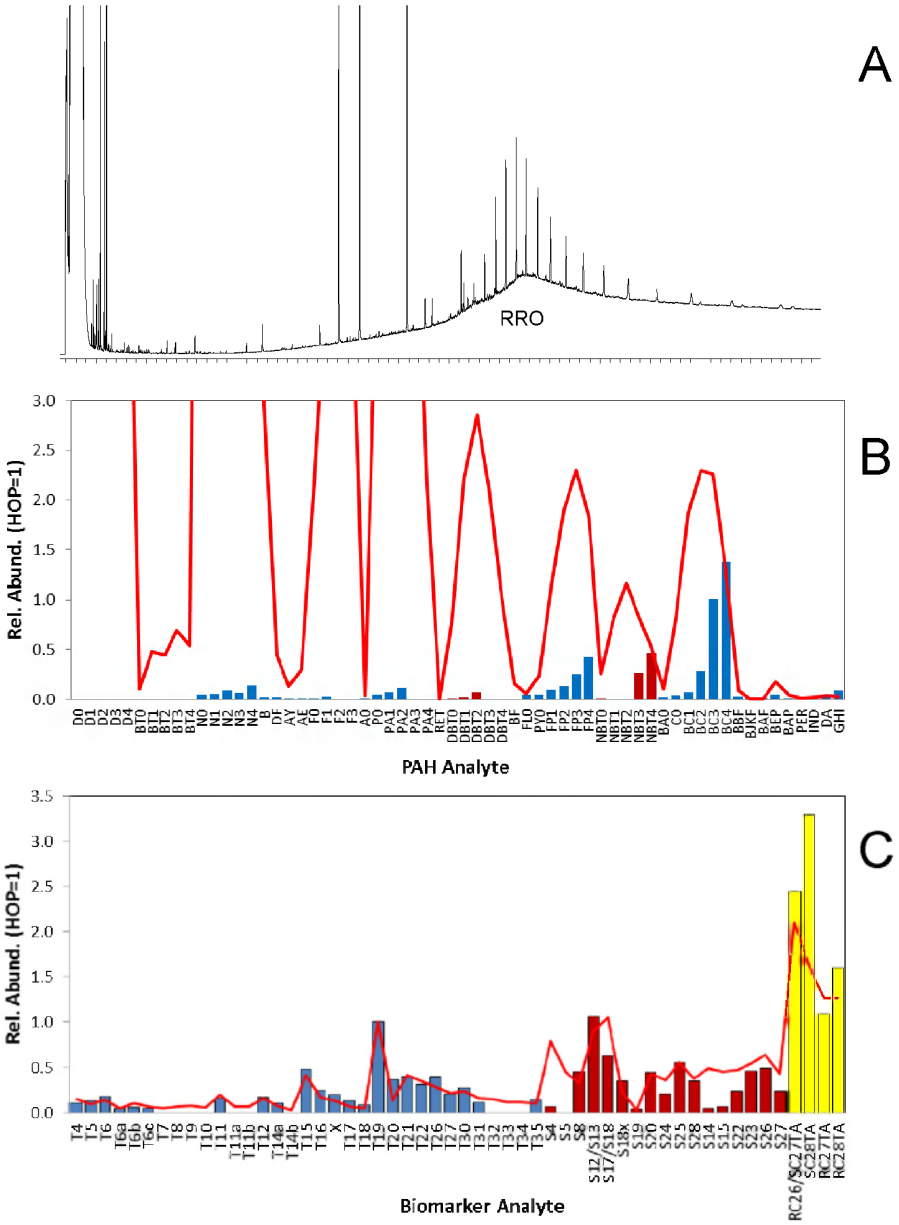

Figure 26: Representative features of the oil found in a surface sediment beyond 5 miles from the well in 2014; RH1-359-E0625-S-MC338-1-HC-4272. (A) GC/FID chromatogram, (B) hopane-normalized PAHs, (C) hopane-normalized biomarkers. See Table 2 for compound abbreviations. RRO-residual range hydrocarbons. Red line reflects distribution in unweathered Macondo oil (Stout, 2015c). Three large peaks in (A) are internal standards.

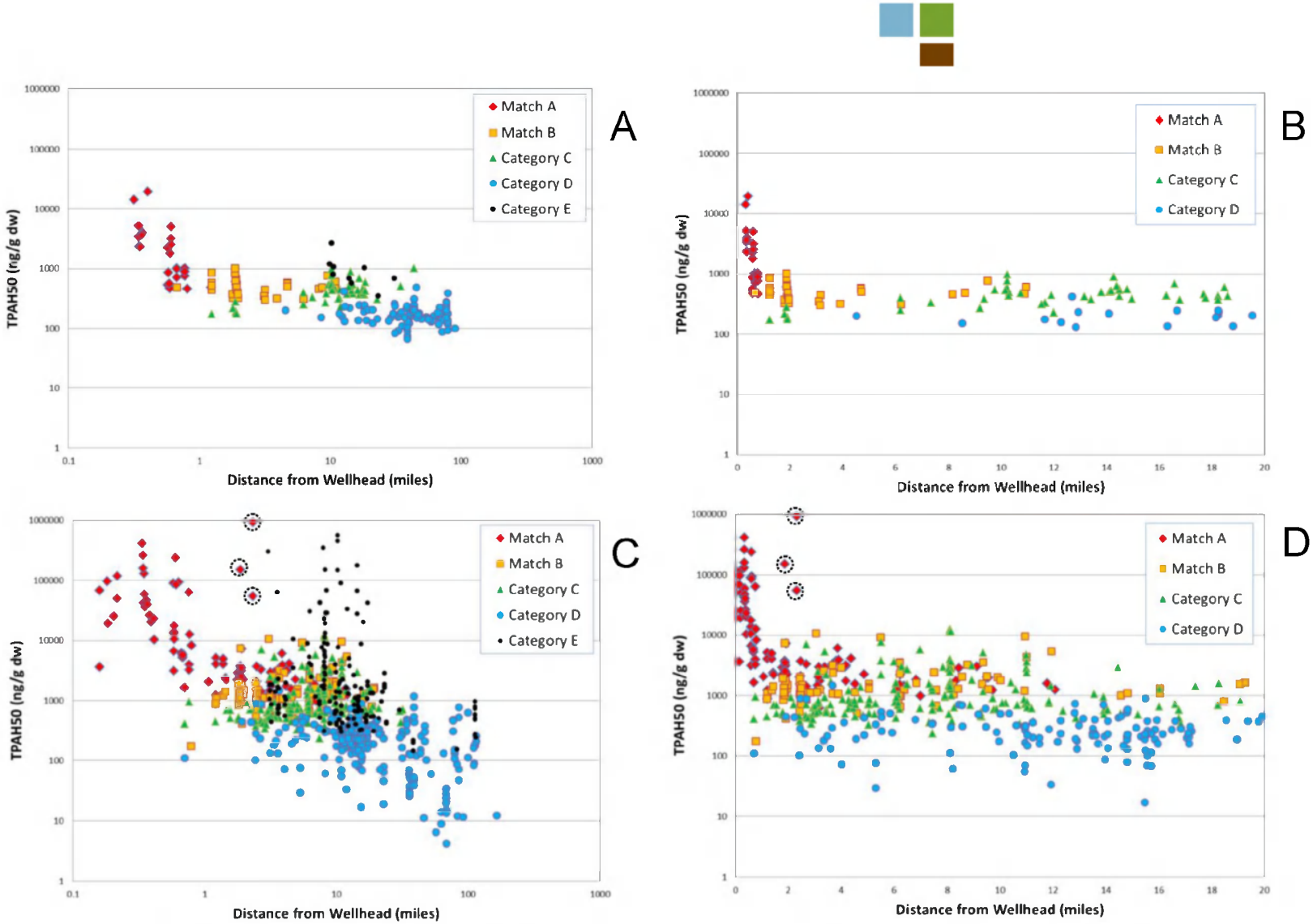

Figure 27: Graphs showing the concentration of $TPAH_{50}$ in surface sediments versus distance from the Macondo well (A) and (B) show results for cores collected in 2014. (C) and (D) show results for cores collected in 2010/2011, reproduced from Figure 17 for ease of comparison. (B) and (D) exclude all "E" samples and sample further than 20 miles from the well. All data from Appendix 1.

Appendix 1 – Tabulated Summary of Fingerprint Classifications and Selected Data

(Samples are sorted by Client ID)